SANDIA REPORT
SAND2017-3372
Unlimited Release
Printed April 2017

RAZORBACK – A Research Reactor Transient Analysis Code, Version 1.0

Volume 3: Verification and Validation Report

Darren G. Talley

Prepared by
Sandia National Laboratories
Albuquerque, New Mexico 87185 and Livermore, California 94550

Sandia National Laboratories is a multi-mission laboratory managed and operated by Sandia Corporation, a wholly owned subsidiary of Lockheed Martin Corporation, for the U.S. Department of Energy's National Nuclear Security Administration under contract DE-AC04-94AL85000.

Issued by Sandia National Laboratories, operated for the United States Department of Energy by Sandia Corporation.

Available to DOE and DOE contractors from
U.S. Department of Energy
Office of Scientific and Technical Information
P.O. Box 62
Oak Ridge, TN 37831

Telephone: (865) 576-8401
Facsimile: (865) 576-5728
E-Mail: reports@osti.gov
Online ordering: http://www.osti.gov/scitech

Available to the public from
U.S. Department of Commerce
National Technical Information Service
5301 Shawnee Rd
Alexandria, VA 22312

Telephone: (800) 553-6847
Facsimile: (703) 605-6900
E-Mail: orders@ntis.gov
Online order: http://www.ntis.gov/search

SAND2017-3372
Unlimited Release
Printed April 2017

RAZORBACK – A Research Reactor Transient Analysis Code, Version 1.0

Volume 3: Verification and Validation Report

Darren G. Talley
Nuclear Safety Technologies
Sandia National Laboratories
P.O. Box 5800
Albuquerque, New Mexico 87185-1141

Abstract

This report describes the work and results of the verification and validation (V&V) of the version 1.0 release of the Razorback code. Razorback is a computer code designed to simulate the operation of a research reactor (such as the Annular Core Research Reactor (ACRR)) by a coupled numerical solution of the point reactor kinetics equations, the energy conservation equation for fuel element heat transfer, the equation of motion for fuel element thermal expansion, and the mass, momentum, and energy conservation equations for the water cooling of the fuel elements. This V&V effort was intended to confirm that the code shows good agreement between simulation and actual ACRR operations.

ACKNOWLEDGMENTS

The author would like to thank the operations staff of the Annular Core Research Reactor for providing the data and log sheets for the pulse operations, installing the spare instrumented element, and executing the power stepdown operation used in this report. In addition, the author would like to thank Gerald Naranjo for his invaluable help in setting up the data acquisition equipment for the power stepdown operation.

CONTENTS

FIGURES

TABLES

NOMENCLATURE

ACRR	Annular Core Research Reactor
$BeO\text{-}UO_2$	Beryllium Oxide-Uranium Dioxide
DOE	Department of Energy
DSA	Documented Safety Analysis
FWHM	Full Width at Half-Maximum
LEHM	Leading Edge (Width) at Half-Maximum
PDS	Pulse Diagnostic System
PPS	Plant Protection System
RHU	Rod Holdup
SNL	Sandia National Laboratories
TEHM	Trailing Edge (Width) at Half-Maximum
TR	Transient Rod
TRW	Transient Rod Withdrawal
V&V	Verification and Validation
ρ	Reactivity
$	Dollar (a unit of reactivity)

1. INTRODUCTION

1.1. Background

Razorback is a computer code designed to simulate the operation of a research reactor (such as the Annular Core Research Reactor (ACRR)) by a coupled numerical solution of the point reactor kinetics equations, the energy conservation equation for fuel element heat transfer, the equation of motion for fuel element material thermal expansion, and the mass, momentum, and energy conservation equations for the water cooling of the fuel elements. Razorback is intended for the performance of analyses related to the ACRR Documented Safety Analysis (DSA). As such, it is necessary that the code be verified to be solving these equations correctly, and also have its predictive results validated against data collected from actual ACRR operation.

1.2. Purpose and Scope

The purpose of this report is to document the work done to verify and validate the version 1.0 release of the Razorback code. This work is intended to address as many verification and validation (V&V) areas for the code as achievable with simple analytical solutions and the currently available ACRR operational data. The V&V results may be used to provide confidence that the code produces acceptable results for ACRR operations, and to provide insight for determining margins to safety/design limits and where conservatism is needed in a given application.

The scope of the verification and validation (V&V) includes addressing analytical solutions as well as data collected under normal operating conditions of the ACRR. The RAZORBACK code can be used to simulate ACRR steady-state, pulse, transient rod withdrawal (TRW), and general operational transient operation. Limitations on its current application include conditions after fuel element materials are considered as failed (i.e., melting, or plastic deformation). In addition, while the code does have the capability to model bulk boiling in the coolant channel, no ACRR boiling data is available for validation in this regime.

1.3. Approach

The V&V is accomplished in five areas: (1) comparison to analytical solutions, (2) comparison to ACRR pulse operations, (3) comparison to ACRR TRW operations, (4) comparison to ACRR steady-state operation, and (5) comparison to a general ACRR transient operation. The comparison to analytical solutions will verify that the relevant physical models (i.e., equations) have been properly implemented within Razorback, and the implementation is providing a correct solution of those equations. The comparison to pulse operations will determine the validity of the coupled reactor kinetics and thermal-hydraulic solutions implemented within Razorback for simulating large rapid reactivity additions at the ACRR. The comparison to TRW and general ACRR transient operations will determine the validity of the coupled reactor kinetics and thermal-hydraulic solutions implemented within Razorback for simulating general ACRR operation. The comparison to ACRR steady-state operation will determine the validity of the thermal-hydraulic solution implemented within Razorback for determining the temperature conditions within an ACRR fuel element for normal operating conditions.

A previous work (Ref. 1) documents the initial V&V of the beta version of RAZORBACK. Some areas of this current V&V report for version 1.0 refer to the V&V results of that previous work. In these cases, either no changes have been made in the associated subroutines, or only changes which do not affect the physical models have been made.

2. GENERAL OVERVIEW OF THE RAZORBACK ACRR MODEL

This section provides a high level discussion of the input data pertinent to the validation modeling of the ACRR presented in this report. A sample input file is included in Appendix A.

2.1. Reactor Kinetics

The reactor kinetics model consists of the point reactor kinetics equations (see Ref. 2) using eight delayed neutron precursor groups. A neutron generation time of 24 μs (Ref. 3) was selected, along with a total delayed neutron fraction of 0.0073 (Ref. 4). The delayed neutron group parameters (group decay constants and production fraction) used are shown in Table 1. These values are from Campbell and Spriggs (Ref. 5).

Table 1. Reactor Kinetics Delayed Neutron Precursor Group Parameters Used.

Delayed Neutron Group	Group Decay Constant λ_i (s^{-1})	Group Fraction β_i
1	1.25×10^{-2}	2.409×10^{-4}
2	2.83×10^{-2}	1.1242×10^{-3}
3	4.25×10^{-2}	6.643×10^{-4}
4	1.33×10^{-1}	1.4381×10^{-3}
5	2.92×10^{-1}	2.4163×10^{-3}
6	6.66×10^{-1}	6.570×10^{-4}
7	1.63	5.913×10^{-4}
8	3.55	1.679×10^{-4}

2.2. Reactivity Control Systems

The differential reactivity worth curve for the CR, SR, and TR banks is input to Razorback in the form

$$\frac{d\rho}{dz} = Asin^2\left[B\left(z - z_o\right) + C\right] \tag{2-1}$$

Where it is noted that the "A" coefficient is normalized to a total bank worth, which is a separate input. The values used for A, B, C, z_o, and bank worth parameters were determined from MCNP analyses (Ref. 15). The coefficients/constants are shown in Table 2.

Table 2. Rod Bank Differential Worth Input Parameters.

Parameter	Control Rod Bank	Safety Rod Bank	Transient Rod Bank
A	0.03003581	0.03003581	0.0282943
B	0.0463939	0.0463939	0.0423011
C	0.425066	0.425066	0.634055
z_o	n/a	n/a	26.0
Bank Worth	$11.57	$2.22	$4.454

To simulate a pulse operation, there are timing issues which must be addressed. First, an actual pulse operation will initiate TR ejection after an initial delay time programmed by the reactor operator in the pulse countdown timer program. This value has typically been set at 165 ms. Thus, the Razorback input herein was set to account for this initial time delay. Additionally, once the 165 ms is attained, there is a delay associated with how quickly the valve which admits high pressure nitrogen to the TR ejection mechanism can open. This delay time is also an input to the Razorback simulation of a pulse. At this point, Razorback determines the acceleration of the TR rod bank based on the input nitrogen pressure, piston area, and TR mass. The pressure was obtained from ACRR operations (65 psig). The piston area (28.96 cm^2) was determined from the piston drawing.[1] The TR mass (13.75 kg) was set based on past measurements of TR position vs. time data. The valve opening delay time was set at a value for which the simulated pulse peak time approximately matched the measured pulse peak time (for the pulse to be simulated).

Lastly, the ACRR pulse operation system sets a "rod holdup time" (RHU). The RHU time value (0.4 seconds for the pulses being simulated) is the time (from t=0) at which a gravity drop of the transient rods, safety rods, and control rods will be initiated. At this point in the pulse simulation, Razorback will initiate all rods dropping after a simulated electric circuit delay (set using the "Scram Delay Time" input), and the downward acceleration of the rods will be determined assuming that the rods would fall by 55.00 cm over the input "Rod Fall Time." The inputs selected (125 ms scram delay time, and 1.0 s rod fall time) were set to attain the impact of the rod drops on the simulated pulse tails.

2.3. Fuel Element

The fuel element model for the ACRR was defined using the dimensions from ACRR drawings. The model explicitly includes the BeO-UO_2 fuel pellets (inner and outer), the niobium fuel cups, the stainless steel cladding, and the gaps (helium filled) between the fuel pellets, niobium, and cladding. The model dimensions are shown in Table 3. The energy deposition factors were determined using MCNP (Ref. 19). Razorback input options were set such that radial thermal expansion of the fuel element materials was computed, and radiation heat transfer across the helium filled gaps was computed.

[1] Automated Concepts Inc. Drawing 2062M205, Rev. A.

Table 3. Fuel Element Model Dimensions.

Material	Inner Radius (cm)	Outer Radius (cm)	Number of Nodes	Energy Deposition Fraction
BeO-UO_2	0.24130	1.09982	30	0.97846[a]
He	1.09982	1.11760	10	0.0
BeO-UO_2	1.11760	1.68402	10	0.97846[a]
He	1.68402	1.73228	10	0.0
Nb	1.73228	1.77038	10	0.00400
He	1.77038	1.82245	10	0.00
SS-304	1.82245	1.87325	10	0.00456

a. As currently configured in Razorback, the energy deposition factor (EDF) applies to the material, and not to the zone. Thus, 97.846% of the energy deposition is in the BeO-UO_2 material. Also, a single fuel pellet (vs. two pellets separated by a small gap) is used in the MCNP model to compute the EDFs. This approach may be revised in future versions for increased generality.

The radial fission density peaking distribution across the BeO-UO_2 fuel pellet in Razorback is of the form

$$f(r) = Ae^{B \cdot r} + C \tag{2-2}$$

Values used for A, B, and C are given in Table 4 (Ref. 6).

The axial fission density peaking distribution over the length of the fuel element in Razorback is of the form

$$f(z) = \sum_{i=0}^{6} a_i \left(\frac{z}{H}\right)^i \tag{2-3}$$

where H is the height of the fuel stack. Values used for the polynomial coefficients are shown in Table 4 (Ref. 6).

Table 4. Pellet Radial and Element Axial Peaking Distribution Parameters.

Fuel Pellet Radial Distribution Coefficients		Fuel Axial Distribution Coefficients	
		a_0	0.7721
A	0.0157	a_1	-0.6252
		a_2	24.0903
B	1.9370 cm^{-1}	a_3	-89.6026
		a_4	141.5383
C	0.8211	a_5	-108.8048
		a_6	33.1631

2.4. Coolant Channel

The coolant channel is the active fuel height (52.25 cm), and the flow wetted perimeter (P_w) and flow area (A_f) based upon the element diameter (3.747 cm), and the hexagonal pitch (4.171 cm) of the element grid. The coolant channel is coupled to the fuel cladding surface by means of a single phase heat transfer coefficient (h) determined from the flow/heat transfer regime dependent Nusselt number. The Nusselt number (Nu) is given by

$$Nu = \frac{hD_h}{k} \tag{2-4}$$

where D_h = channel hydraulic diameter ($4A_f/P_w$), and
k = coolant thermal conductivity.

For very low flow natural convection regimes, Nu is given by

$$Nu = CRa^n \tag{2-5}$$

where C = correlation coefficient,
n = correlation exponent, and
Ra = Rayleigh number.

The Rayleigh number is given by

$$Ra = \frac{\rho^2 g\beta(T_w - T_b){D_h}^4}{\mu^2} \tag{2-6}$$

where ρ = coolant density,
g = acceleration of gravity,
β = coolant volumetric expansion coefficient,
T_w = cladding wall temperature,
T_b = bulk coolant temperature, and
μ = coolant absolute viscosity.

The Razorback simulations use C = 0.272 and n = 0.25 from a correlation determined by Kim and El-Genk (Ref. 23).

For laminar flow regimes, Nu is given by

$$Nu = CRe^m Pr^n \tag{2-7}$$

where C = correlation coefficient,
Re = Reynolds number,
m = correlation exponent for Re,
Pr = Prandtl number, and
n = correlation exponent for Pr.

$$Re = \frac{\rho V D}{\mu} \tag{2-8}$$

where V = coolant flow velocity.

$$Pr = \frac{\mu c_p}{k} \tag{2-9}$$

where c_p = coolant specific heat capacity.

The Razorback simulations use C = 1.061, m = 0.34, and n = 0.33 from a correlation determined by Kim and El-Genk (Ref. 23).

For turbulent flow regimes, Nu is given by

$$Nu = CRe^m Pr^n \tag{2-10}$$

The Razorback simulations use C = 0.023, m = 0.8, and n = 0.4 from the Dittus-Boelter correlation (Ref. 24).

Once the cladding surface temperature exceeds the local coolant saturation temperature, the heat transfer will transition to a two-phase subcooled boiling heat transfer superposition of the single phase heat flux characterized by Eqs. 2-7 or 2-10 and the subcooled boiling heat flux. The subcooled boiling heat flux is characterized by the Jens-Lottes correlation (Ref. 25) in Razorback. The Jens-Lottes correlation (adjusted for SI units) is given by

$$\frac{q''_{JL}}{10^6} = \frac{exp(\frac{4p}{62})}{25^4}(T_w - T_{sat})^4 \tag{2-11}$$

where q''_{JL} = heat flux (W/m^2),
p = coolant pressure (bar),
T_w = cladding surface temperature (°C), and
T_{sat} = local coolant saturation temperature (°C).

In Razorback, the superposition is formed using the relation

$$q''_{scb} = \sqrt{q''^{\,2}_{sp} + \left(q''_{JL} - q''_{ib}\right)^2} \tag{2-12}$$

where q''_{scb} = subcooled boiling heat flux,
q''_{sp} = single phase heat flux (Eqs. 2-7 or 2-10),
q''_{JL} = Jens-Lottes subcooled boiling heat flux, and
q''_{ib} = incipient boiling heat flux.

The heat flux of incipient boiling (q_{ib}'') is determined in Razorback using the Bergles-Rohsenow (Ref. 26) relation (adjusted for SI units)

$$q''_{ib} = 1082p^{1.156}\left[1.8\left(T_w - T_{sat}\right)\right]^{2.1598/p^{0.0234}} \quad (2\text{-}13)$$

where q''_{ib} = heat flux (W/m^2),
p = coolant pressure (bar),
T_w = cladding surface temperature (°C), and
T_{sat} = local coolant saturation temperature (°C).

2.5. Reactivity Feedback

Razorback utilizes five reactivity feedback mechanisms that compensate for control system reactivity inputs which are determined from MCNP calculations:

- Fuel temperature: representing the Doppler broadening of the fuel absorption cross section.
- Fuel expansion: representing the local fuel density change, as well as the outer fuel surface area change.
- Cladding expansion: representing the change in local moderator-to-fuel ratio as the coolant channel area changes with clad expansion/contraction.
- Coolant density: representing the change in moderation and absorption as the density of the coolant changes.
- Coolant temperature: representing the change in the local neutron energy spectrum as the coolant temperature changes.

The reactivity feedback coefficient for fuel temperature is given by

$$\frac{d\rho}{dT}^{fuel} = A_{ft} + \frac{B_{ft}}{\sqrt{T_{fuel}}} \quad (2\text{-}14)$$

where T_{fuel} is the absolute temperature. The coefficients for this relation are A_{ft} = -0.000988 \$/K and B_{ft} = -0.079422 \$/K$^{0.5}$ (Ref. 16).

The reactivity feedback coefficient for fuel expansion is given by the summation of three components, where the first component is

$$\frac{d\rho}{dR}^{f\_outer} = C_{fo} \quad (2\text{-}15)$$

where R_{f_outer} is the outer radius of the outer fuel pellet. The coefficient is C_{fo} = 47.50 \$/cm (Ref. 16).

The second component of the reactivity feedback coefficient for fuel expansion is given by

$$\frac{d\rho}{dR}_{f\_inner} = C_{fi} \tag{2-16}$$

where R_{f_inner} is the innermost radius of the fuel pellets (the gap between the inner and outer pellets is essentially ignored). The coefficient is C_{fi} = -6.31 \$/cm (Ref. 16).

The third component of the reactivity feedback coefficient for fuel expansion is given by

$$\frac{d\rho}{d\rho_f} = C_{fd} \tag{2-17}$$

where ρ_f is the local density of the fuel. The coefficient is C_{fd} = 11.26 \$/(g/cm^3) (Ref. 16).

The reactivity feedback coefficient for clad expansion is also given by the summation of three components, where the first component is

$$\frac{d\rho}{dR}_{c\_outer} = C_{co} \tag{2-18}$$

where R_{c_outer} is the outer radius of the clad. The coefficient is C_{co} = -122.51 \$/cm (Ref. 17).

The second component of the reactivity feedback coefficient for clad expansion is given by

$$\frac{d\rho}{dR}_{c\_inner} = C_{ci} \tag{2-19}$$

where R_{c_inner} is the inner radius of the clad. The coefficient is C_{ci} = 104.46 \$/cm (Ref. 17).

The third component of the reactivity feedback coefficient for clad expansion is given by

$$\frac{d\rho}{d\rho_c} = C_{cd} \tag{2-20}$$

where ρ_c is the local density of the clad. The coefficient is C_{cd} = -0.71 \$/(g/cm) (Ref. 17).
The coolant density feedback[2] is given as -0.382 \$/%void (Ref. 18). The coolant temperature feedback is given as -0.00116\$/K (Ref. 18).

[2] The unit "%void" is calculated as $(\rho_o-\rho)/\rho_o*100$, where ρ_o is the initial reference density of the coolant, and ρ is the "current" density of the coolant.

[This page intentionally left blank.]

3. COMPARISON TO ANALYTICAL SOLUTIONS

3.1. Reactor Kinetics

The reactor kinetics model of the code has been evaluated previously in Ref. 8. In this previous evaluation, the code was used to simulate benchmark cases for step, ramp, and sinusoidal reactivity additions which were documented in Ref. 9. The code results were in excellent agreement with the benchmark results. Tables 5 through 10 below present selected results from Ref. 8.

Table 5. Point Kinetic Benchmark Evaluation for -$1.0 Step Addition.

Time (s)	Code Result	Benchmark	% Difference
0.1	5.2049990E-01	5.205642866E-01	-0.012369
1.0	4.3332231E-01	4.333334453E-01	-0.002570
10.0	2.3610794E-01	2.361106508E-01	-0.001148
100.0	2.8667533E-02	2.866764245E-02	-0.000382

Table 6. Point Kinetic Benchmark Evaluation for -$0.5 Step Addition.

Time (s)	Code Result	Benchmark	% Difference
0.1	6.9885920E-01	6.989252256E-01	-0.009447
1.0	6.0704475E-01	6.070535656E-01	-0.001452
10.0	3.9607494E-01	3.960776907E-01	-0.000694
100.0	7.1582682E-02	7.158285444E-02	-0.000241

Table 7. Point Kinetic Benchmark Evaluation for $0.5 Step Addition.

Time (s)	Code Result	Benchmark	% Difference
0.1	1.5332115E+00	1.533112646E+00	0.006448
1.0	2.5115239E+00	2.511494291E+00	0.001179
10.0	1.4215038E+01	1.421502524E+01	0.000090
100.0	8.0060942E+07	8.006143562E+07	-0.000617

Table 8. Point Kinetic Benchmark Evaluation for $1.0 Step Addition.

Time (s)	Code Result	Benchmark	% Difference
0.1	2.5158849E+00	2.515766141E+00	0.004721
0.5	1.0362726E+01	1.036253381E+01	0.001855
1.0	3.2183405E+01	3.218354095E+01	-0.000422
10.0	3.2469217E+09	3.246978898E+09	-0.001762
100.0	---*	2.596484646E+89	---*

*Run terminated shortly after 10.0 seconds due to prohibitively slow run time.

Table 9. Point Kinetic Benchmark Evaluation for $0.1/s Ramp Addition.

Time (s)	Code Result	Benchmark	% Difference
2.00	1.3382200E+00	1.338200050E+00	0.001491
4.00	2.2284412E+00	2.228441897E+00	-0.000031
6.00	5.5818737E+00	5.582052449E+00	-0.003202
8.00	4.2780238E+01	4.278629573E+01	-0.014158
10.00	4.5061295E+05	4.511636239E+05	-0.122056
11.00	1.7852862E+16	1.792213607E+16	-0.386528

Table 10. Point Kinetic Benchmark Evaluation for $2.0 Step Addition with Feedback.

Time (s)	Code Result	Benchmark	% Difference
10.0	1.0338084E+02	1.033808535E+02	-0.000013
20.0	3.9138865E+01	3.913886903E+01	-0.000010
30.0	2.2003775E+01	2.200377721E+01	-0.000010
40.0	1.4493671E+01	1.449367193E+01	-0.000006
50.0	1.0318610E+01	1.031861108E+01	-0.000010
60.0	7.6633185E+00	7.663319203E+00	-0.000009
70.0	5.8293948E+00	5.829395378E+00	-0.000010
80.0	4.4994266E+00	4.499427073E+00	-0.000011
90.0	3.5074223E+00	3.507422663E+00	-0.000010
100.0	2.7551266E+00	2.755126886E+00	-0.000010

3.2. Fuel Element Heat Transfer

The fuel element heat transfer routine was verified against a steady-state analytical solution. A simple fuel element model was developed for this verification effort, and is shown in Fig. 1. The simple model comprises a cylindrical geometry fuel element with an inner void, a BeO-UO_2 fuel region, a niobium inner can region, and a stainless steel cladding region.

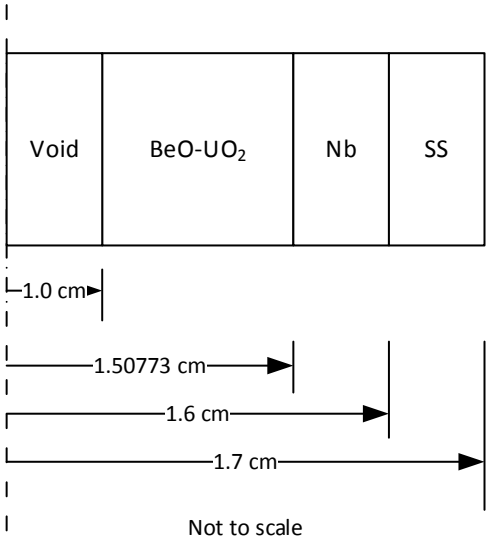

Figure 1. Schematic of Fuel Element for Analytical Verification of Heat Transfer.

To facilitate an analytical solution, the thermal conductivities of the materials were set at constant (i.e., non-temperature dependent) values of 0.16 W/cm-K, 0.5 W/cm-K, and 0.2 W/cm-K for the BeO-UO_2, niobium, and stainless steel, respectively. The inner radius boundary condition was a zero temperature gradient (zero net heat flux/symmetry), and the outer radius boundary condition was a constant 120°C surface temperature. The thermal expansion option in Razorback was turned off. The height of the element was set at 50 cm. The power level was set at 20 kW, which results in a power density in the BeO-UO_2 region of 100 W/cm^3.

Figure 2 shows the resulting steady-state temperature profile within this simplified fuel element model. The Razorback results clearly align well with the analytical solution. Figure 3 presents the actual relative error between the Razorback results and the analytical solution. The relative error across the element model is bounded by $\pm 10^{-4}$.

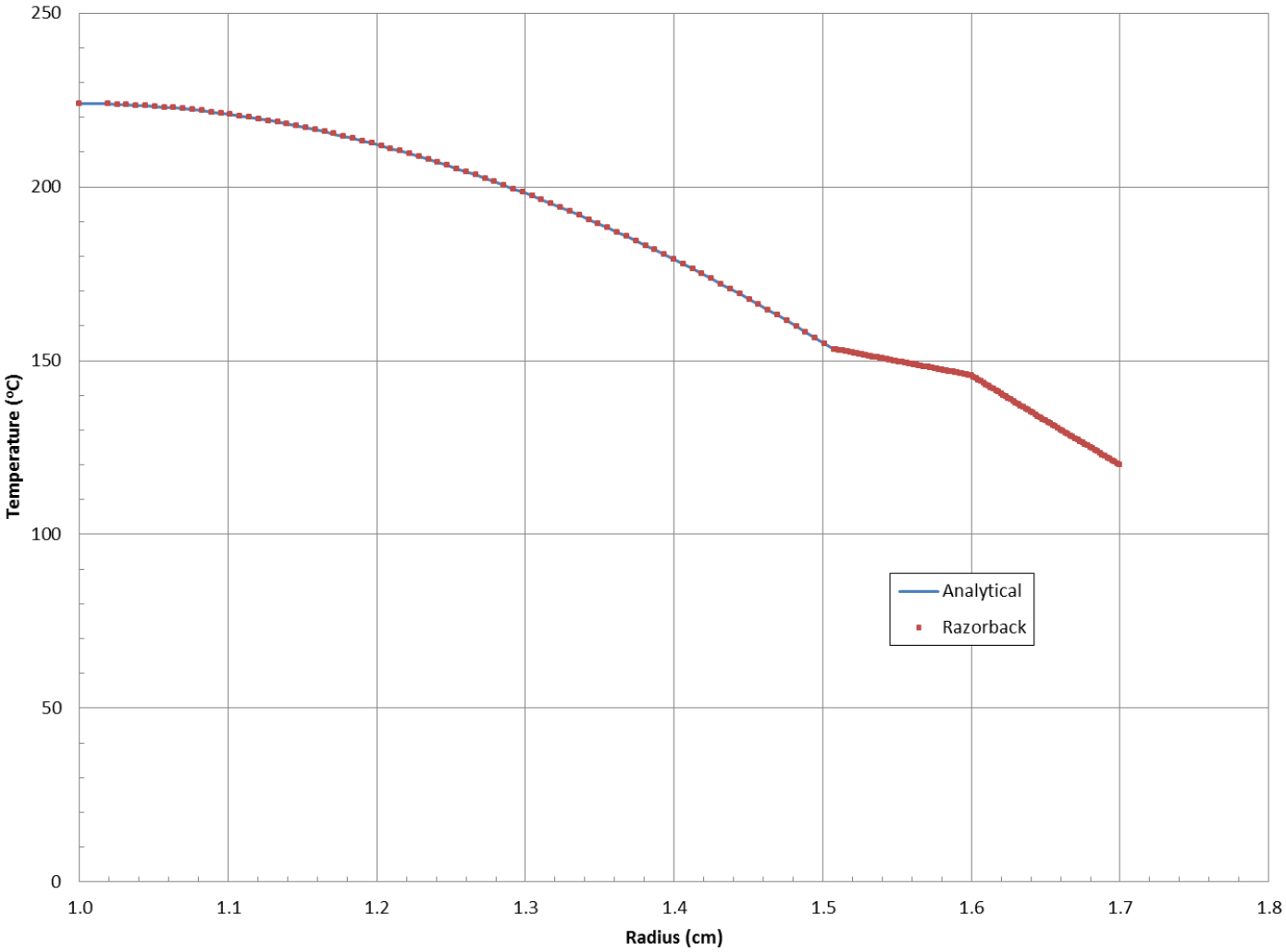

Figure 2. Razorback Fuel Element Temperature vs. the Analytical Result.

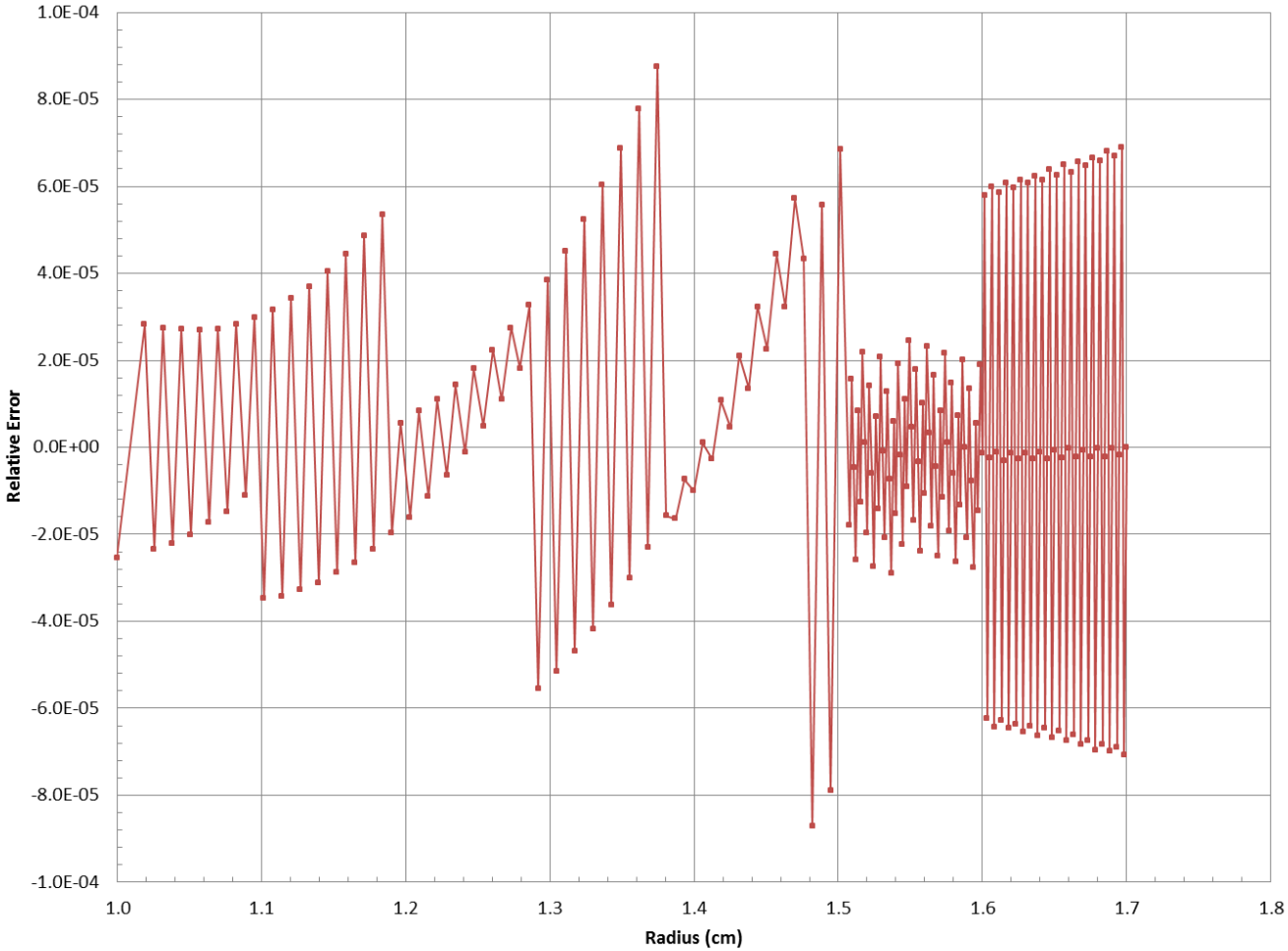

Figure 3. Relative Error of Fuel Temperature Prediction and Analytical Solution.

[This page intentionally left blank.]

3.3. Fuel Element Thermal Expansion

The fuel element thermal expansion routine was verified against a steady-state analytical solution. The ACRR fuel element model (described in Sect. 2.3) was used for this verification effort. The thermal expansion routine in Razorback assumes plane stress conditions (i.e., axial stress is zero).

The analytical solution for plane stress thermal expansion for a particular temperature distribution T(r) is given in Ref. 14 as

$$u(r) = \alpha(1+\nu)\frac{1}{r}\int_a^r (T(r) - T_{ref})rdr + C_1(r)r + \frac{C_2}{r}$$

$$C_1(r) = \frac{(1-\nu)}{(1+\nu)}\frac{1}{a^2}C_2 - \frac{1-\nu}{E}p_i$$

$$C_2 = \alpha(1+\nu)\frac{a^2}{b^2-a^2}\int_a^b (T(r) - T_{ref})rdr + \frac{1+\nu}{E}\frac{a^2b^2}{b^2-a^2}(p_i - p_o)$$

To facilitate an analytical solution, the linear thermal expansion coefficients (α), Young's moduli (E) and Poisson's ratios (ν) of the materials were set at constant (i.e., non-temperature dependent) values shown in Table 11.[3] Razorback was run in steady-state mode with a reactor power of 2.39 MW in order to produce a temperature distribution for the analytical check. The Razorback radial fuel element temperature data at an axial node approximately halfway up the fuel was selected, and a polynomial fit was determined for T(r) for each material. The reference temperature T_{ref} was 20°C. The boundary condition for each fuel material was zero pressure ($p_i = p_o = 0$) on both inner and outer radii (a and b).

Table 11. Material properties used for verification of thermal expansion routine.

Material	α (1/K)	E (GPa)	ν
BeO-UO_2	$8.5\text{x}10^{-6}$	345	0.26
Niobium	$8\text{x}10^{-6}$	105	0.4
Stainless Steel	$17.3\text{x}10^{-6}$	190	0.3

Figures 4 through 7 show the resulting steady-state temperature profile within the inner and outer BeO-UO_2 fuel pellets, niobium cup, and stainless steel cladding. Figures 8 through 15 show the comparison to the analytical solution and the relative error of the predicted radial displacements for each of these regions. The agreement is good in all cases. The largest absolute value of the relative error considering the results for all four regions is ~0.095%.

[3] Note that thermal expansion is only computed within the solid materials (i.e., not for gas-filled gaps).

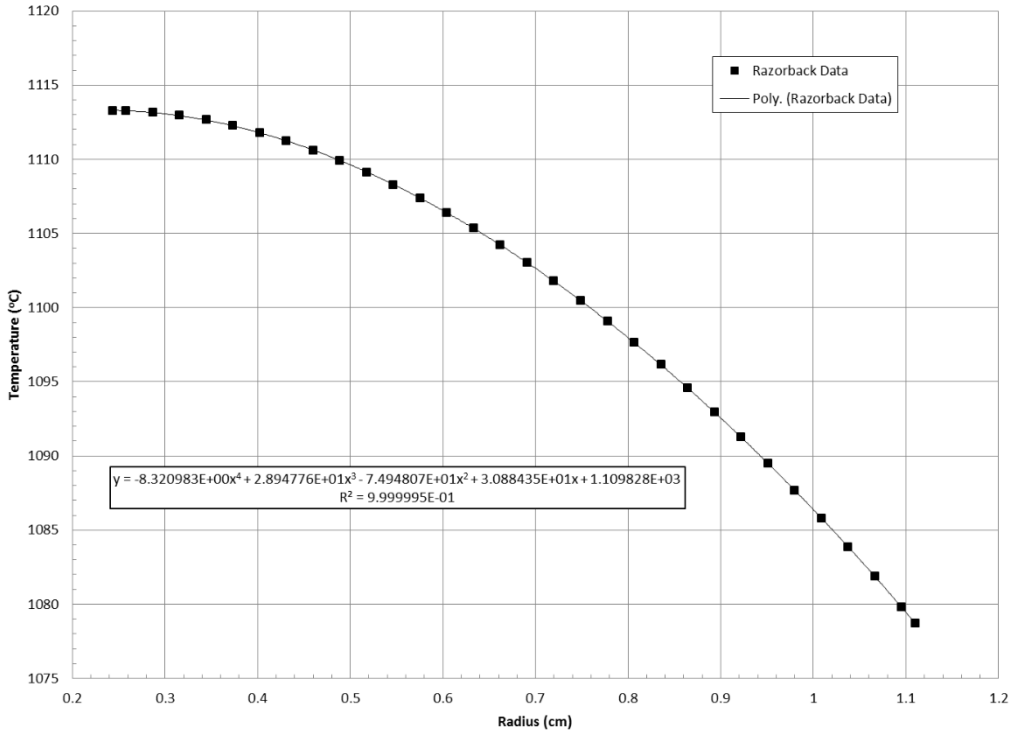

Figure 4. Inner fuel pellet temperature distribution for thermal expansion verification.

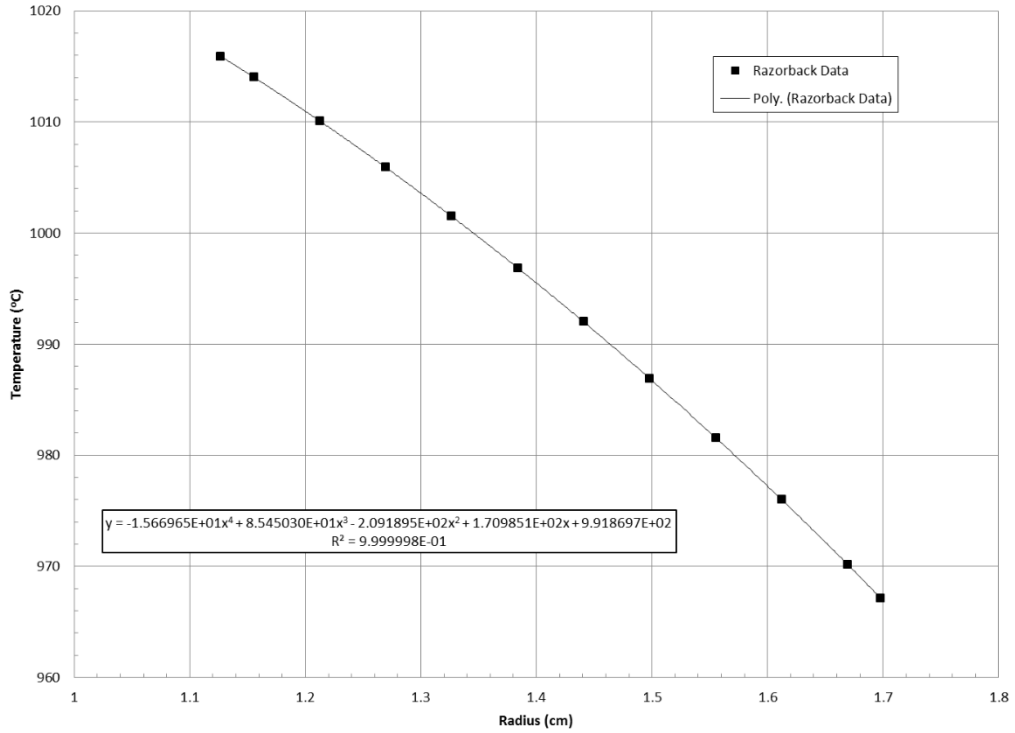

Figure 5. Outer fuel pellet temperature distribution for thermal expansion verification.

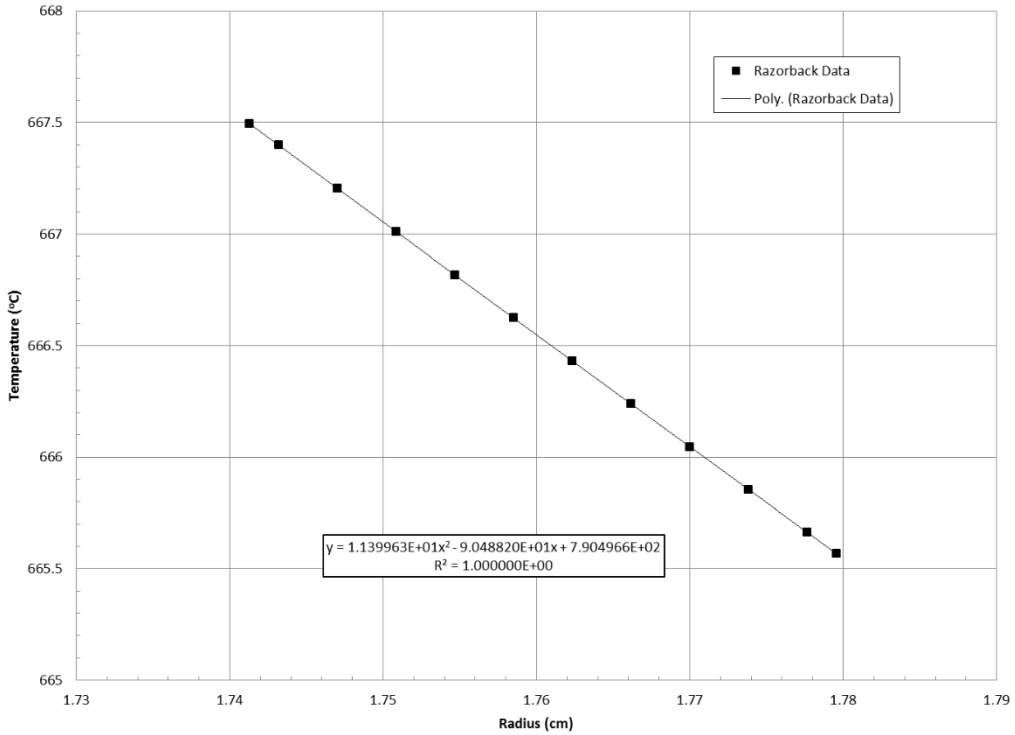

Figure 6. Niobium cup temperature distribution for thermal expansion verification.

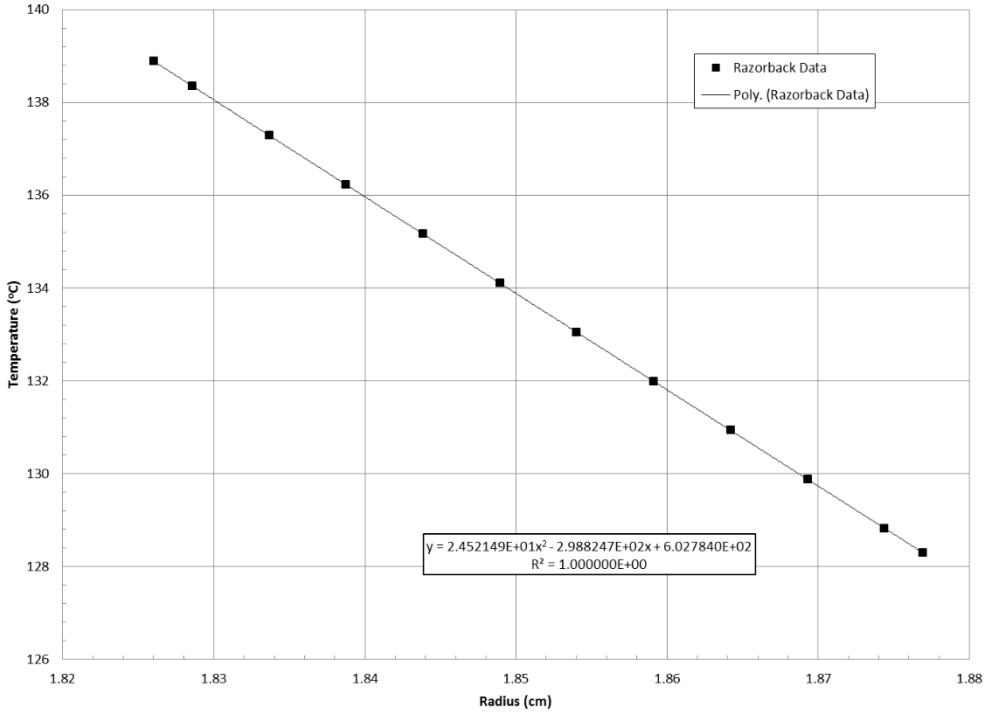

Figure 7. Stainless steel cladding temperature distribution for thermal expansion verification.

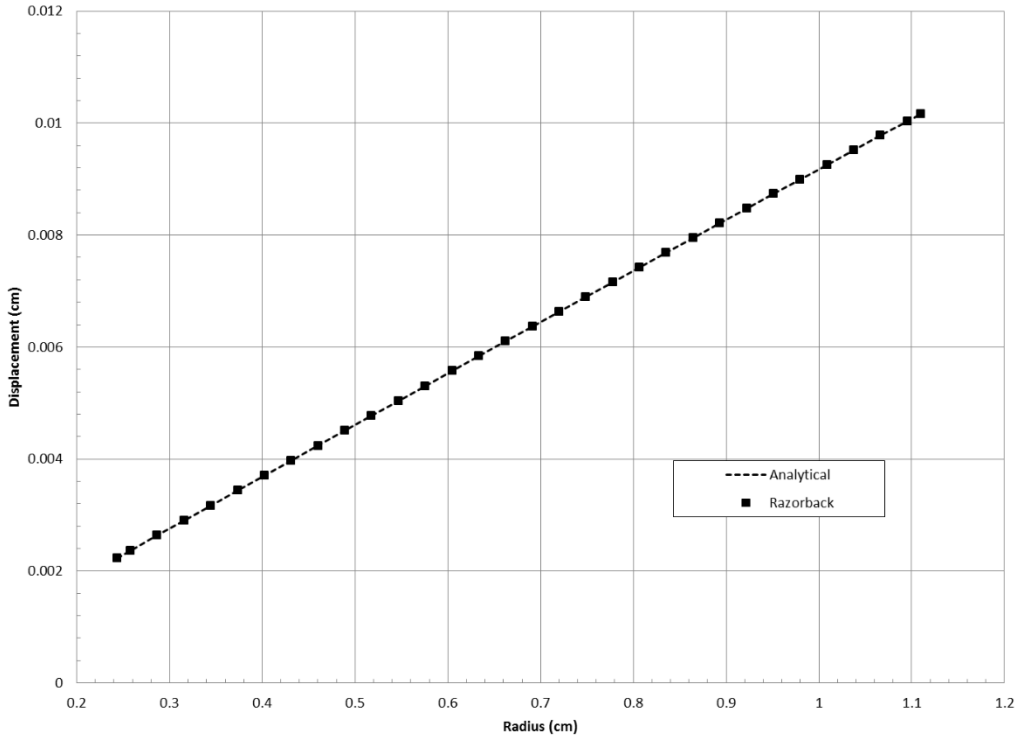

Figure 8. Inner fuel pellet radial displacement due to thermal expansion compared to analytical solution.

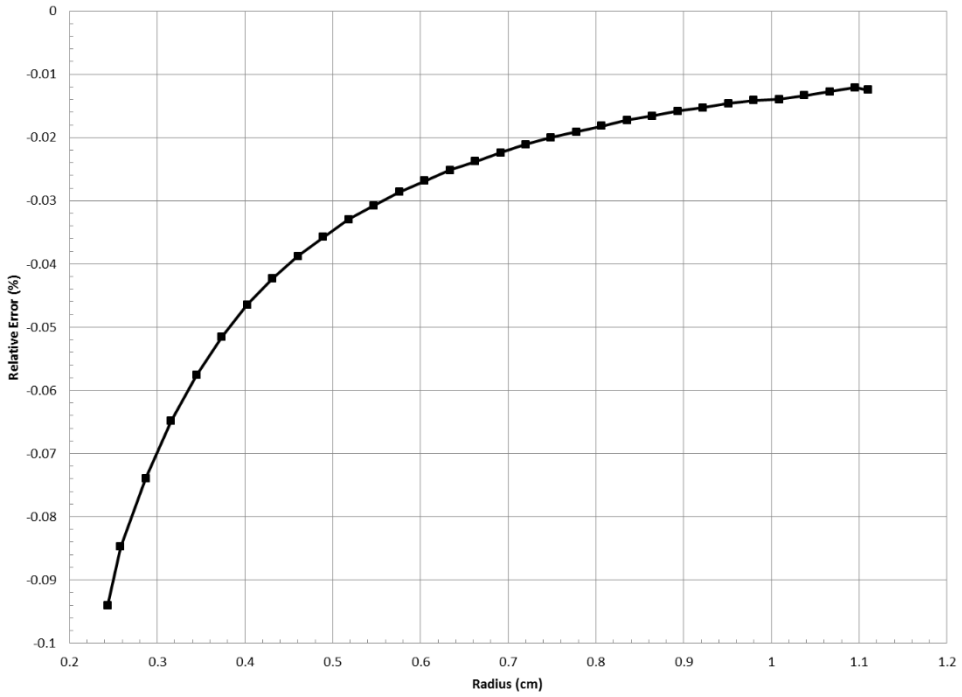

Figure 9. Relative error for verification of inner fuel pellet radial displacement due to thermal expansion.

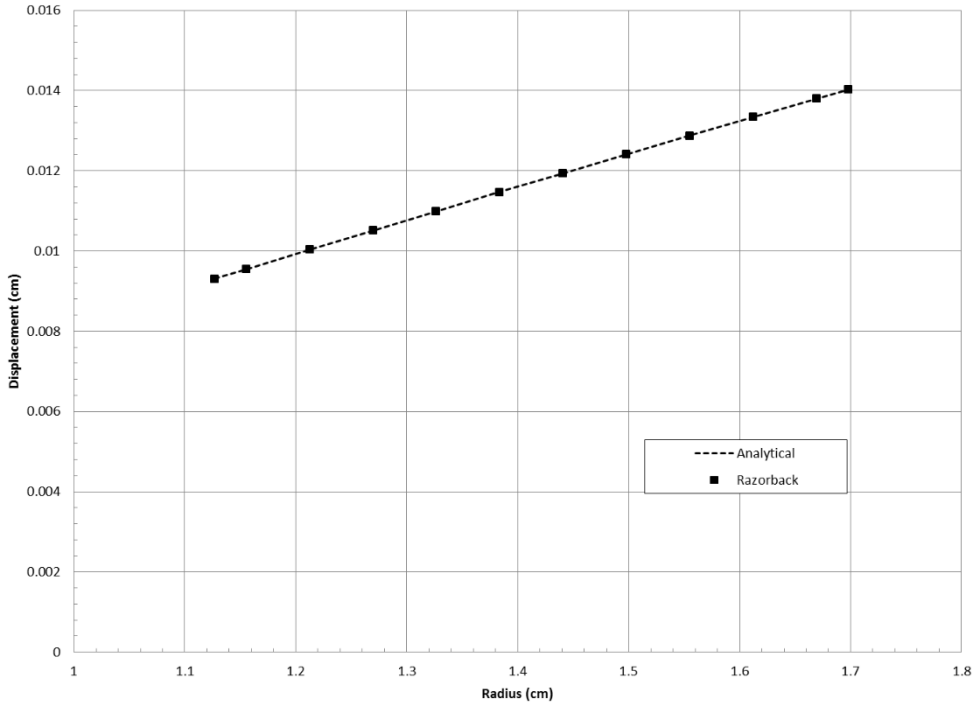

Figure 10. Outer fuel pellet radial displacement due to thermal expansion compared to analytical solution.

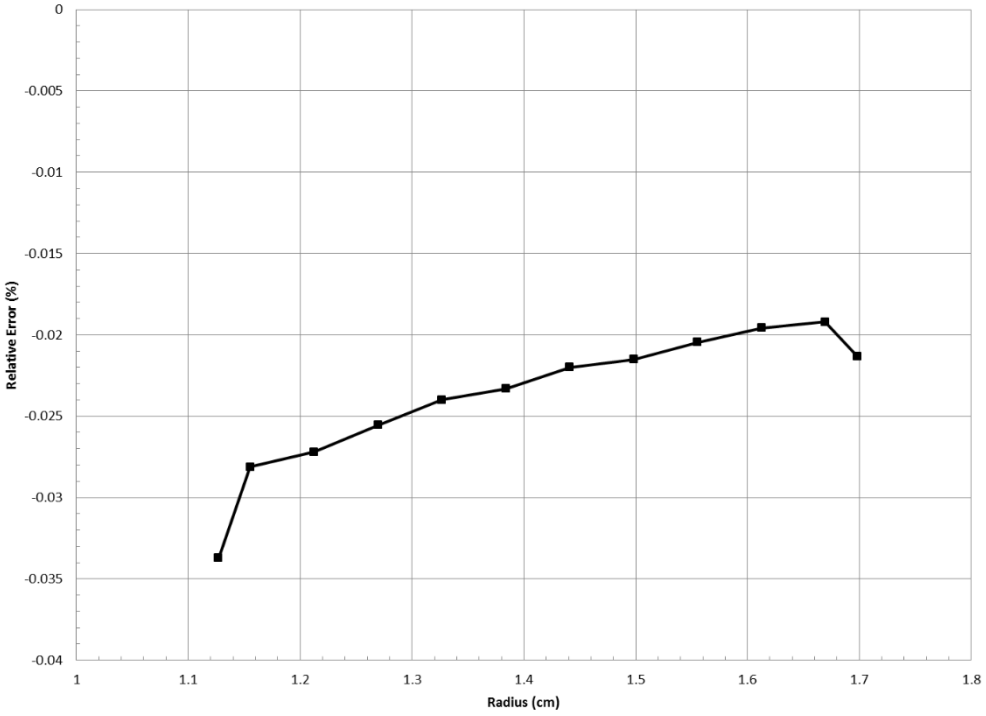

Figure 11. Relative error for verification of outer fuel pellet radial displacement due to thermal expansion.

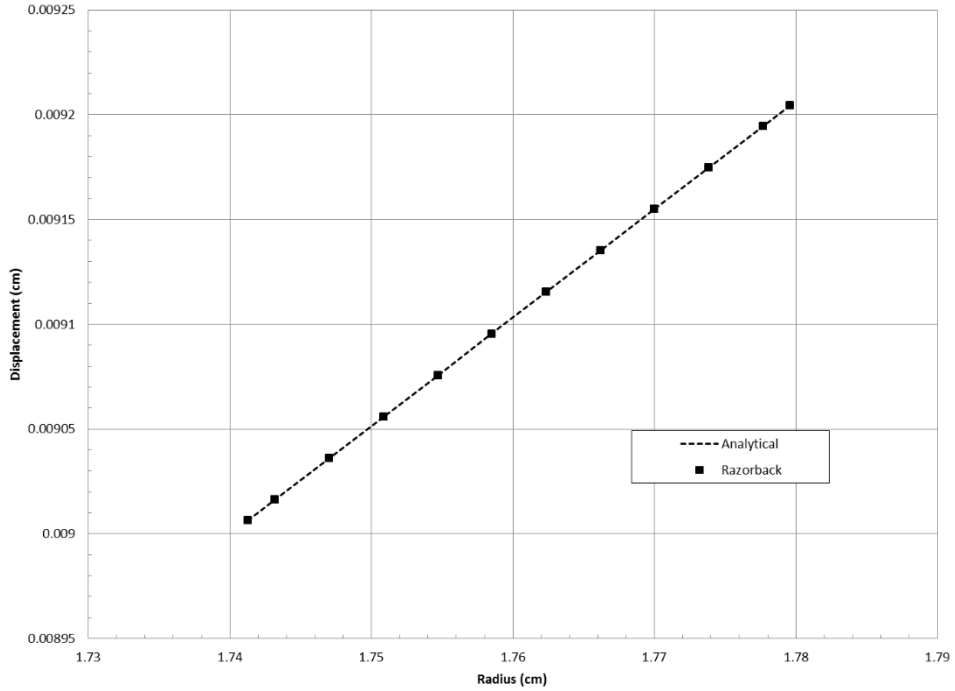

Figure 12. Niobium cup radial displacement due to thermal expansion compared to analytical solution.

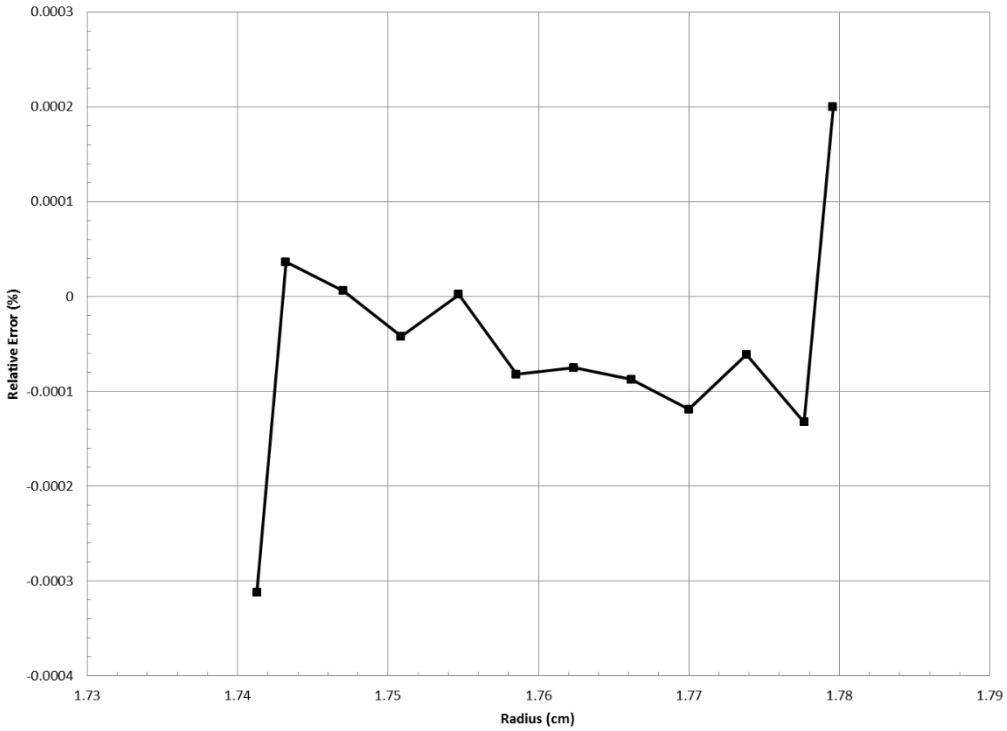

Figure 13. Relative error for verification of niobium cup radial displacement due to thermal expansion.

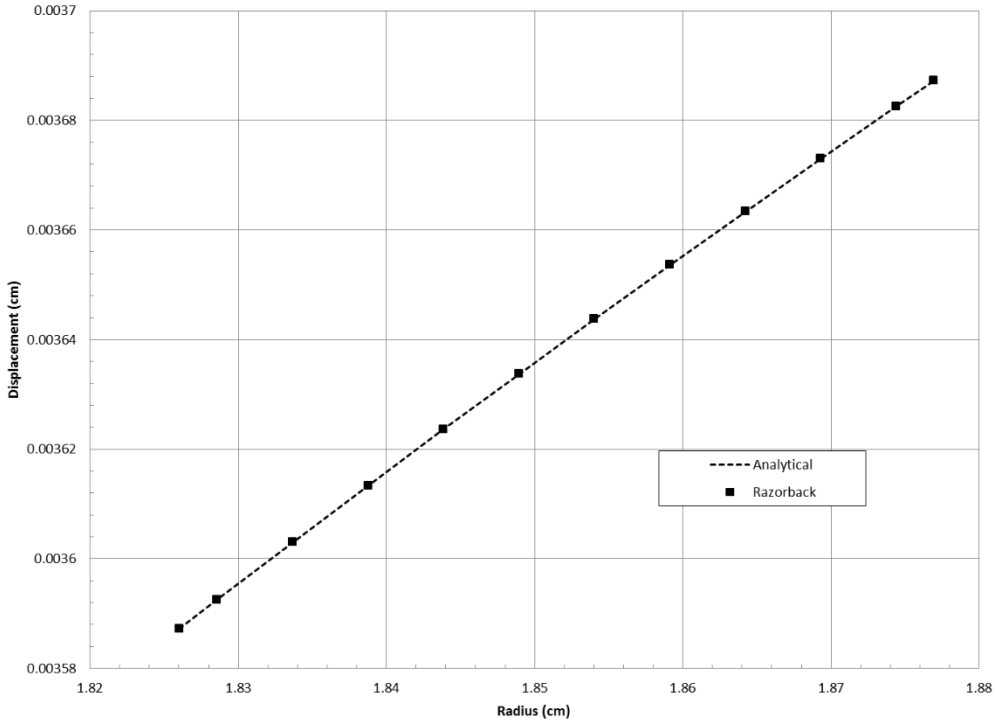

Figure 14. Stainless steel cladding radial displacement due to thermal expansion compared to analytical solution.

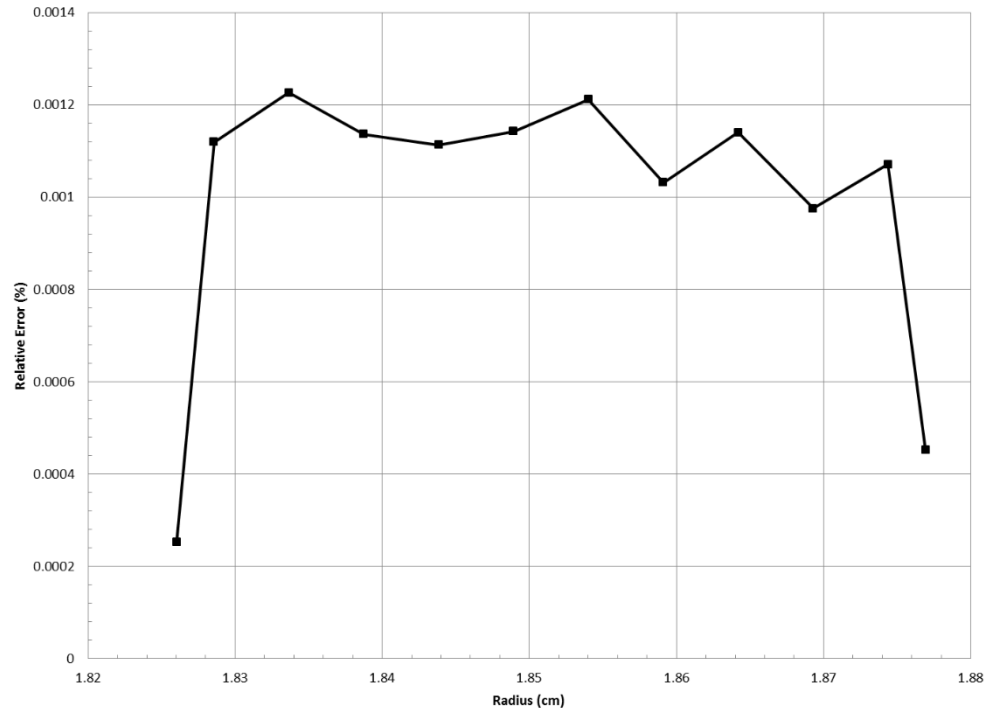

Figure 15. Relative error for verification of stainless steel cladding radial displacement due to thermal expansion.

[This page intentionally left blank.]

3.4. Fuel Element Stress

The verification of the fuel element thermal expansion routine is presented in Section 3.3. The thermal expansion routine uses the radial displacement results to compute the radial, azimuthal, and axial stress in the component materials of the fuel element. This section presents the verification of the stress results using the data from the same thermal expansion Razorback runs of Section 3.3.

The analytical solution for radial, azimuthal, and axial stress under the plane stress assumption is also given in Ref. 14 as

$$\sigma_r(r) = -\alpha E \frac{1}{r^2}\int_a^r \left(T(r) - T_{ref}\right) r dr + \frac{E}{1-\nu^2}\left[(1+\nu)C_1(r) - (1-\nu)\frac{C_2}{r^2}\right]$$

$$\sigma_\theta(r) = \alpha E \frac{1}{r^2}\int_a^r \left(T(r) - T_{ref}\right) r dr - \alpha E\left(T(r) - T_{ref}\right) + \frac{E}{1-\nu^2}\left[(1+\nu)C_1(r) - (1-\nu)\frac{C_2}{r^2}\right]$$

$$\sigma_z(r) \equiv 0$$

$$C_1(r) = \frac{(1-\nu)}{(1+\nu)}\frac{1}{a^2}C_2 - \frac{1}{(1+\nu)}\frac{p_i}{E}$$

$$C_2 = \alpha E \frac{a^2}{b^2 - a^2}\int_a^b \left(T(r) - T_{ref}\right) r dr + \frac{1}{1-\nu}\frac{a^2 b^2}{b^2 - a^2}(p_i - p_o)$$

Razorback also computes the von Mises stress (σ_{vm}) at each location using $\sigma_1 = \sigma_r$, $\sigma_2 = \sigma_\theta$, and $\sigma_3 = \sigma_z$ in the following equation

$$\sigma_{vm} = \left[\frac{(\sigma_1 - \sigma_2)^2}{2} + \frac{(\sigma_2 - \sigma_3)^2}{2} + \frac{(\sigma_1 - \sigma_3)^2}{2}\right]^{\frac{1}{2}}$$

The linear thermal expansion coefficients (α), Young's moduli (E) and Poisson's ratios (ν) of the materials were those shown in Table 11 in Section 3.3. Razorback was run in steady-state mode with a reactor power of 2.39 MW in order to produce a temperature distribution for the analytical check. The Razorback radial fuel element temperature data at an axial node approximately halfway up the fuel was selected, and a polynomial fit was determined for T(r) for each material. The reference temperature T_{ref} was 20°C. The boundary conditions for the materials within the cladding was a pressure of 2 atm. on both the inner and outer radii ($p_i = p_o$ = 29.932 psia =

0.20265 MPa). The boundary conditions for the cladding was a pressure of 2 atm. on the inner radius ($p_i = p_o$ = 29.932 psia = 0.20265 MPa) and 20 psia on the outer radius (p_o = 20.0 psia = 0.13789 MPa).

Tables 12, 13, and 14 present the results comparing Razorback predictions to analytical solutions for the radial, azimuthal, and von Mises stresses, respectively, in the fuel element components. The maximum radial stress will be equal to the negative of the pressure on each surface (-0.1 to -0.2 MPa). For the thicker fuel pellets, the magnitude of the absolute error is on the same order, and the relative error can be quite high (see Table 12). For thinner components, such as the niobium cup and cladding, the relative error is considerably smaller. For all cases, the absolute error is on the order of 1 MPa, which is small compared to typical yield strengths of 100-500 MPa.

Table 12. Component radial stress predictions compared to analytical solution.

Component	Minimum Radial Stress (MPa)		Absolute Error (MPa)	Relative Error (%)
	Razorback	Analytical		
Inner Fuel Pellet	-16.60	-16.45	-0.15	0.88
Outer Fuel Pellet	-7.67	-7.42	-0.25	3.31
Niobium Cup	-0.210	-0.207	-0.003	1.40
Stainless Steel Cladding	-0.299	-0.291	-0.008	2.45
Component	**Maximum Radial Stress (MPa)**		**Absolute Error (MPa)**	**Relative Error (%)**
	Razorback	**Analytical**		
Inner Fuel Pellet	0.46	-0.20	0.66	327.58
Outer Fuel Pellet	0.58	-0.20	0.78	385.88
Niobium Cup	-0.196	-0.203	0.007	3.31
Stainless Steel Cladding	-0.092	-0.138	0.046	32.94

Table 13. Component azimuthal stress predictions compared to analytical solution.

Component	Minimum Azimuthal Stress (MPa)		Absolute Error (MPa)	Relative Error (%)
	Razorback	Analytical		
Inner Fuel Pellet	-49.90	-46.86	-3.04	6.50
Outer Fuel Pellet	-71.91	-70.77	-1.14	1.61
Niobium Cup	-1.021	-1.018	-0.003	0.35
Stainless Steel Cladding	-15.314	-15.298	-0.016	0.11
Component	**Maximum Azimuthal Stress (MPa)**		**Absolute Error (MPa)**	**Relative Error (%)**
	Razorback	**Analytical**		
Inner Fuel Pellet	54.31	54.55	-0.24	-0.44
Outer Fuel Pellet	71.91	72.29	-0.38	-0.53
Niobium Cup	0.604	0.602	0.002	0.39
Stainless Steel Cladding	19.454	19.440	0.014	0.07

Table 14. Component von Mises stress predictions compared to analytical solution.

Component	Minimum von Mises Stress (MPa)		Absolute Error (MPa)	Relative Error (%)
	Razorback	Analytical		
Inner Fuel Pellet	13.53	13.64	-0.11	-0.80
Outer Fuel Pellet	8.11	7.55	0.56	7.42
Niobium Cup	0.179	0.180	-0.001	-0.31
Stainless Steel Cladding	0.696	0.694	0.002	0.33
Component	Maximum von Mises Stress (MPa)		Absolute Error (MPa)	Relative Error (%)
	Razorback	Analytical		
Inner Fuel Pellet	54.08	54.65	-0.57	-1.05
Outer Fuel Pellet	71.62	72.39	-0.77	-1.06
Niobium Cup	0.934	0.933	0.001	0.12
Stainless Steel Cladding	19.500	19.510	-0.01	-0.05

Figures 16 through 19 show the comparison to the analytical solution and the absolute error of the predicted radial and azimuthal stress (recall $\sigma_z = 0$) for the inner BeO-UO_2 fuel pellet. Figures 20 and 21 show the comparison to the analytical solution and the relative error of the predicted von Mises stress within the inner BeO-UO_2 fuel pellet. The relative error of the von Mises stress is within ±7%.

Figures 22 through 25 show the comparison to the analytical solution and the absolute error of the predicted radial and azimuthal stress (recall $\sigma_z = 0$) for the outer BeO-UO_2 fuel pellet. Figures 26 and 27 show the comparison to the analytical solution and the relative error of the predicted von Mises stress within the outer BeO-UO_2 fuel pellet. The relative error of the von Mises stress is within ±8%.

Figures 28 through 31 show the comparison to the analytical solution and the absolute error of the predicted radial and azimuthal stress (recall $\sigma_z = 0$) for the niobium cup. Figures 32 and 33 show the comparison to the analytical solution and the relative error of the predicted von Mises stress within the niobium cup. The relative error of the von Mises stress is within ±1%.

Figures 34 through 37 show the comparison to the analytical solution and the absolute error of the predicted radial and azimuthal stress (recall $\sigma_z = 0$) for the stainless steel cladding. Figures 38 and 39 show the comparison to the analytical solution and the relative error of the predicted von Mises stress within the stainless steel cladding. The relative error of the von Mises stress is within ±0.4%.

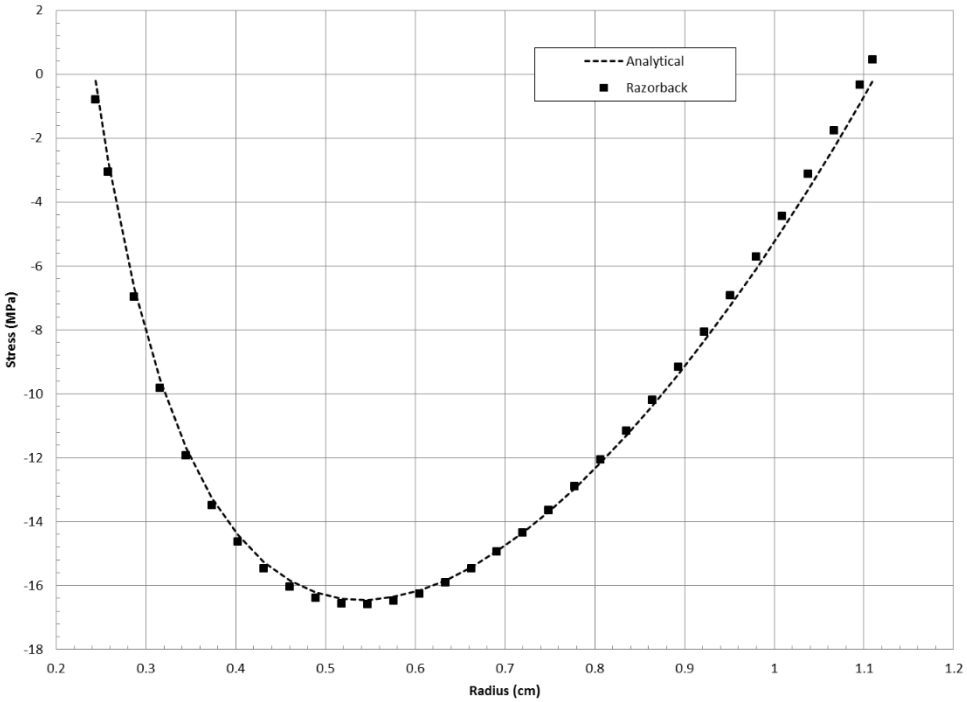

Figure 16. Inner fuel pellet radial stress compared to analytical solution.

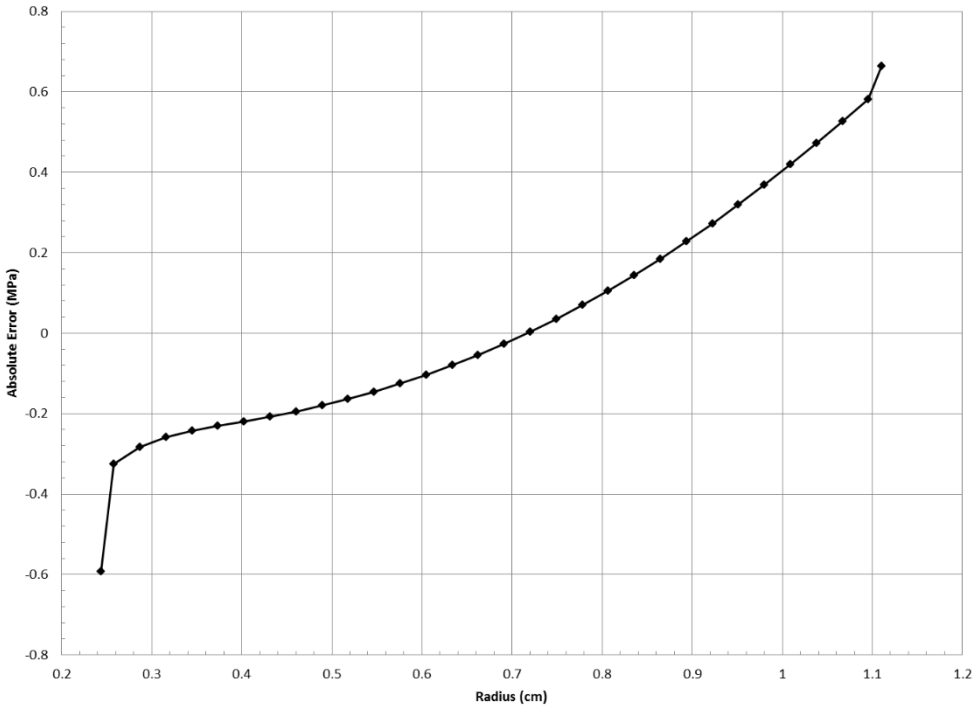

Figure 17. Absolute error for verification of inner fuel pellet radial stress.

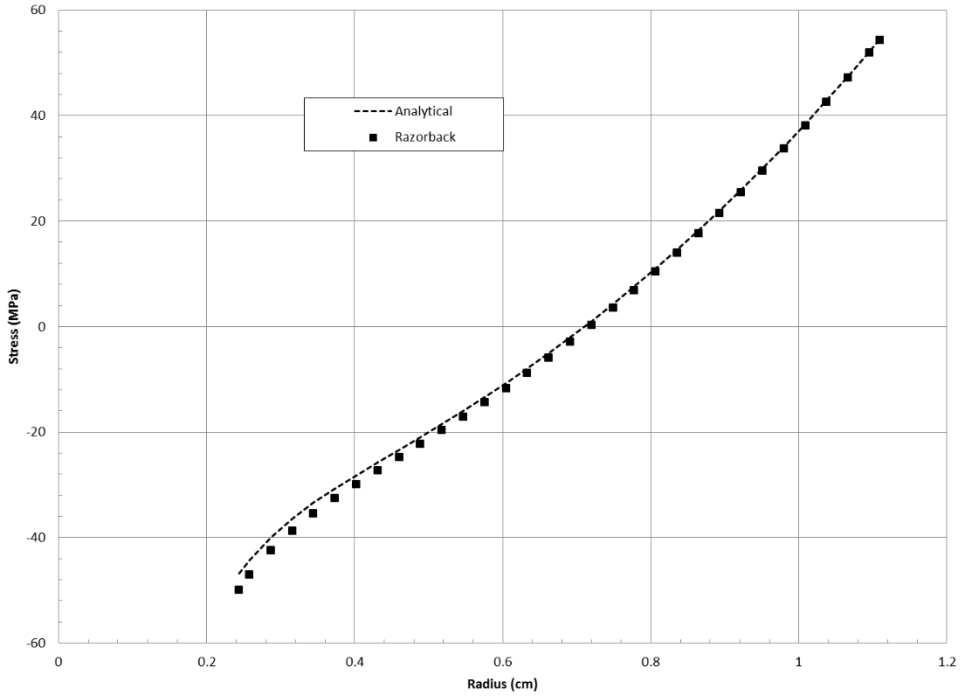

Figure 18. Inner fuel pellet azimuthal stress compared to analytical solution.

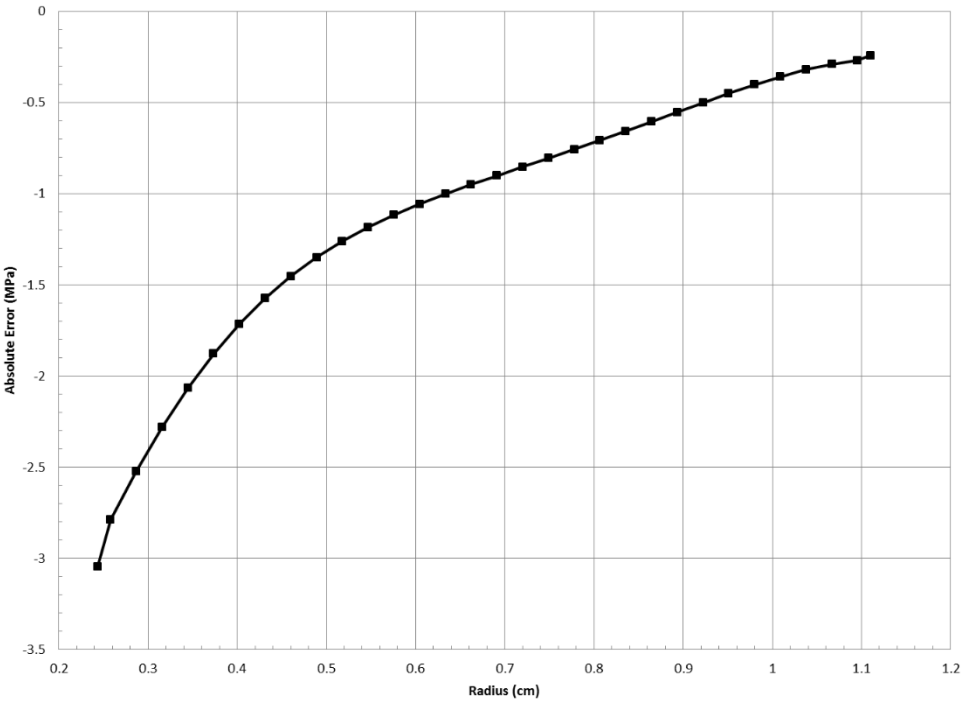

Figure 19. Absolute error for verification of inner fuel pellet azimuthal stress.

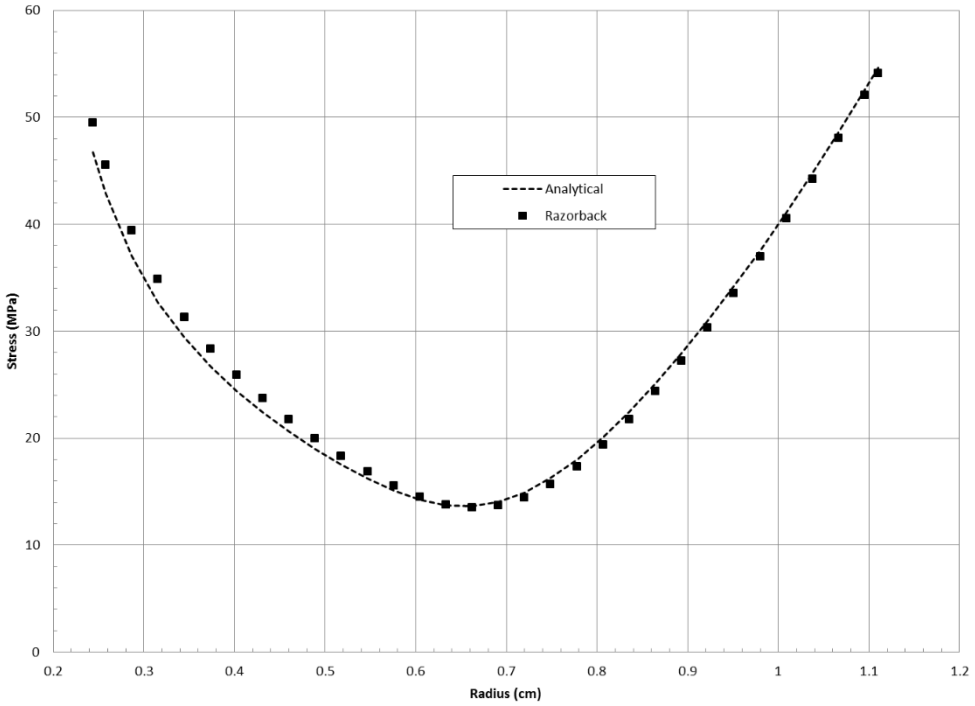

Figure 20. Inner fuel pellet von Mises stress compared to analytical solution.

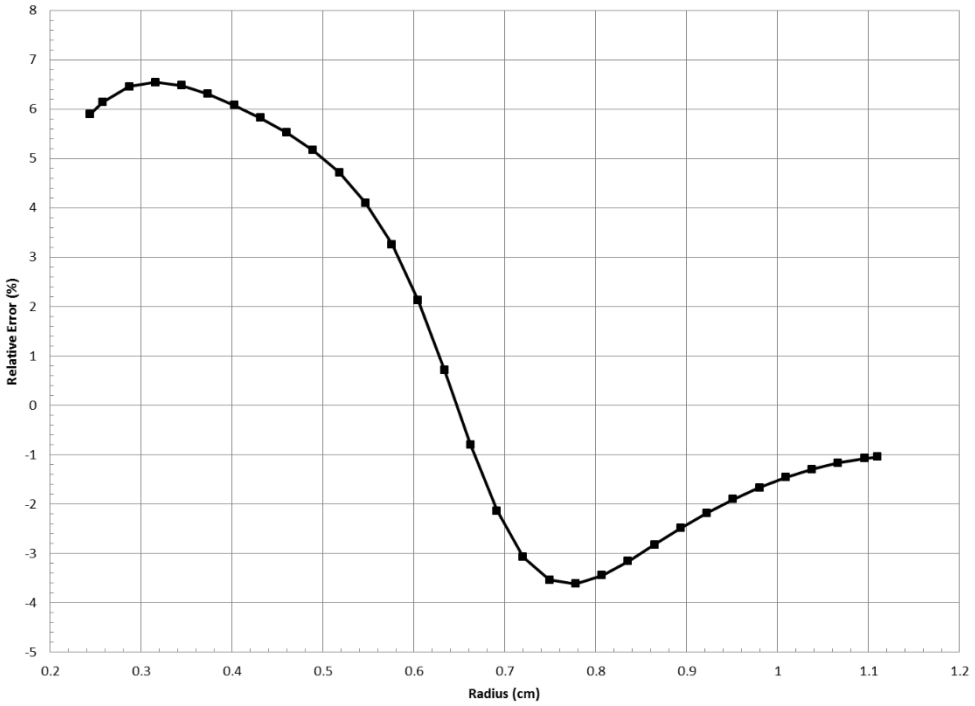

Figure 21. Relative error for verification of inner fuel pellet von Mises stress.

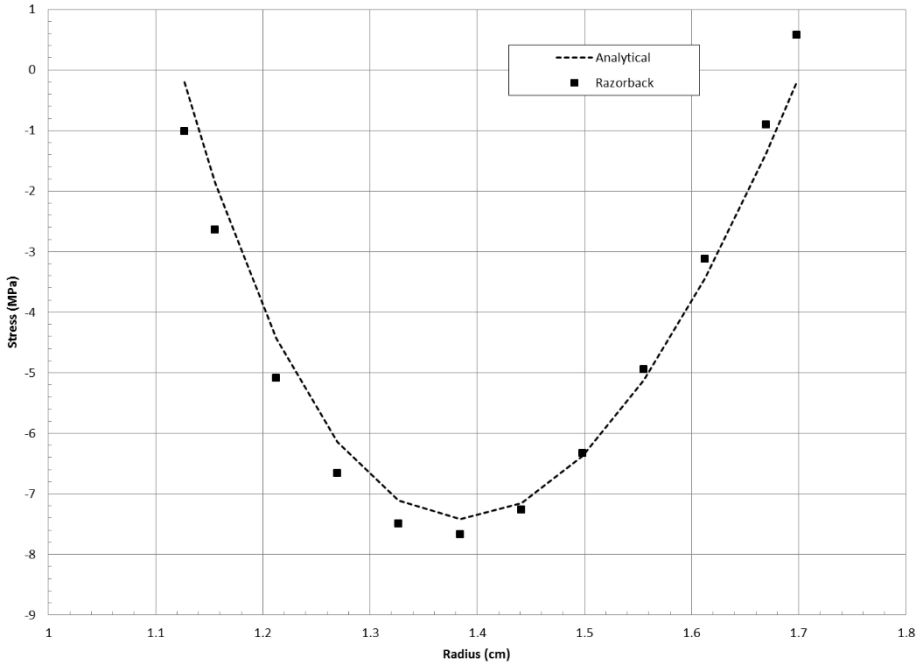

Figure 22. Outer fuel pellet radial stress compared to analytical solution.

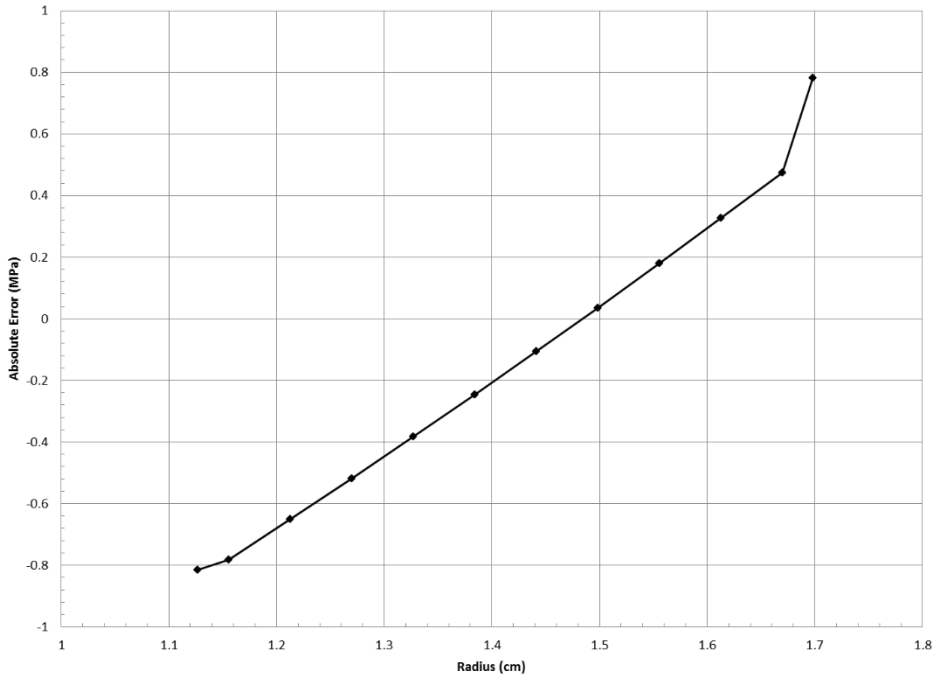

Figure 23. Absolute error for verification of outer fuel pellet radial stress.

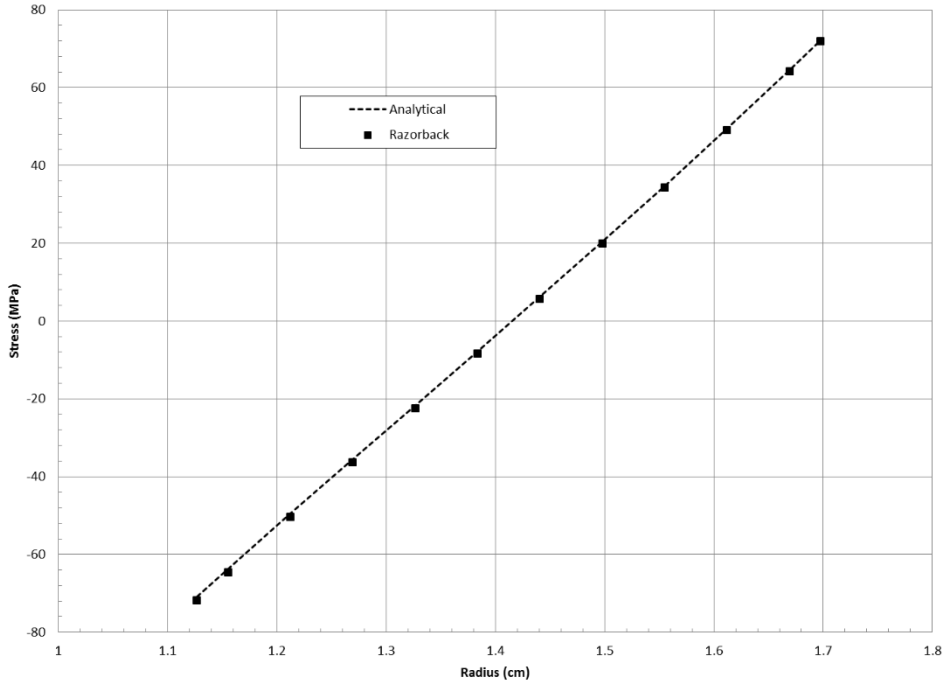

Figure 24. Outer fuel pellet azimuthal stress compared to analytical solution.

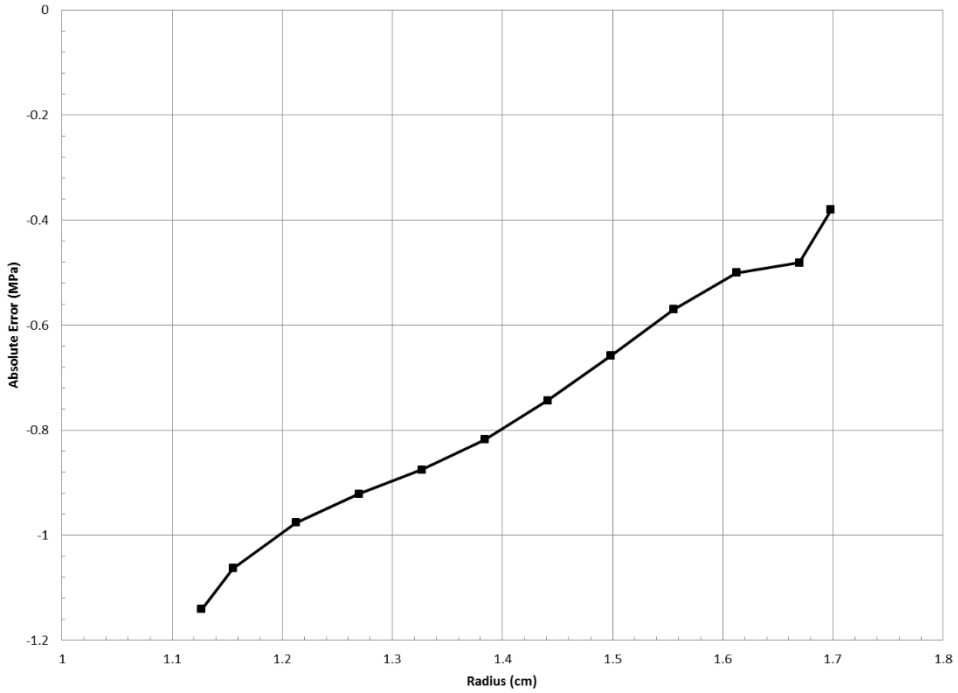

Figure 25. Absolute error for verification of outer fuel pellet azimuthal stress.

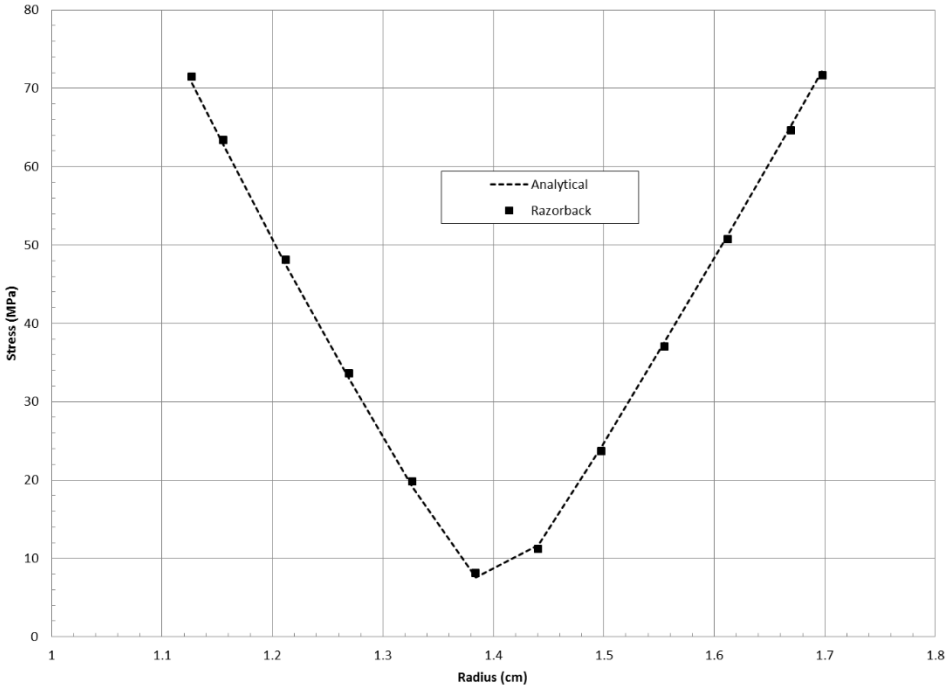

Figure 26. Outer fuel pellet von Mises stress compared to analytical solution.

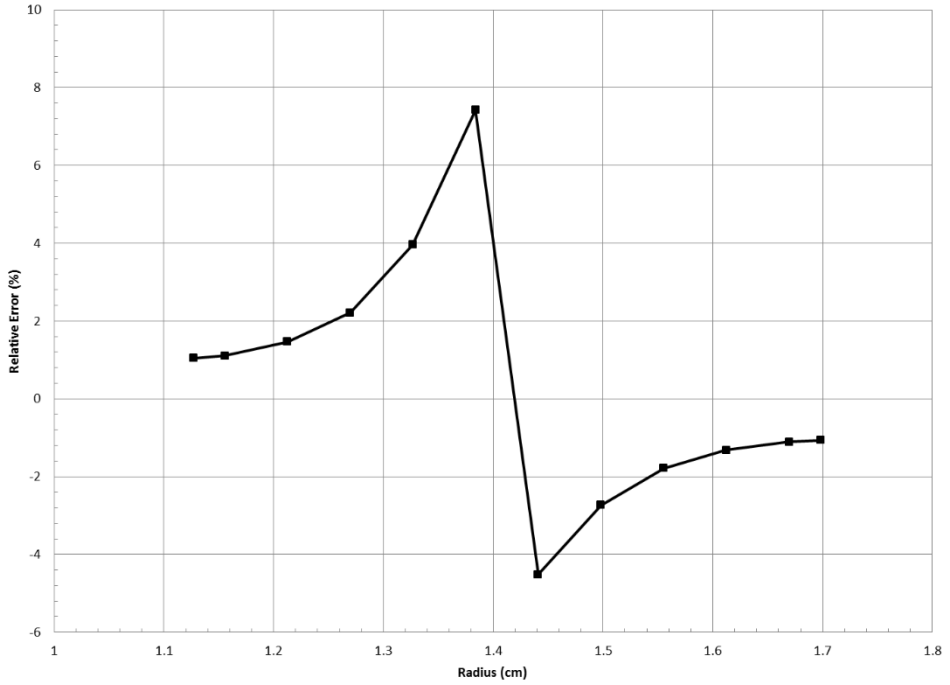

Figure 27. Relative error for verification of outer fuel pellet von Mises stress.

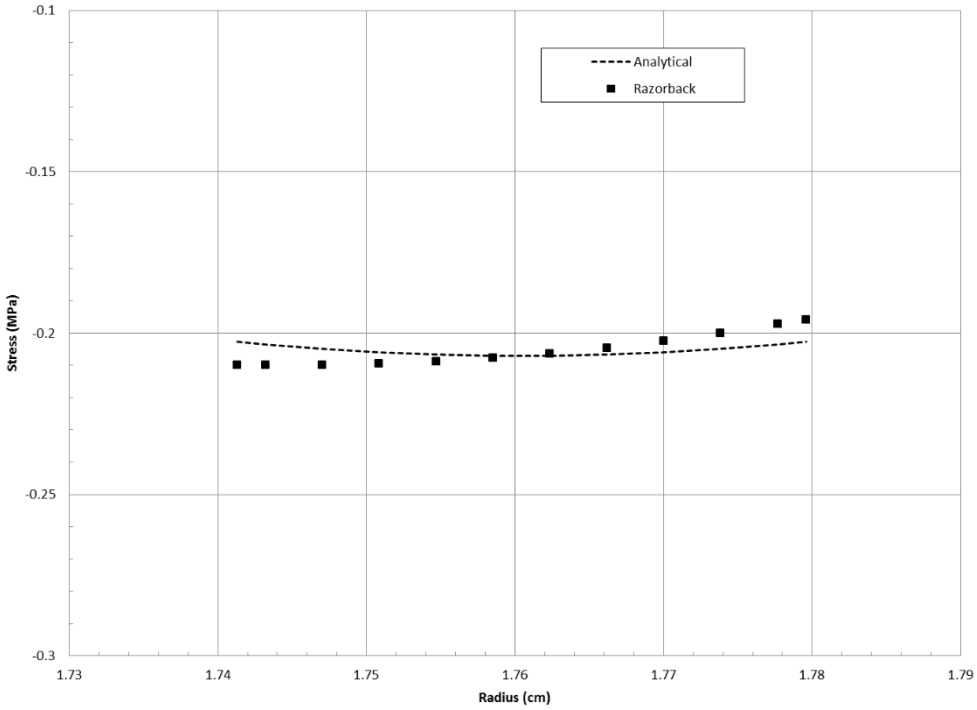

Figure 28. Niobium cup radial stress compared to analytical solution.

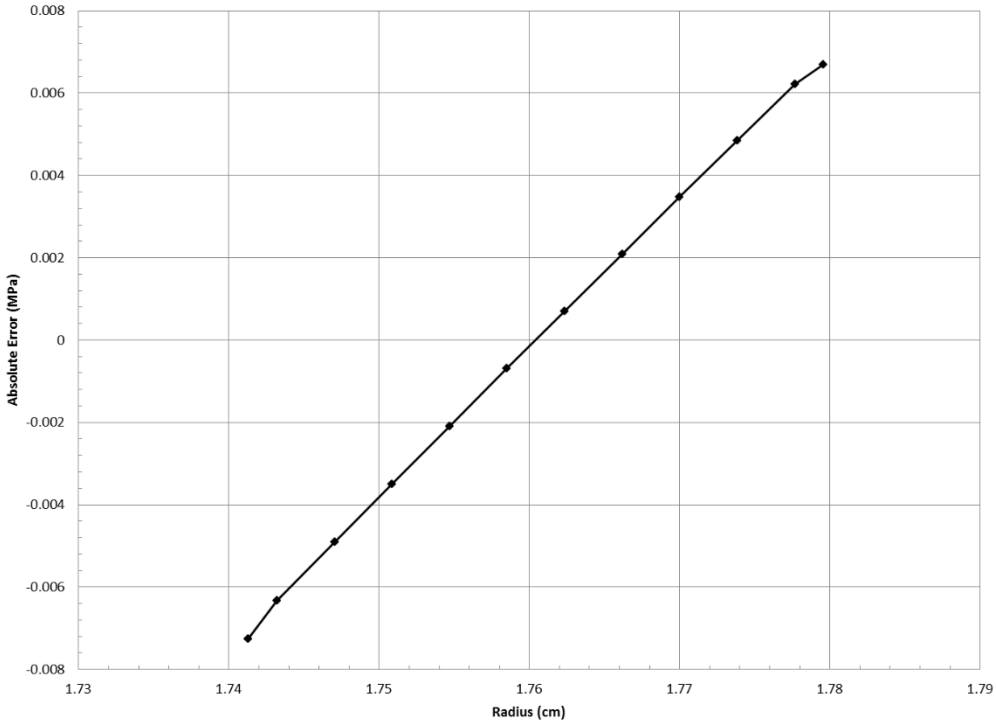

Figure 29. Absolute error for verification of niobium cup radial stress.

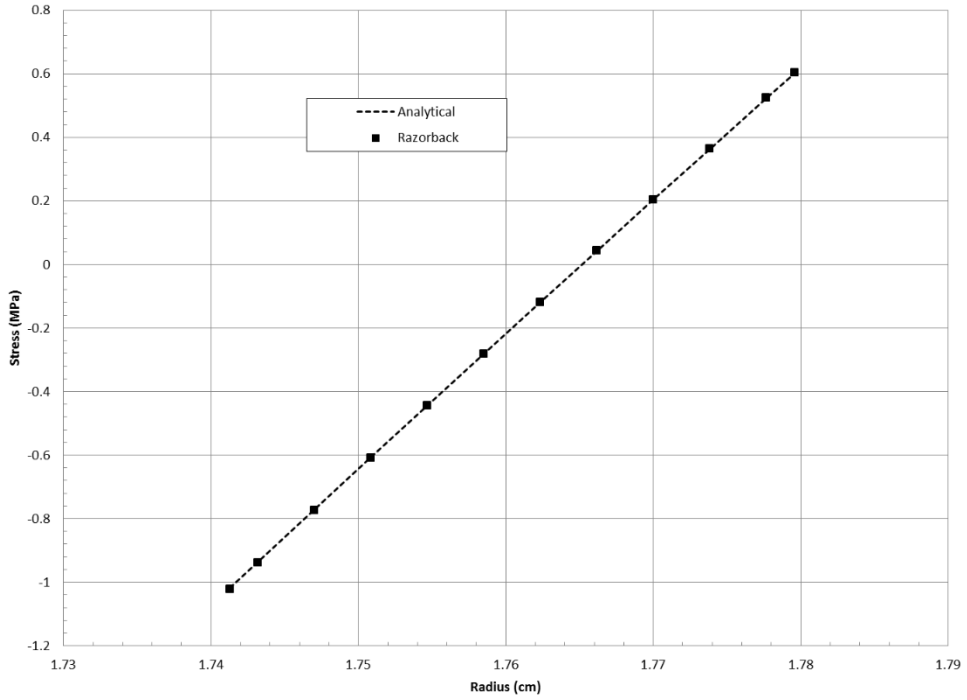

Figure 30. Niobium cup azimuthal stress compared to analytical solution.

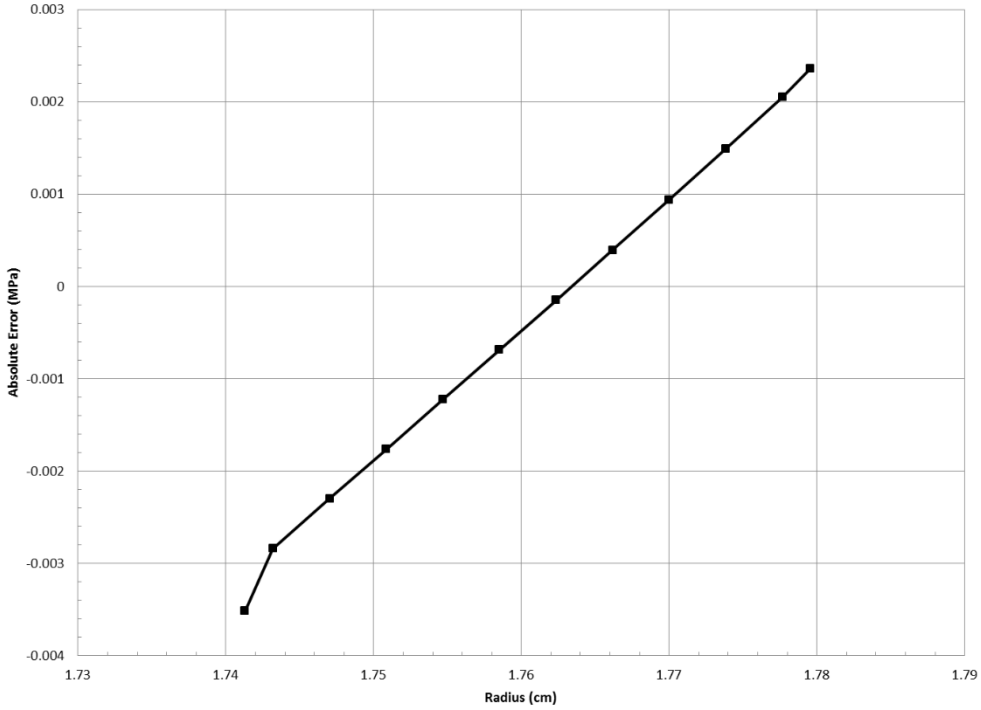

Figure 31. Absolute error for verification of niobium cup azimuthal stress.

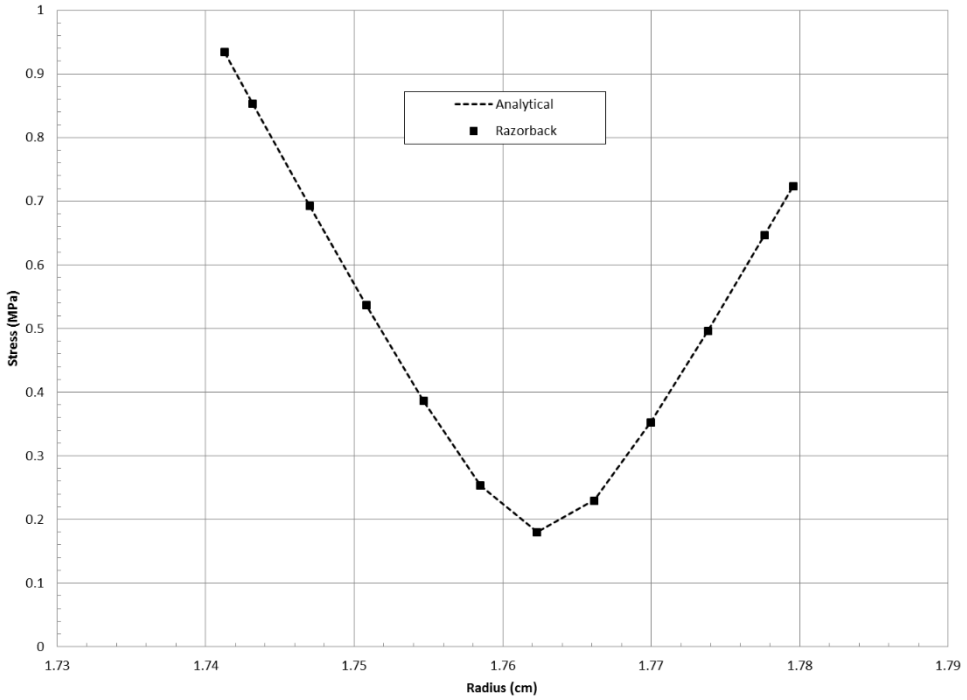

Figure 32. Niobium cup von Mises stress compared to analytical solution.

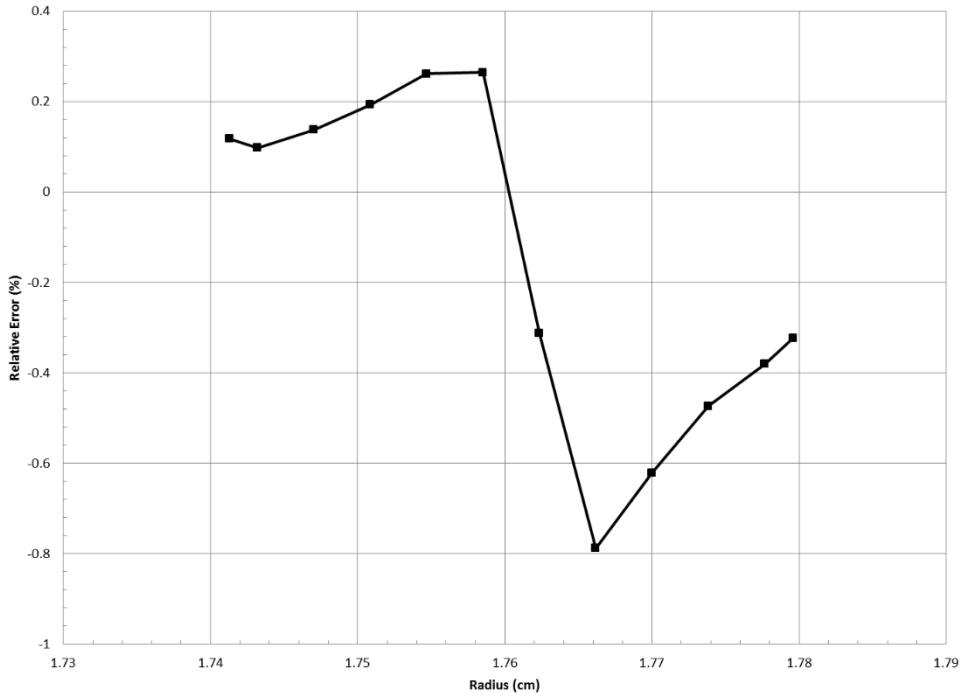

Figure 33. Relative error for verification of niobium cup von Mises stress.

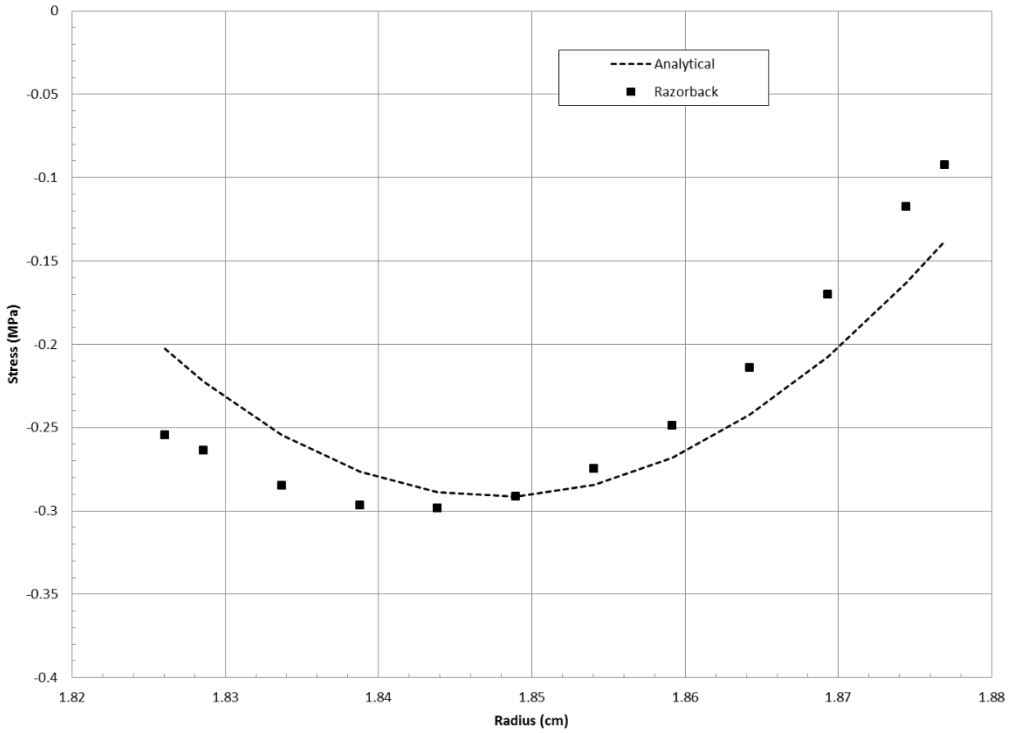

Figure 34. Stainless steel cladding radial stress compared to analytical solution.

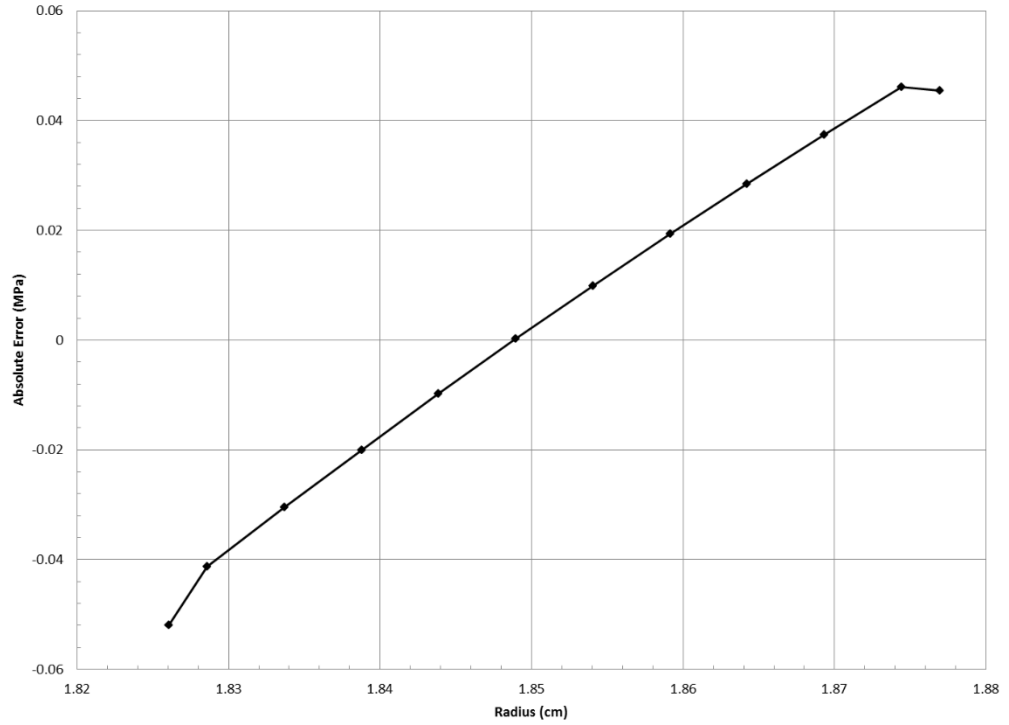

Figure 35. Absolute error for verification of stainless steel cladding radial stress.

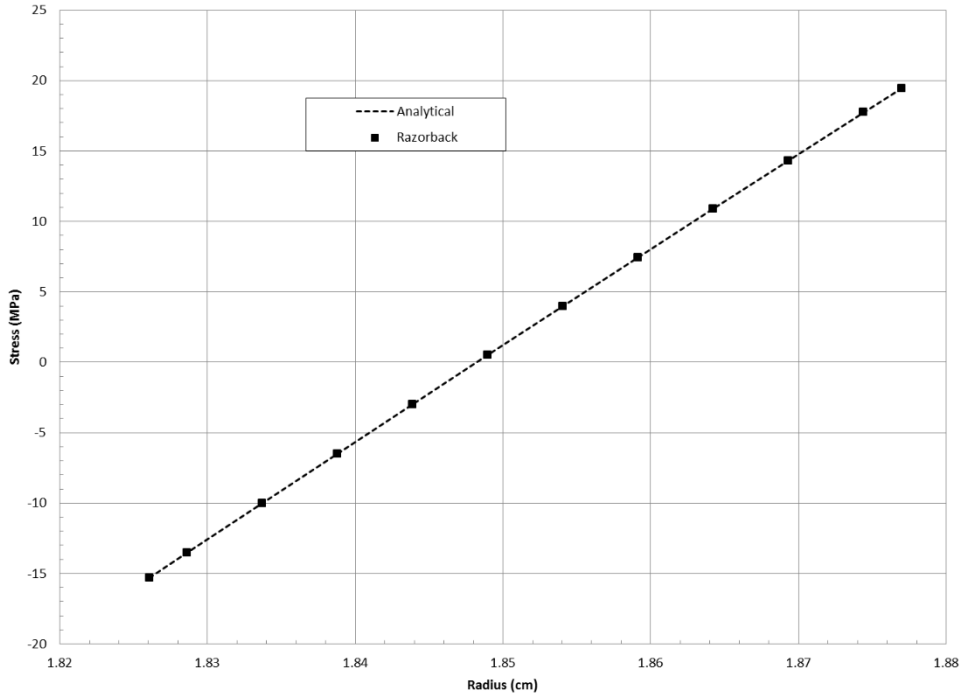

Figure 36. Stainless steel cladding azimuthal stress compared to analytical solution.

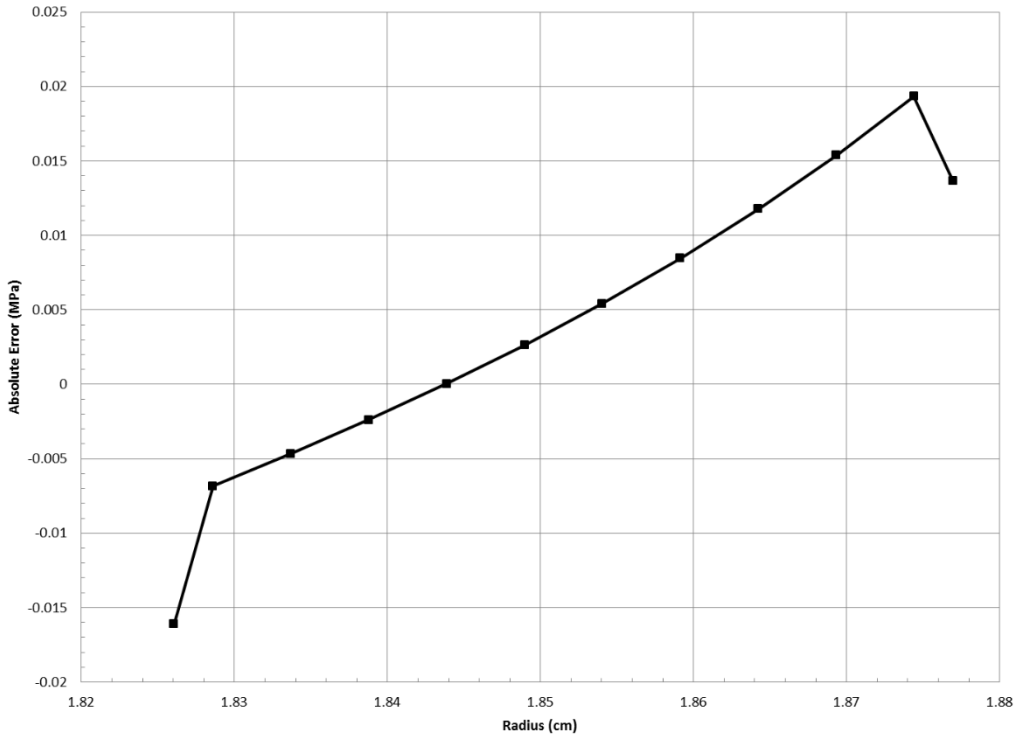

Figure 37. Absolute error for verification of stainless steel cladding azimuthal stress.

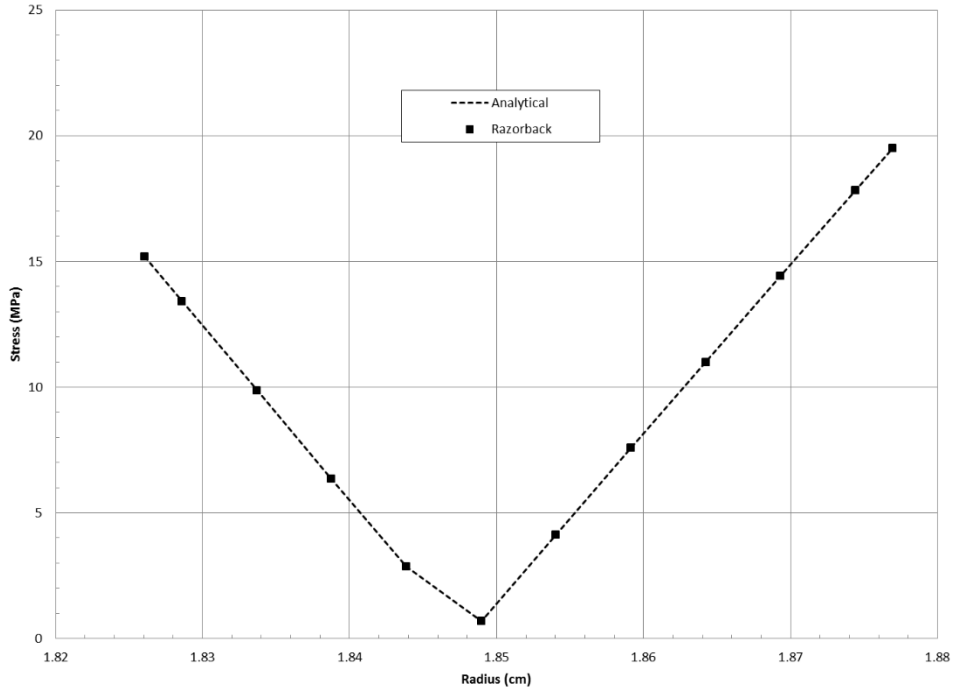

Figure 38. Stainless steel von Mises stress compared to analytical solution.

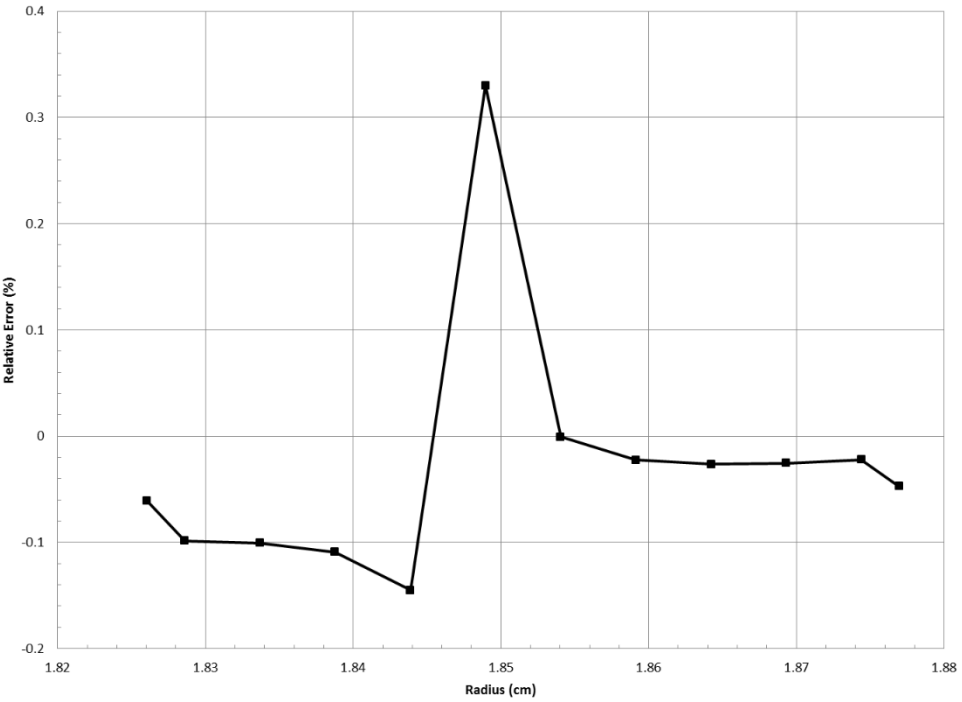

Figure 39. Relative error for verification of stainless steel cladding von Mises stress.

[This page intentionally left blank.]

4. COMPARISON TO ACRR PULSE OPERATIONS

Razorback was run to simulate the pulse operations 9720, 9719, 9718, and 9716 which were annual calibration pulses performed in January 2011, and pulse operations 11694, 11703, 11704, and 11705 which were annual calibration pulses performed in January 2016. For both years, these were, respectively, nominal $3.00, $2.50, $2.00, and $1.50 pulse operations. The data from these 2011 and 2016 operations were selected because the necessary Pulse Diagnostic System (PDS) data files (i.e., the PDS report and the Console Log report) were available on the ACRR Operations department network drive. Excerpts from the PDS reports and the Console Log reports are included in Appendix B.

The PDS used to measure power and evaluate pulse operations is not a formally calibrated system, nor are its components calibrated (e.g., analog-to-digital converters). The sensitivities (e.g., nA/MW) of the self-powered neutron detectors (SPND) have been calibrated to ACRR power operation in the past (Ref. 10), but that practice no longer continues. Instead, the sensitivities are adjusted regularly so that reactor yield via the SPNDs better matches the yield determined by exposure of dosimetry in the ACRR's central cavity. There is a report which documents reasonable agreement of the reactor yield determined by the PDS with dosimetry measurements (Ref. 13). While the PDS data is believed to reasonably characterize the performance of the ACRR, work is clearly needed to provide a documented calibration basis for the results.

The input TR reactivity worth to be used in the Razorback simulations was obtained information on the Console Logs in Appendix B. Each Console Log reports a control rod bank position for a delayed critical condition established at two TR bank positions: (1) TR bank fully withdrawn "TR UP DC", and (2) TR bank at the position from which the pulse will be executed "Setup DC". Next to these positions are the control rod bank reactivity worth at that control rod bank position. The difference in the control rod bank reactivity worth between the TR UP DC and Setup DC is the reactivity worth of the pulse operation. However, the control rod bank reactivity worth values recorded on the Console Log were not used. Instead, the control rod bank reactivity was determined using the control rod worth vs. bank position curve developed in Ref. 20. Table 15 below shows the Razorback input worth as determined using the Console Log and Ref. 20.

Table 15. Input reactivity determination for pulse simulations.

Operation #	**9720**	**9719**	**9718**	**9716**	**11705**	**11704**	**11703**	**11694**
Nominal Pulse Worth ($)	1.50	2.00	2.50	3.00	1.50	2.00	2.50	3.00
Setup DC Position (units)	1973	2112	2257	2400	2004	2156	2301	2428
Setup DC Worth ($)	7.692	7.24	6.758	6.276	7.593	7.095	6.61	6.181
TR UP DC Position (units)	1491	1485	1484	1488	1528	1536	1539	1499
TR UP DC Worth ($)	9.135	9.152	9.154	9.143	9.033	9.011	9.002	9.113
Razorback Input Worth ($)	1.443	1.912	2.396	2.867	1.440	1.916	2.392	2.932

In the simulations, a TR bank initial position was selected to achieve this desired pulse input reactivity worth from Table 15, and Razorback was run. If the desired total reactivity worth was not achieved, then the initial TR bank position was changed, and Razorback was run again.

Once the desired reactivity worth was achieved, then the Razorback simulation was "officially" run.

Actual ACRR pulse operations do not pneumatically eject the transient rods at t=0. Rather, the ejection of the transient rods is set to occur at a prescribed time delay (typically on the order of 130-170 ms after time zero). After this prescribed delay time, another time delay occurs associated with the time required for the opening of the valves which provide the pressurized nitrogen gas which drives the transient rods upward. The timing of the transient rod ejection in the simulations (i.e., the initial pulse start time and nitrogen valve delay time) were set in the Razorback input so that the resulting times of the pulse peaks would match the ACRR data. This allows for a time-matched comparison of the power traces when plotted on the same time scale.

The ACRR pulses were performed in Pulse Reduced Tail submode. In this submode, after a preset Rod Hold Up (RHU) time, a signal is sent through the ACRR scram system to drop the control, safety, and transient rod banks. As such, the Pulse Reduced Tail submode was selected in the Razorback simulations. In its simulation, Razorback accounts for a time delay in the electrical circuitry of the RHU/scram system between the initial RHU/scram signal, and the initiation of dropping rods. Values from 100-125 ms were used for the 2011 pulse simulations. Values from 150-350 ms were used for the 2016 pulses. No speculation will be made as to why two different values were needed. Razorback also accounts for the time required for the rods to fall from a full up position. The simulations for the 2011 pulses here utilized values of 0.5 s, 0.5 s, and 1.0 s for the control rods, safety rods, and transient rods, respectively. The simulations for the 2016 pulses utilized the same values for two of the pulses, while values of 0.75 s, 0.75 s, and 1.25 s were necessary for the other two pulses. All of these values were selected (via trial-and-error) based upon producing a reasonable visual fit to the power tail decay.

The initial power level of the reactor before the pulse was executed was provided by the ACRR Operations group[4] for each of the 2016 calibration pulses as 0.00009% (Pulse 11694), 0.00042% (Pulse 11703), 0.000275% (Pulse 11704), and 0.000225% (Pulse 11705). This data was not available for the 2011 calibration pulses, so an initial power of 0.0001% was assumed for all four 2011 pulses.

The ACRR pool water temperature before the pulse was executed was provided by the ACRR Operations group[5] for each of the 2016 calibration pulses as 16°C (Pulse 11694), 20°C (Pulse 11703), 21°C (Pulse 11704), and 18°C (Pulse 11705). This data was not available for the 2011 calibration pulses, so a pool water temperature of 20°C was assumed for all four 2011 pulses.

Figures 40 through 55[6] show the results of the Razorback simulations superimposed on the ACRR PDS power measurement channel results. The agreement between the simulation and the PDS data is quite good. Sections 4.1 through 4.5 provide more focused comparison and discussion of various pulse parameters associated with the data presented in Figs. 40 through 55.

[4] Private communication, e-mail from R. D. Clovis to D. G. Talley, Subject: ACRR 2016 cal pulse data," 7/5/2016.
[5] Ibid.
[6] Note that on Figures 40 through 55, even noisy power traces from ACRR PDS were included unless, in the author's opinion, the trace needed to be removed from the plot for clarity.

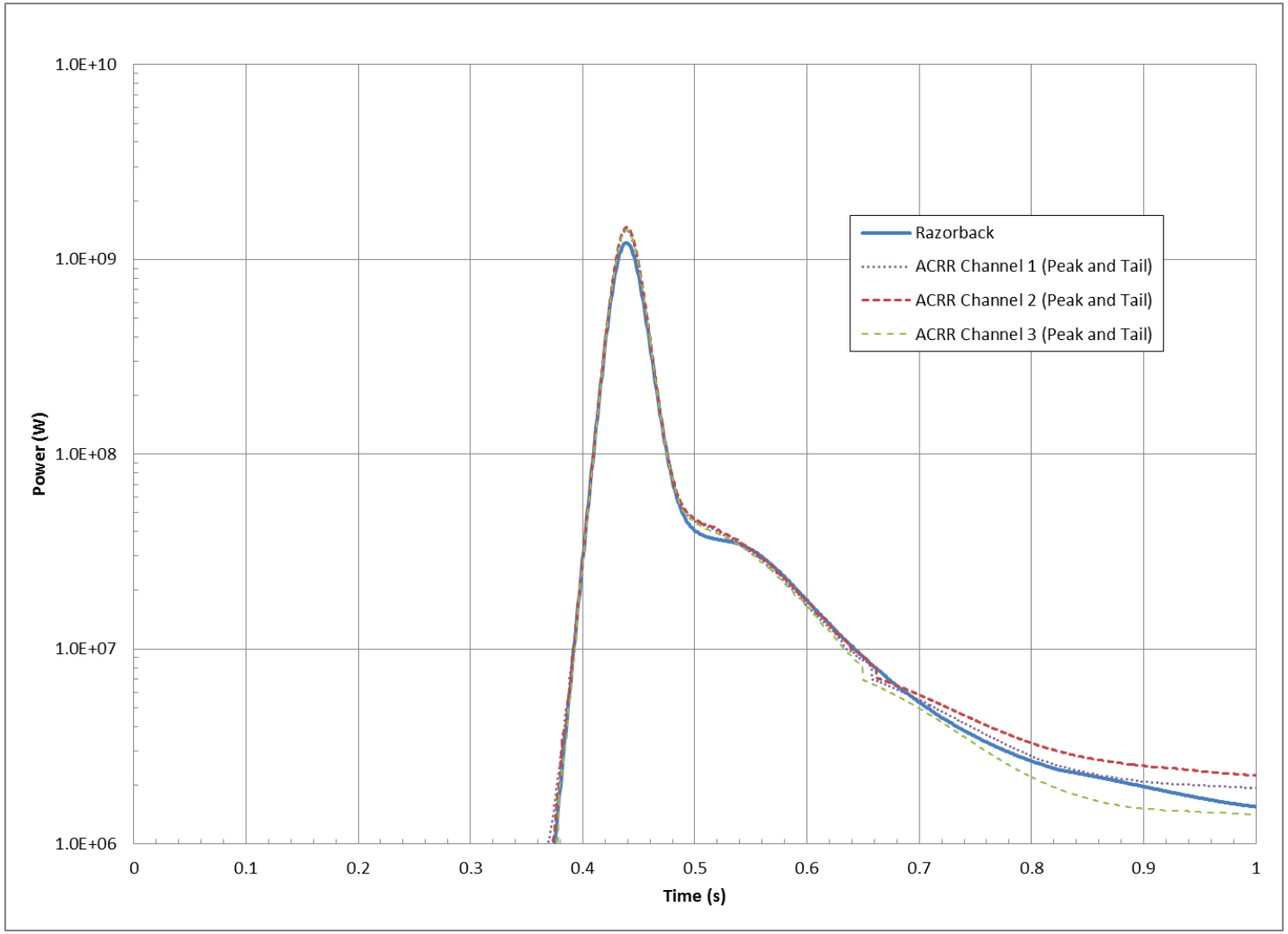

Figure 40. Razorback Simulation of a $1.50 Pulse Operation (#9720).

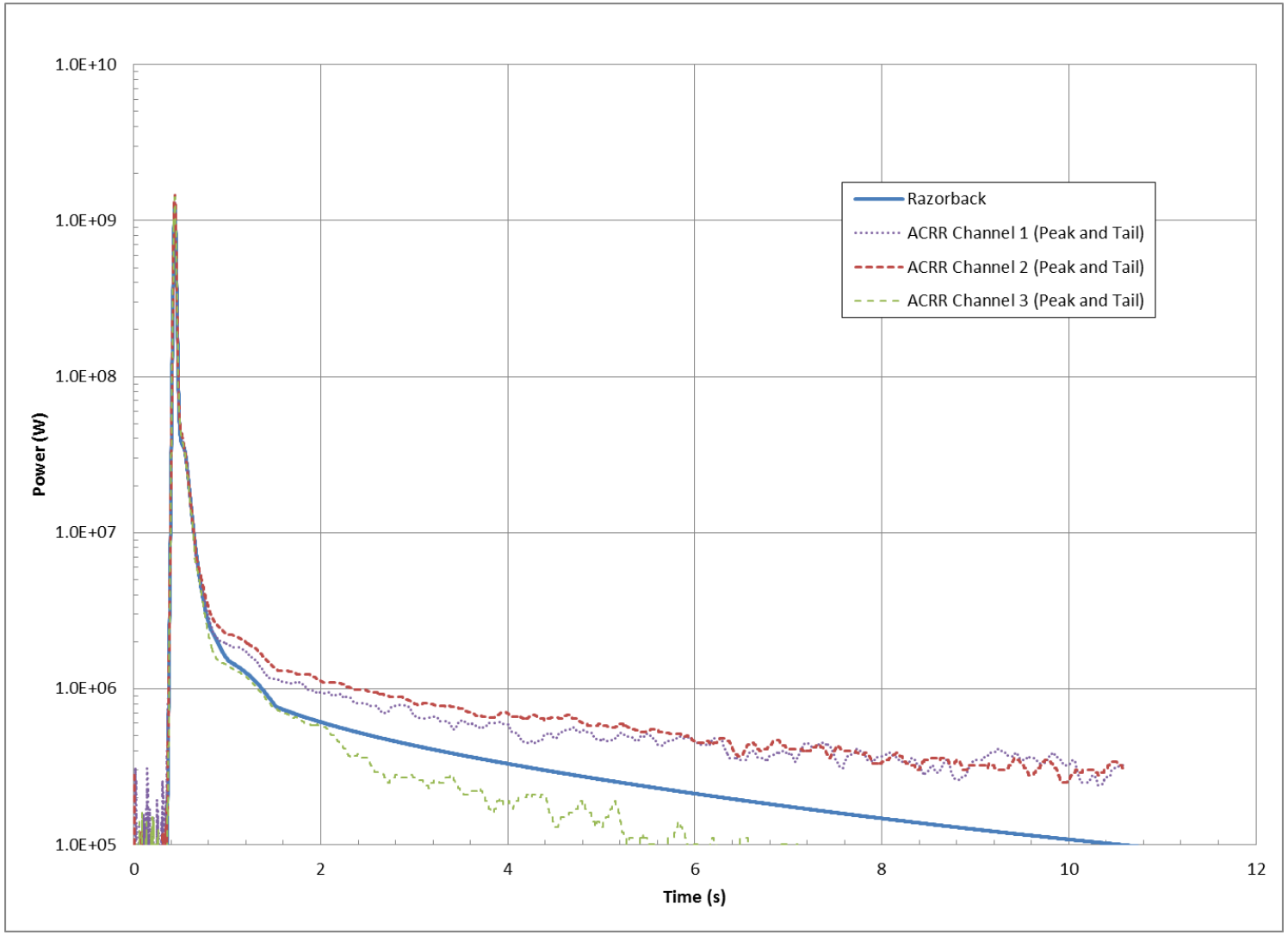

Figure 41. Razorback Simulation of a $1.50 Pulse Operation (#9720) Showing the Pulse Tail.

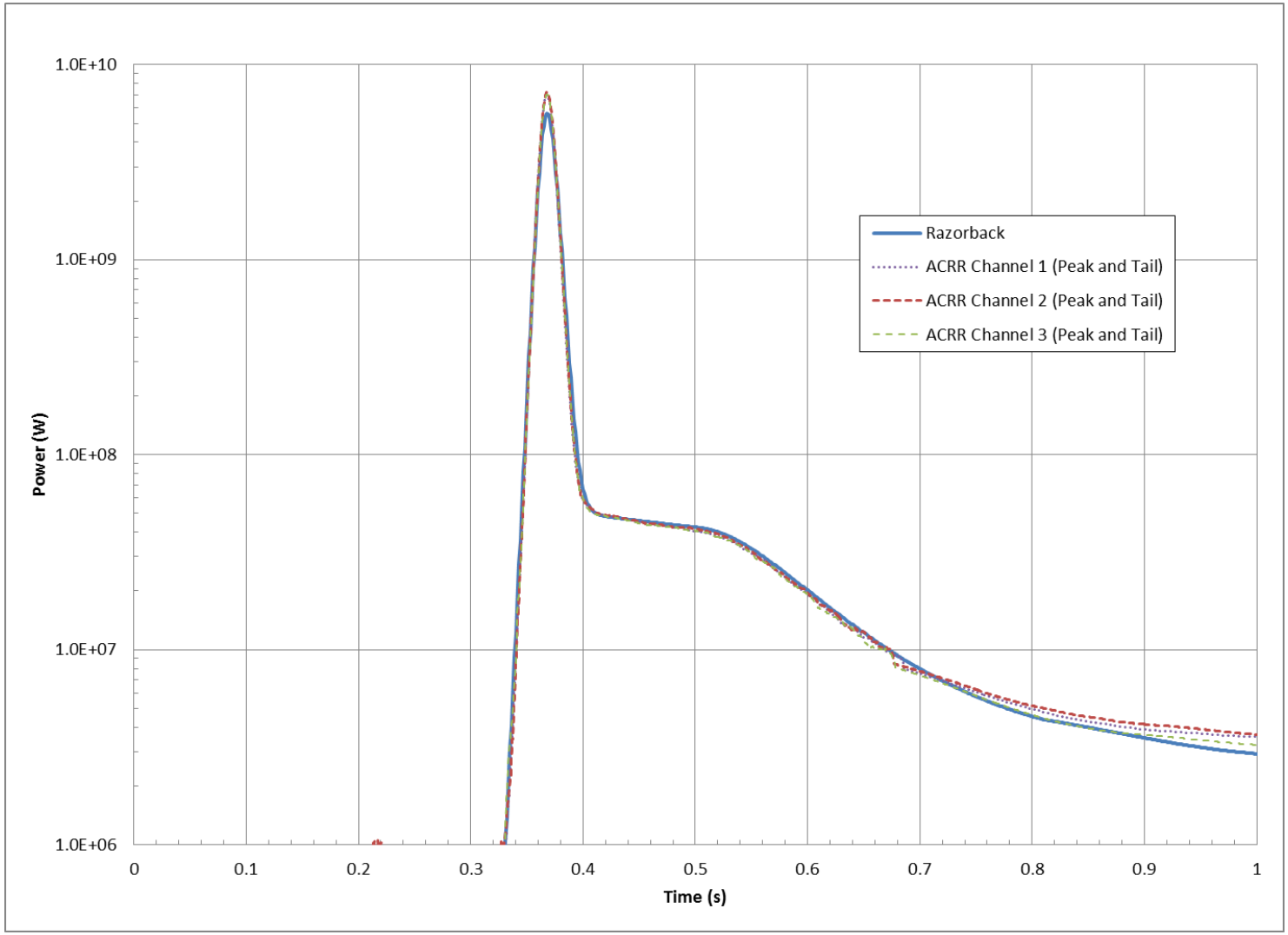

Figure 42. Razorback Simulation of a $2.00 Pulse Operation (#9719).

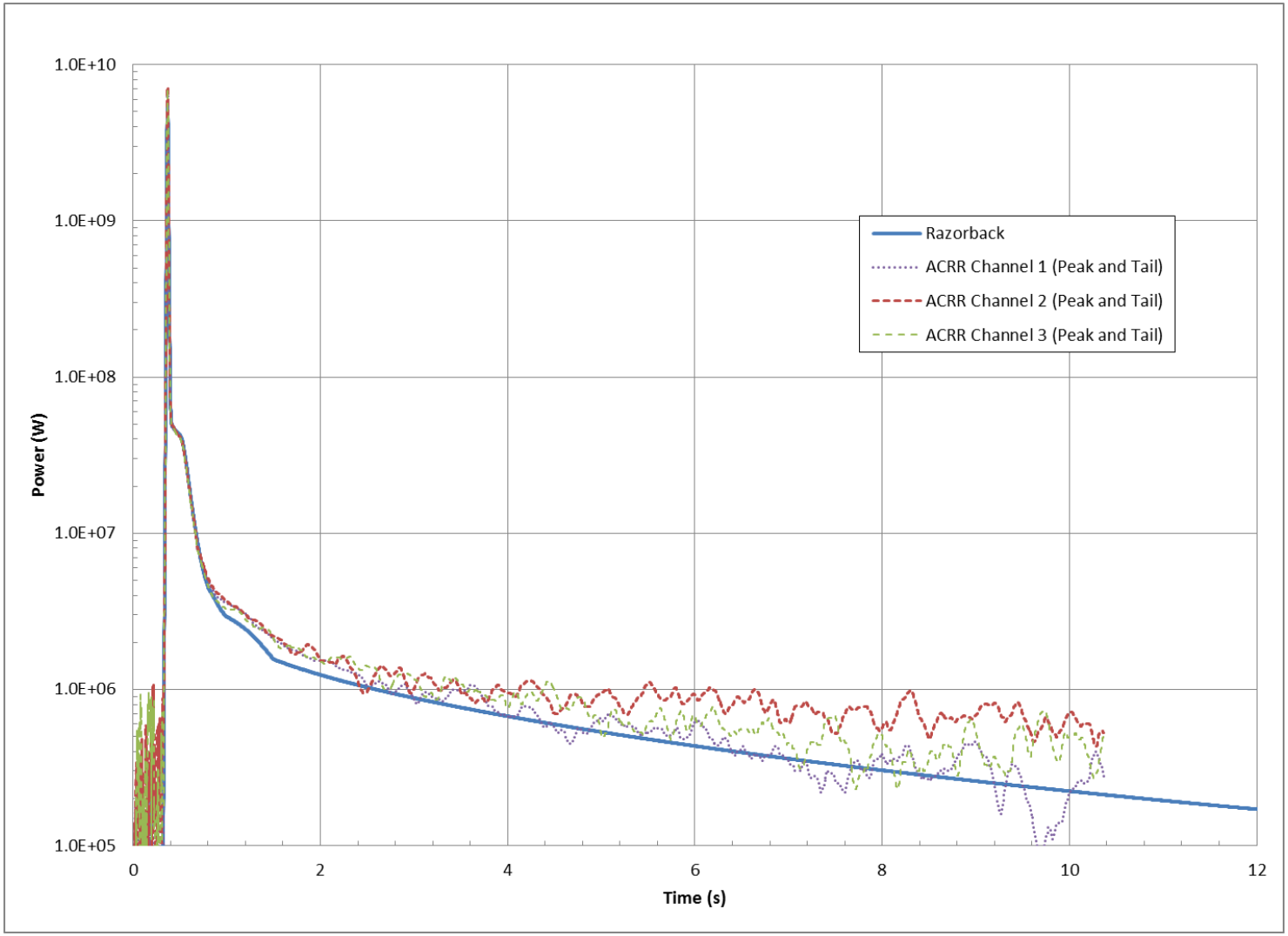

Figure 43. Razorback Simulation of a $2.00 Pulse Operation (#9719) Showing the Pulse Tail.

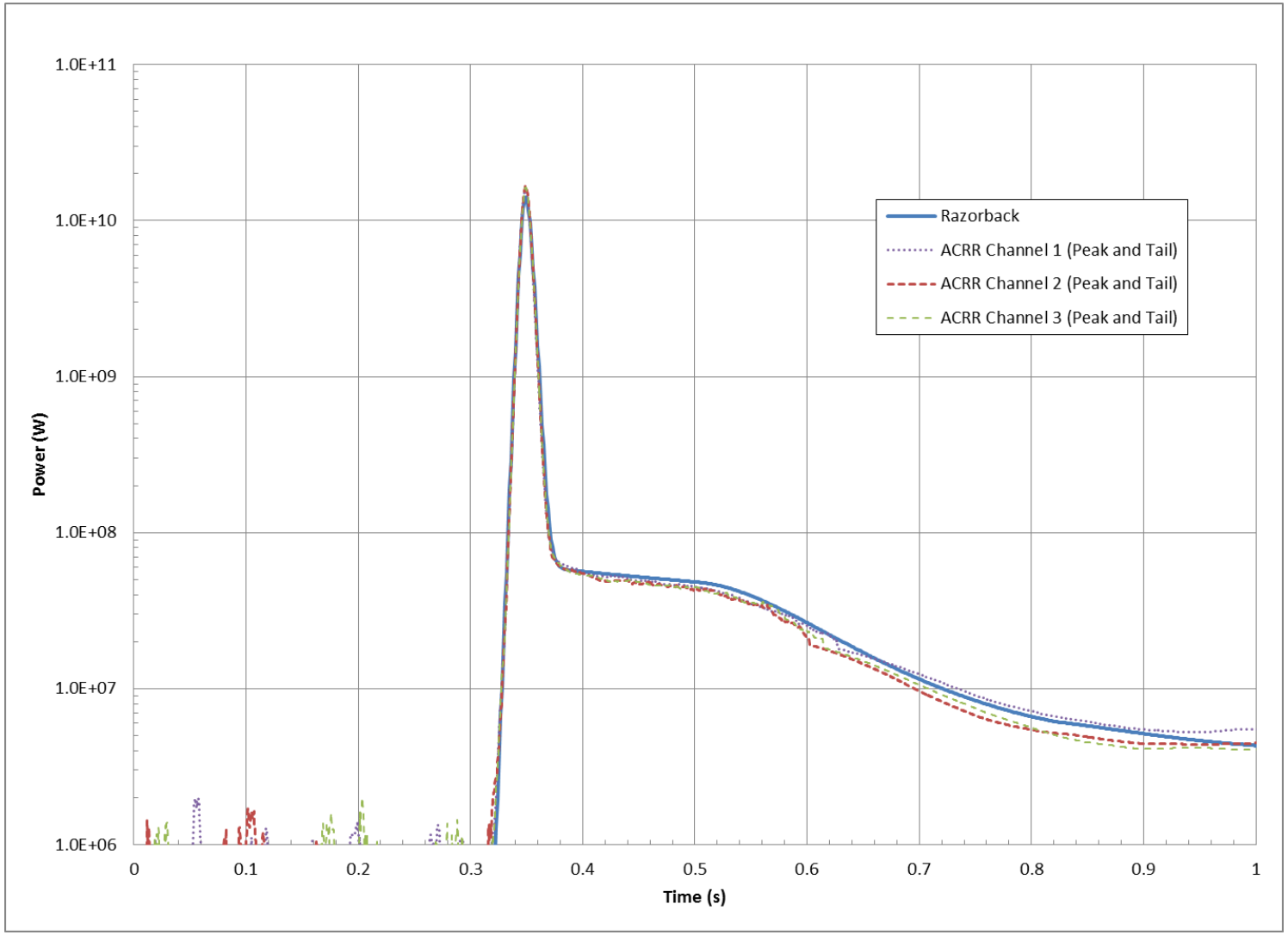

Figure 44. Razorback Simulation of a $2.50 Pulse Operation (#9718).

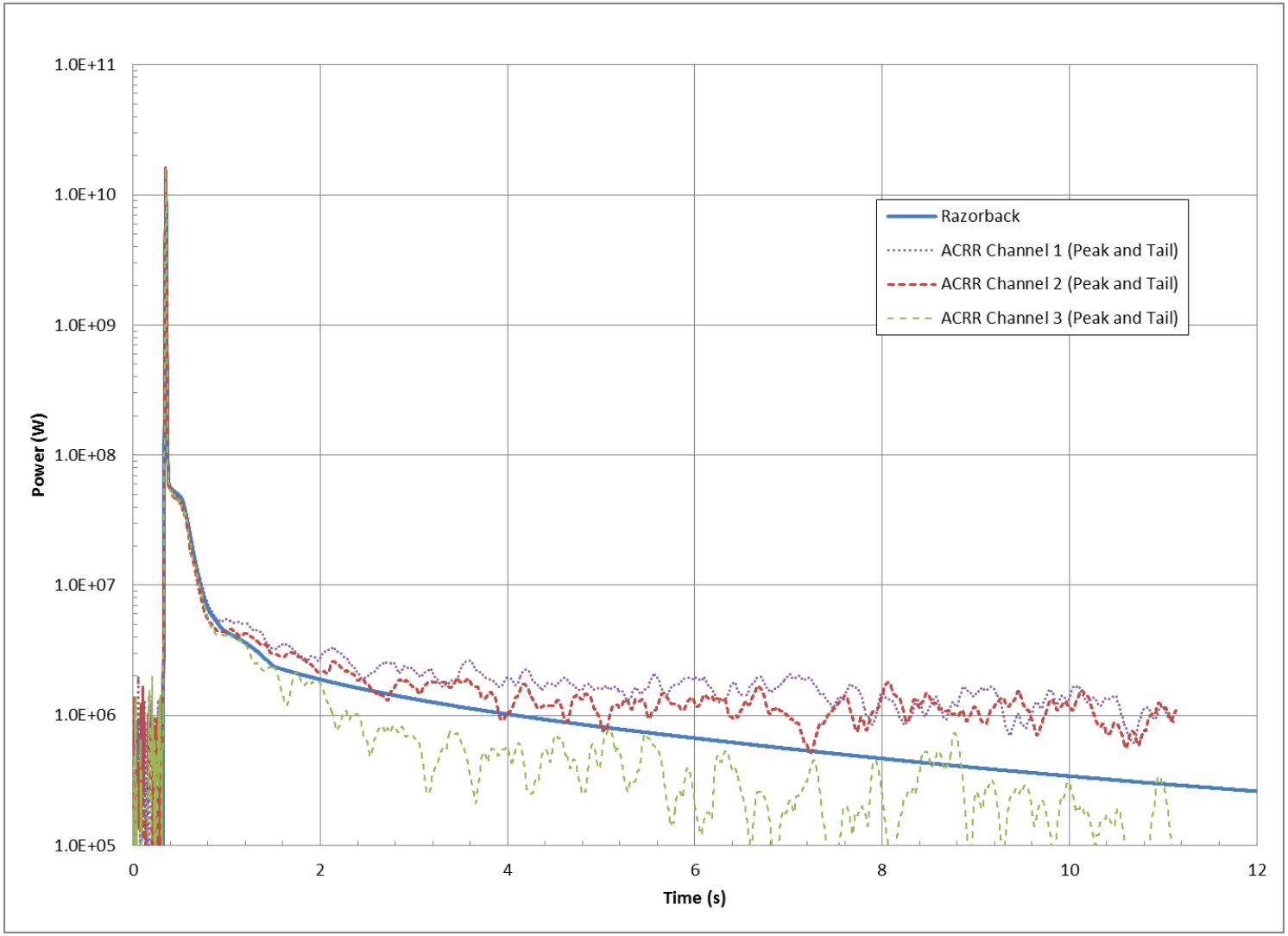

Figure 45. Razorback Simulation of a $2.50 Pulse Operation (#9718) Showing the Pulse Tail.

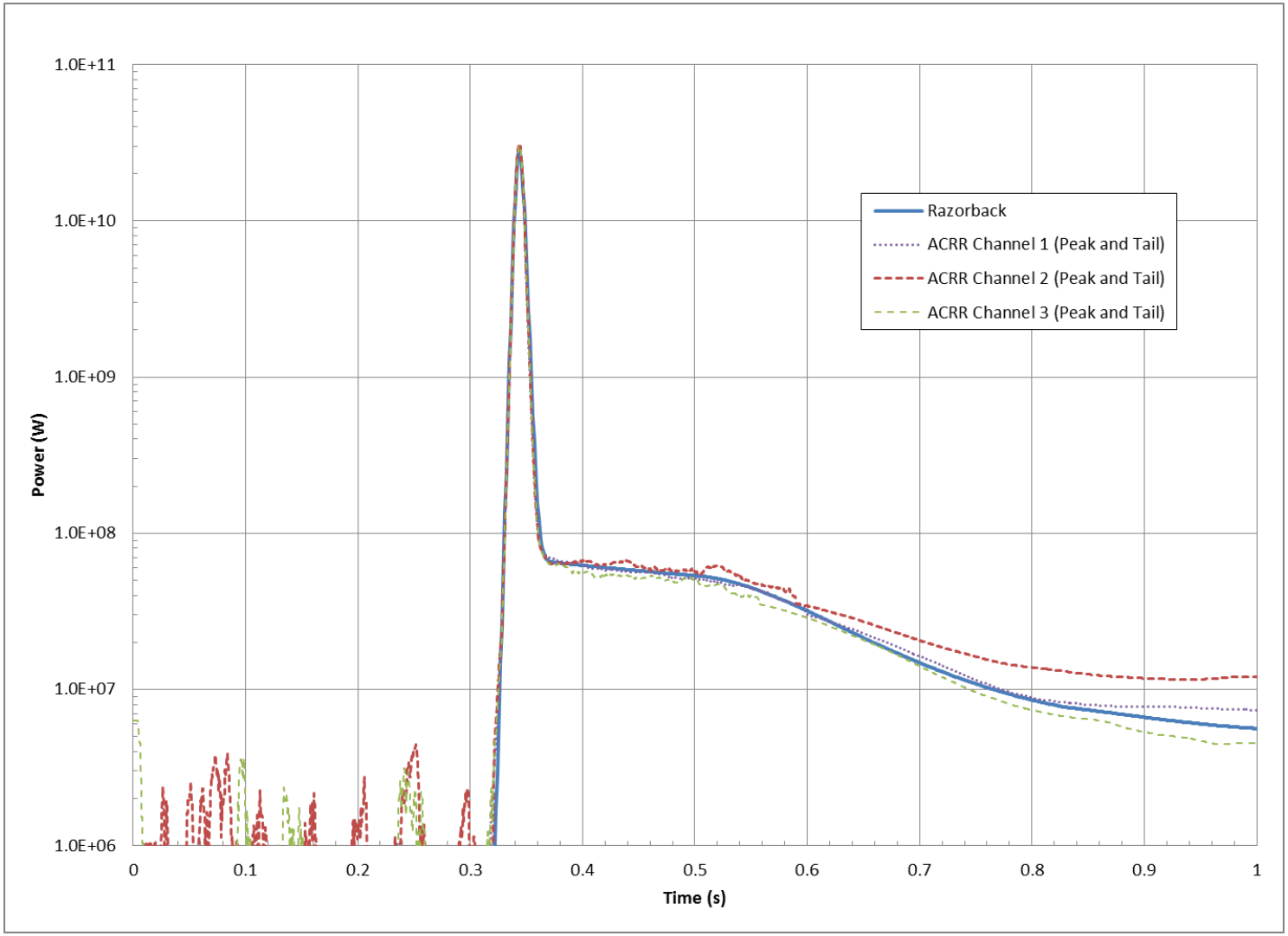

Figure 46. Razorback Simulation of a $3.00 Pulse Operation (#9716).

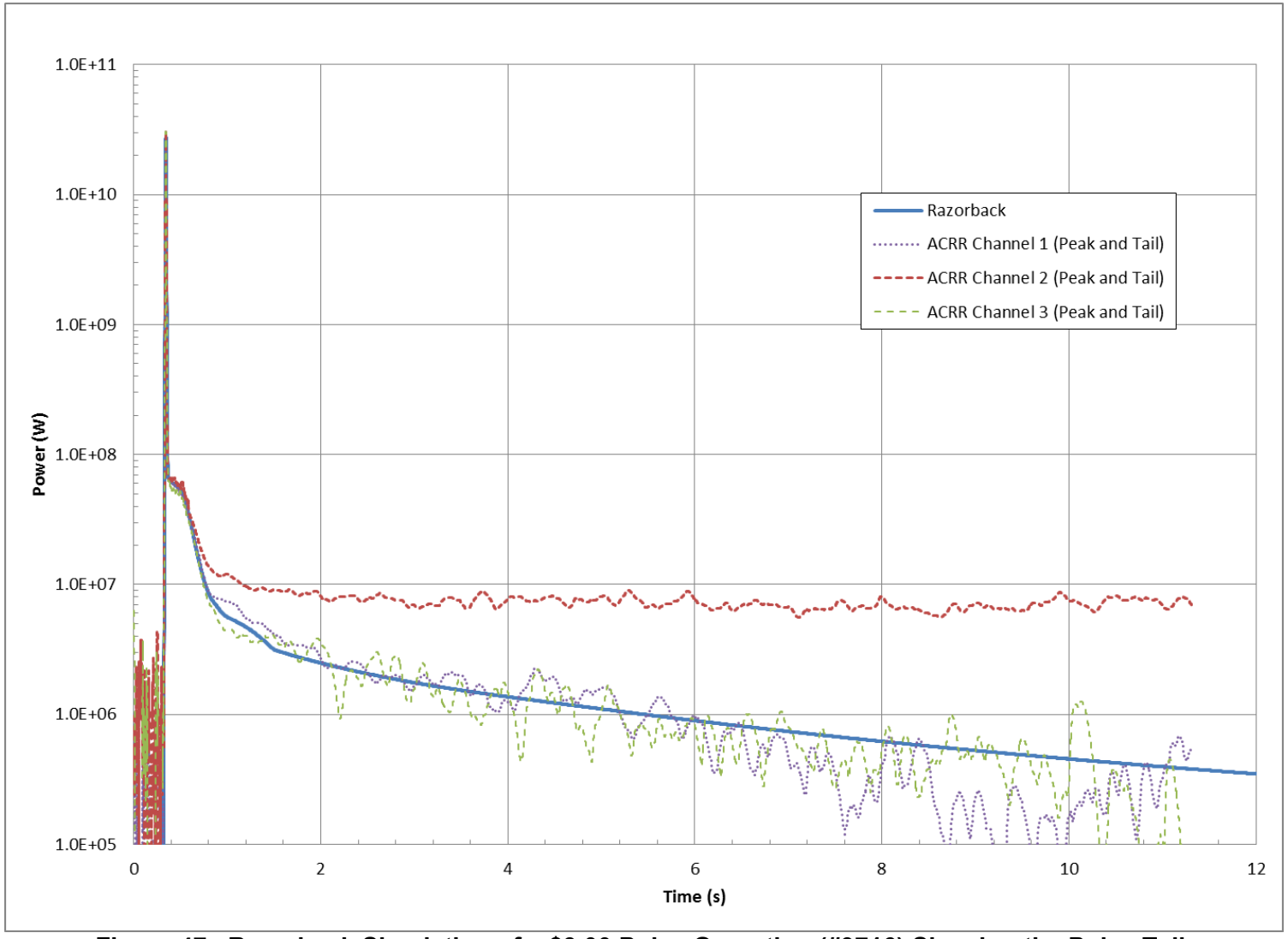

Figure 47. Razorback Simulation of a $3.00 Pulse Operation (#9716) Showing the Pulse Tail.

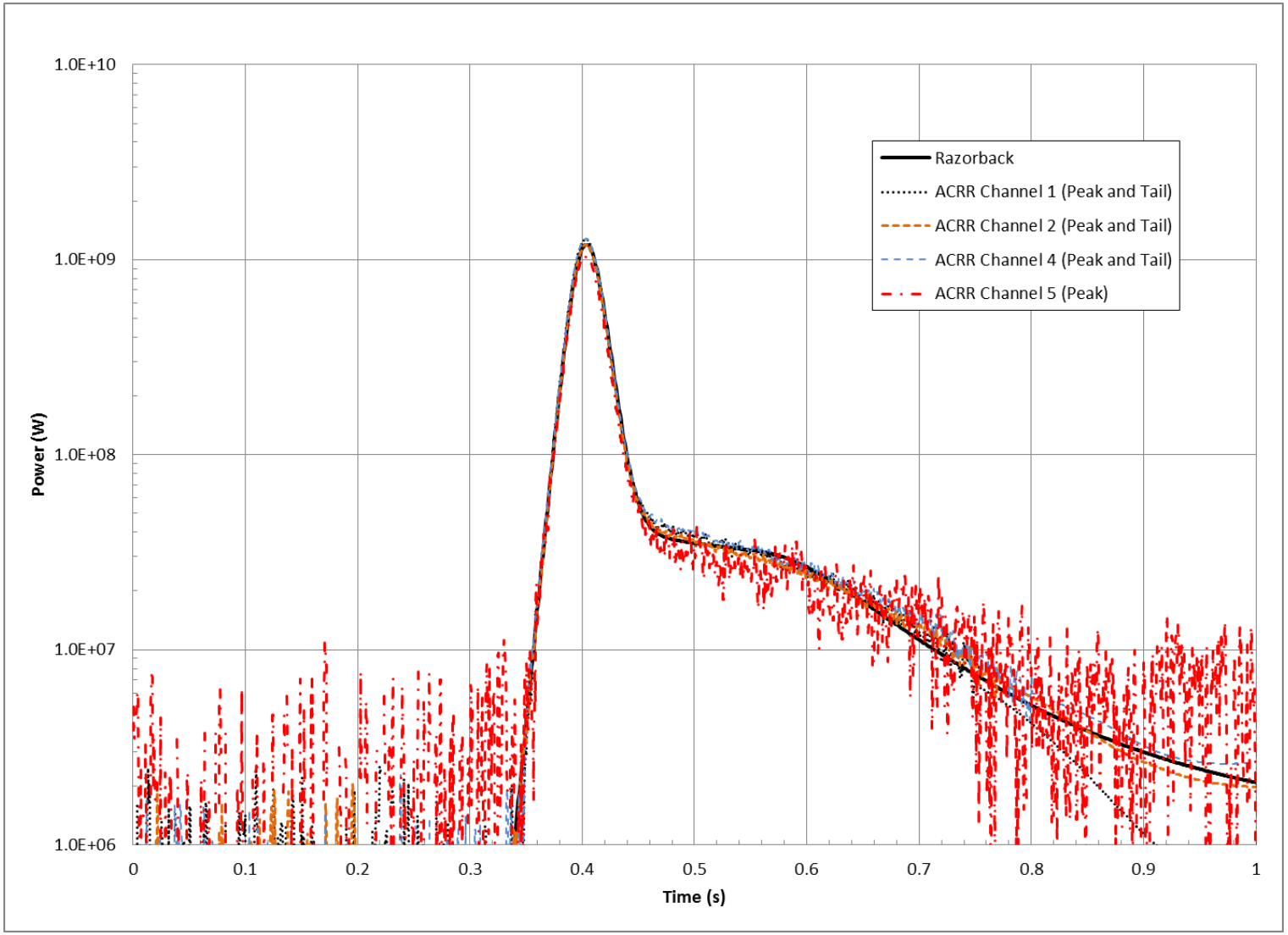

Figure 48. Razorback Simulation of a $1.50 Pulse Operation (#11705).

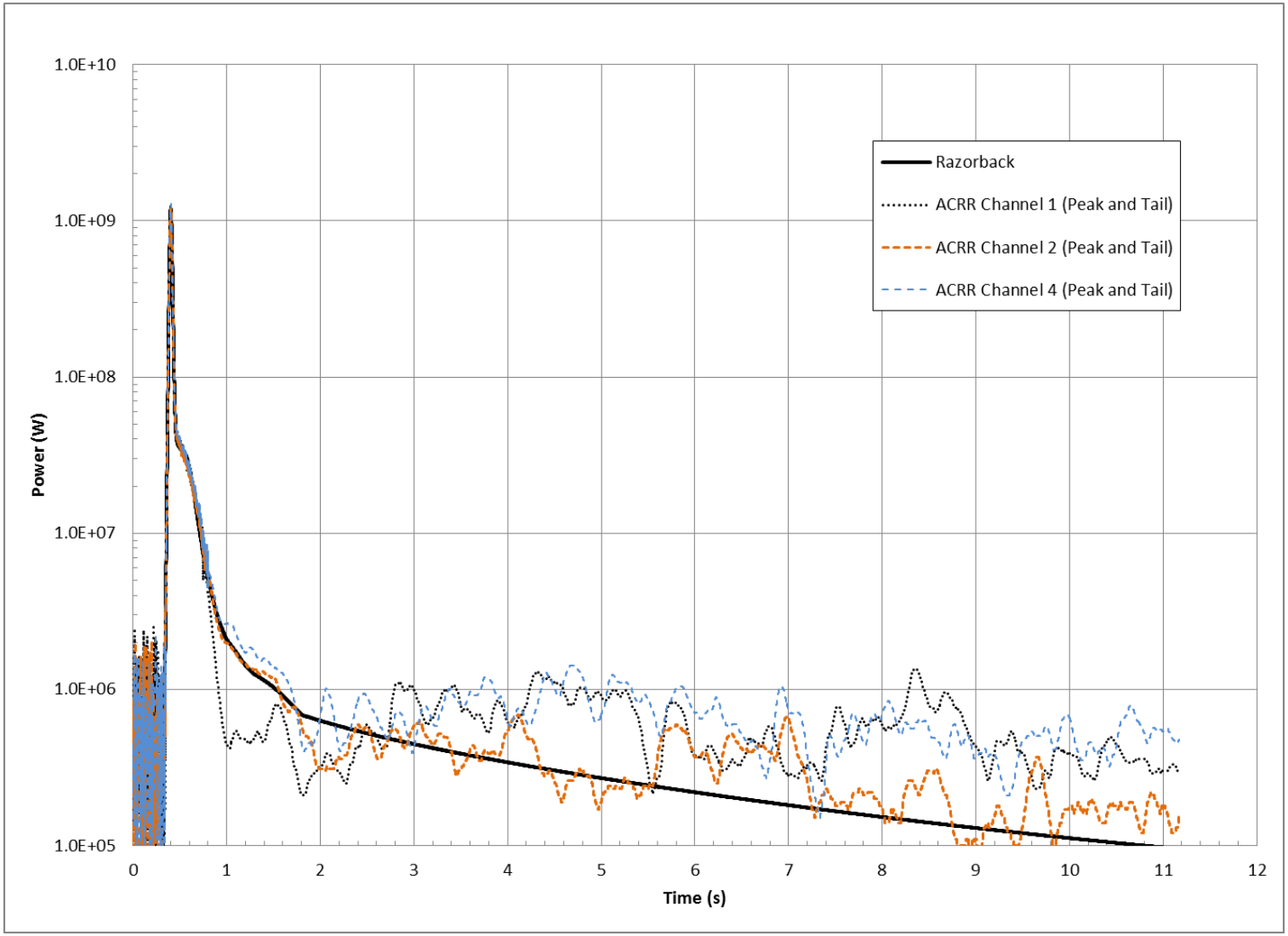

Figure 49. Razorback Simulation of a $1.50 Pulse Operation (#11705) Showing the Pulse Tail.

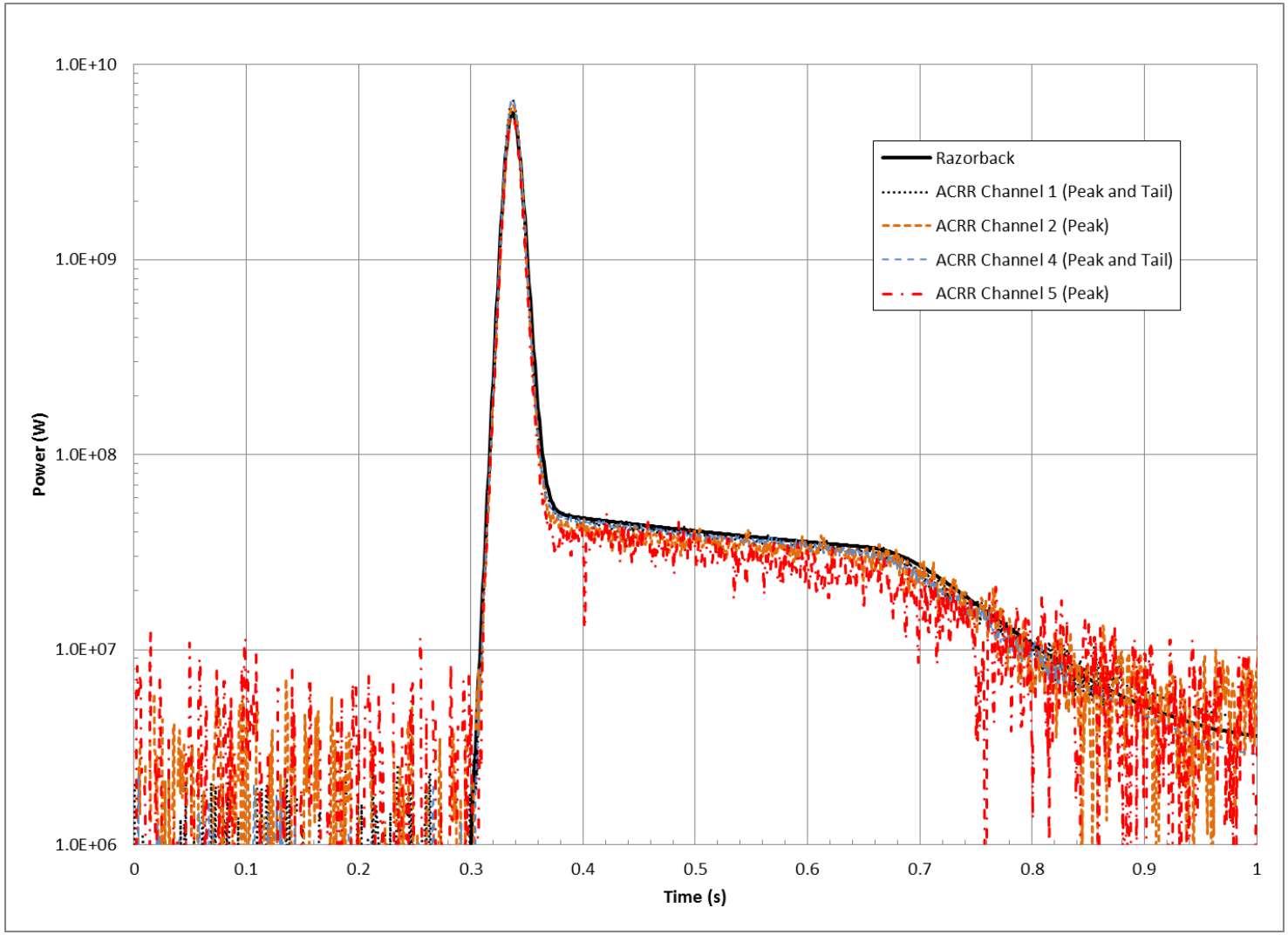

Figure 50. Razorback Simulation of a $2.00 Pulse Operation (#11704).

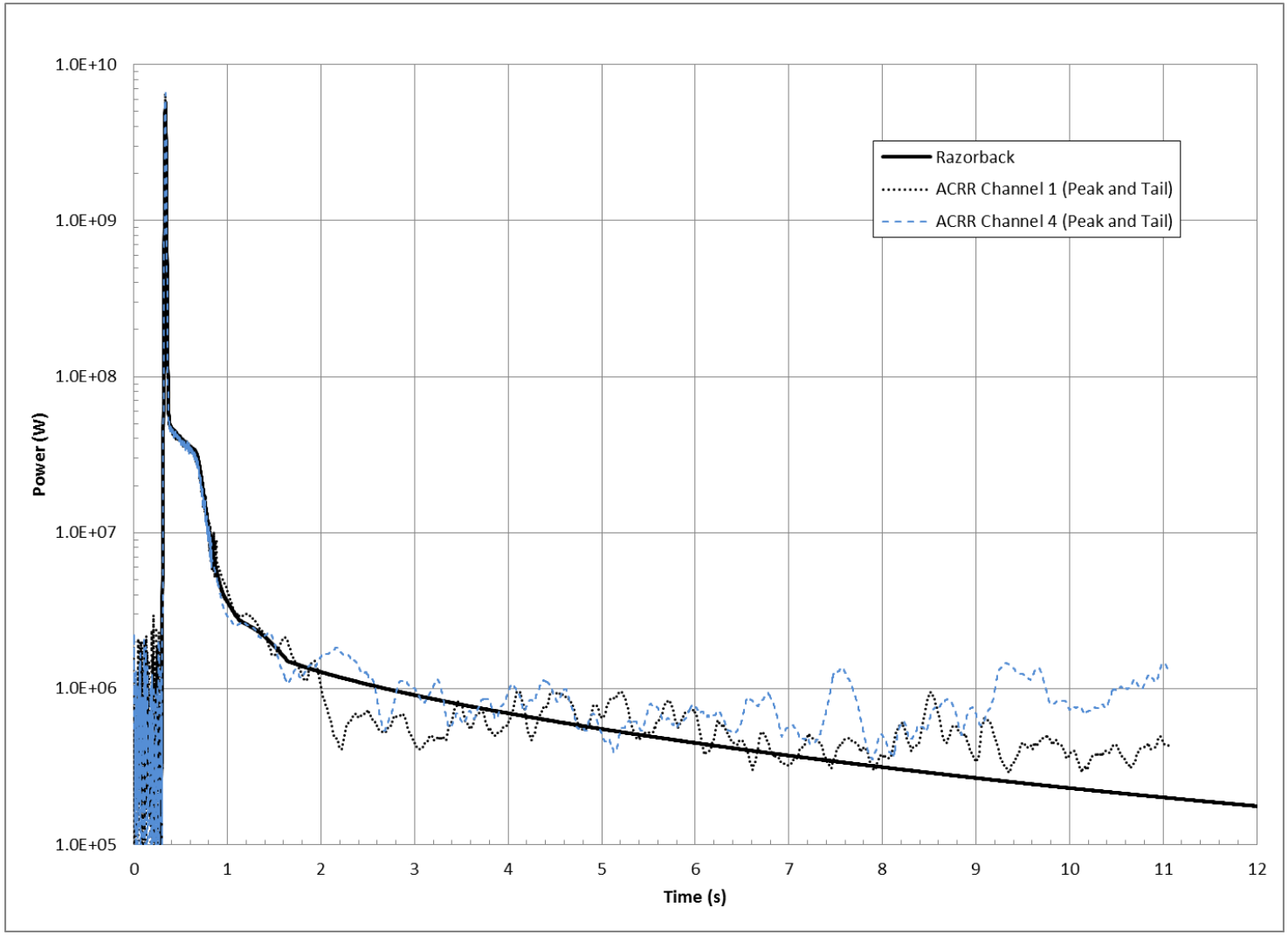

Figure 51. Razorback Simulation of a $2.00 Pulse Operation (#11704) Showing the Pulse Tail.

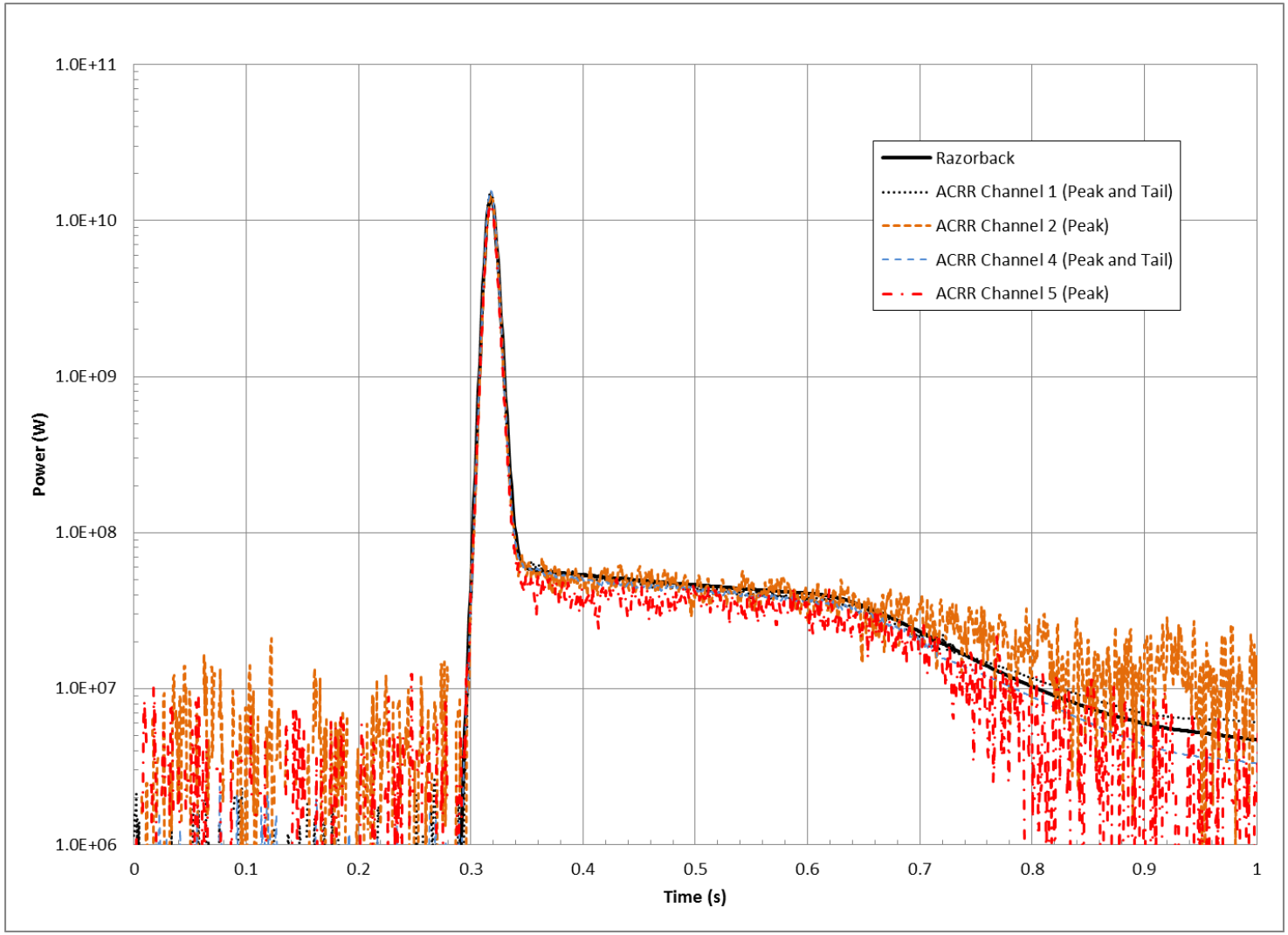

Figure 52. Razorback Simulation of a $2.50 Pulse Operation (#11703).

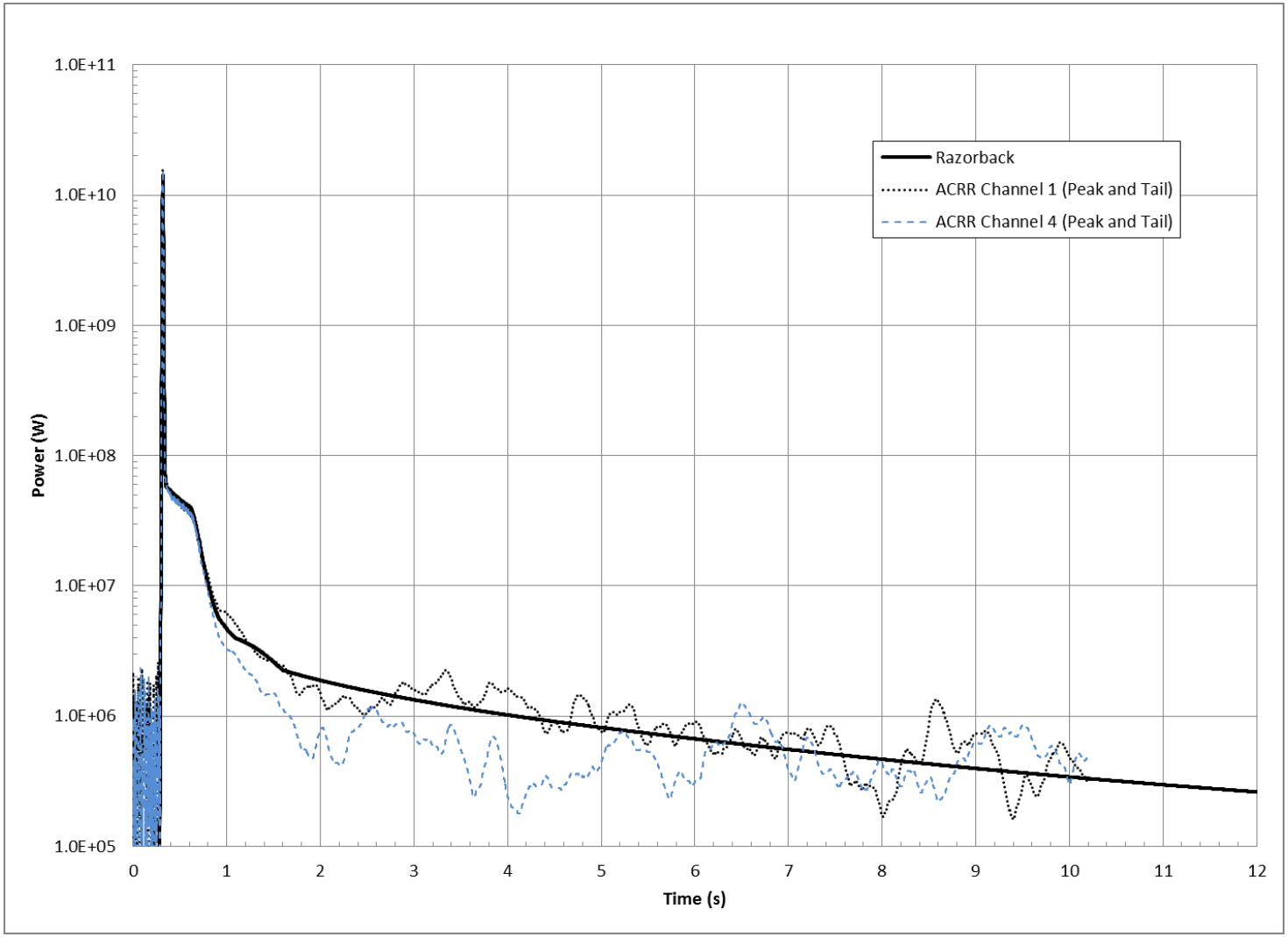

Figure 53. Razorback Simulation of a $2.50 Pulse Operation (#11703) Showing the Pulse Tail.

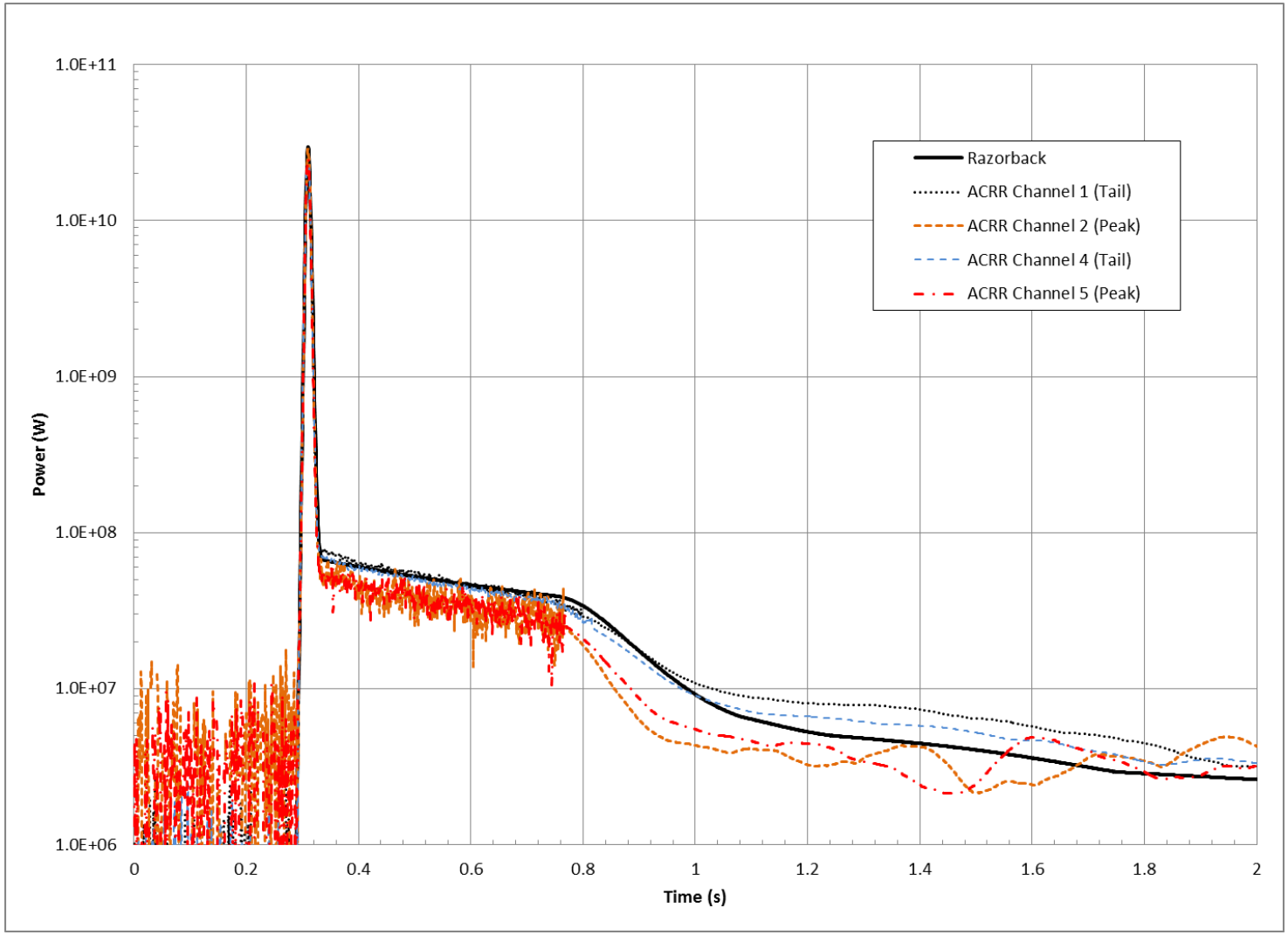

Figure 54. Razorback Simulation of a $3.00 Pulse Operation (#11694).

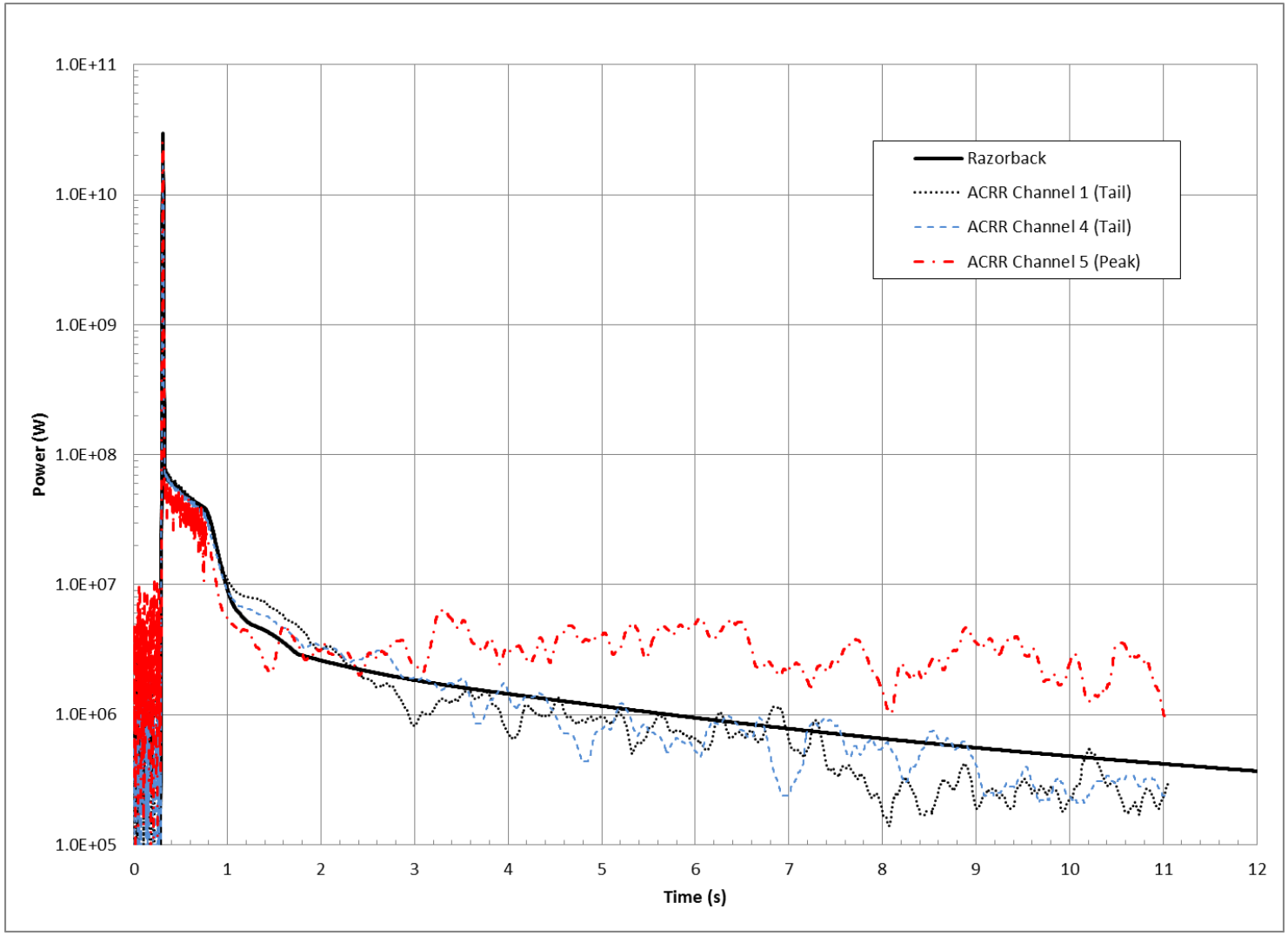

Figure 55. Razorback Simulation of a $3.00 Pulse Operation (#11694) Showing the Pulse Tail.

4.1. Predicted Reactor Peak Power

A comparison of the peak measured reactor power from the ACRR's Pulse Diagnostic System and those predicted by Razorback are shown in Table 16. Figure 56 displays the results in Table 16 graphically. Pulse Diagnostic System peak power results are consistent for the nominal \$1.50 and \$2.00 pulses. The Pulse Diagnostic System begins to evidence some scatter in the peak power results for the nominal \$2.50 and \$3.00 pulses, with the peak power for the \$3.00 pulse being lower than would be expected from the apparent trend.

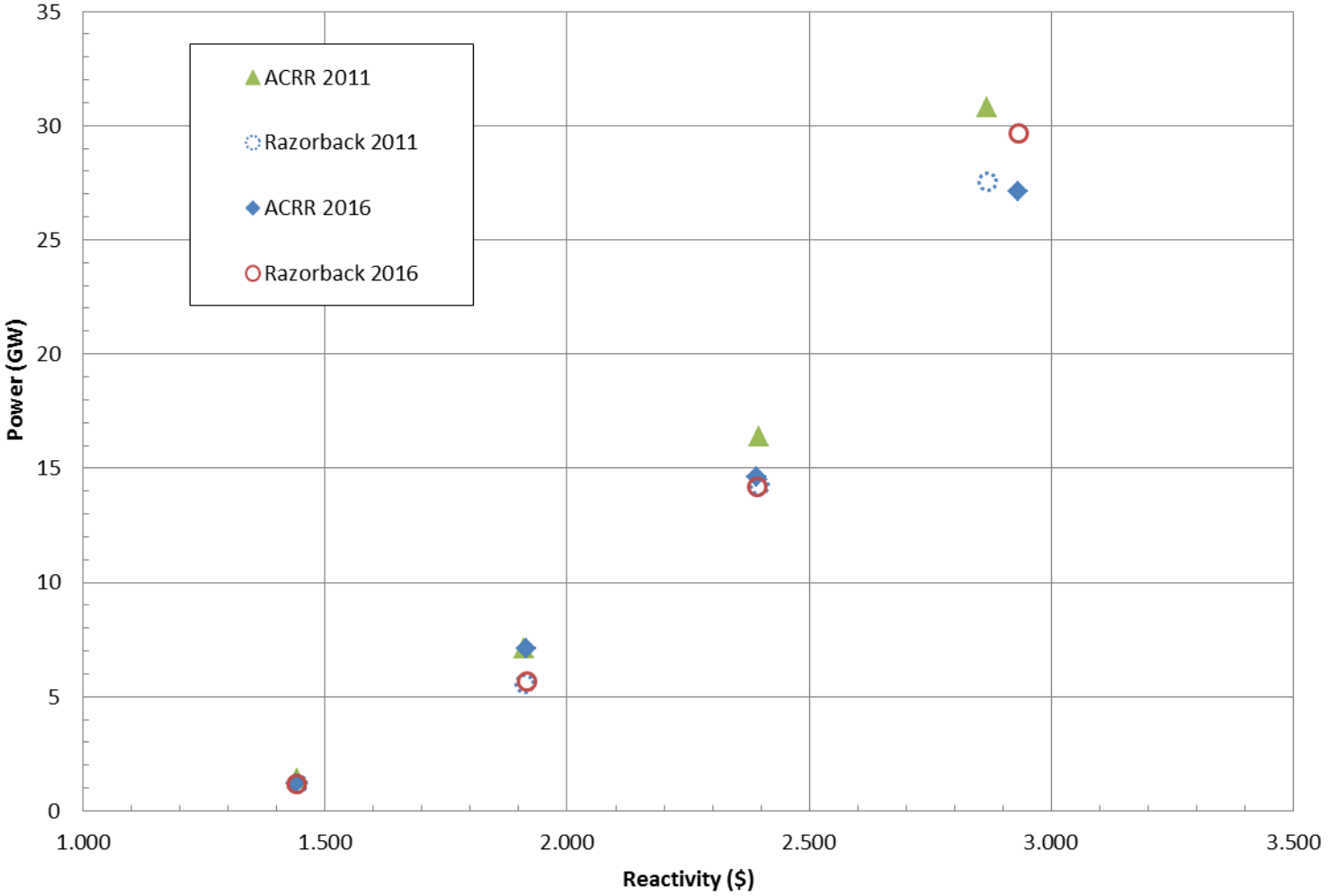

Figure 56. Comparison of Predicted and ACRR Peak Power for Several Pulses.

Table 16. Reactor Peak Power Comparison for Pulse Operations.

RUN #	**9720**	**9719**	**9718**	**9716**	**11705**	**11704**	**11703**	**11694**
Pulse Size ($) (nominal)	1.50	2.00	2.50	3.00	1.50	2.00	2.50	3.00
Pulse Size ($)	1.443	1.912	2.396	2.867	1.440	1.916	2.392	2.932
ACRR Diagnostic System Peak Power (GW)	1.4	7.1	16.4	30.8	1.2	7.1	14.6	27.1
Razorback Peak Power (GW)	1.2	5.6	14.3	27.5	1.2	5.7	14.2	29.7
Deviation	-14.8%	-21.0%	-13.1%	-10.6%	-0.3%	-20.0%	-2.5%	9.6%

4.2. Predicted Reactor Yield

The reactor yield parameters used to characterize a pulse at the ACRR are as follows:

- Yield at Peak: This parameter is determined by integrating the pulse power history up to the time of the pulse peak.
- Yield at Peak + 3FWHM: This parameter is determined by integrating the pulse power history up to a time equal to the time of the pulse peak plus three times the FWHM (full width at half-maximum (see Section 4.4)). This time span is intended to result in value which characterizes the energy release of the pulse prior to significant delayed neutron effects.
- Total Yield: This parameter is determined by integrating the pulse power history all the way to the end time of the Diagnostic System data recording. This is typically approximately 12 seconds from time zero for the pulse operation. This time span is intended to result in value which characterizes the total energy release of the pulse including the pulse "tail" which is due to delayed neutron effects.

Figure 57 illustrates the integration timespans for each of these yield parameters.

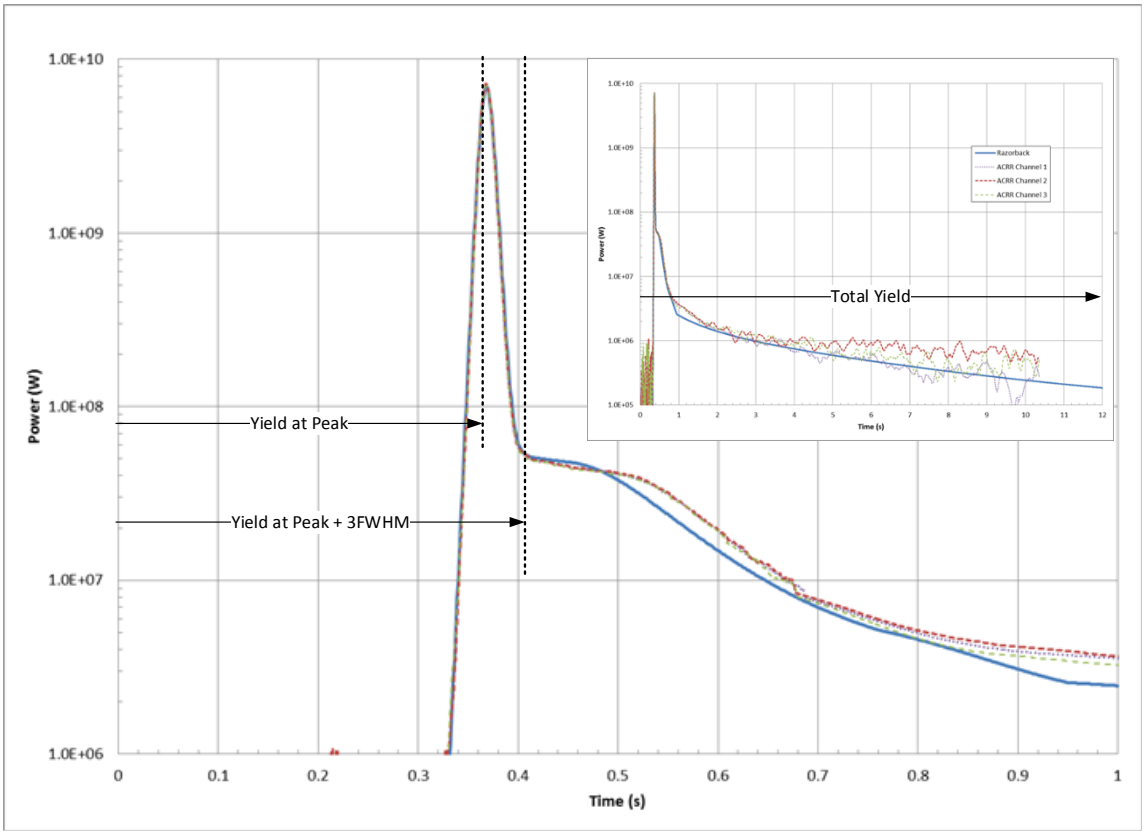

Figure 57. Depiction of the Integration Ranges of the Reactor Yield Parameters.

A comparison of the reactor yield (i.e., the pulse energy release determined by integrating the pulse power history) from the ACRR's PDS and that predicted by Razorback for the 2011 and 2016 calibration pulses is shown in Table 17. The results are in reasonable agreement with the ACRR data, but the deviation can be as large as 13%-17%. Figures 58-60 display the results in Table 17 graphically.

It is of interest to note the trends of the ACRR data vs. that of the Razorback data. With respect to the ACRR data, Razorback appears to be under predicting yield for the $1.50 and $2.00 pulses of 2016, while over predicting yield for the $2.50 and $3.00 pulses of 2016. However, Razorback seems to generally under predict for the 2011 pulses. It can be shown (Ref. 21) that reactor yield should follow a concave upward parabolic curve based on a Fuchs-Nordheim analysis assuming the fuel Doppler reactivity feedback to be inversely proportional to the square root of the fuel temperature. With this in mind, it appears that the yield results for the 2016 pulses may be trending toward a concave downward parabolic curve. It should be noted that the collection of self-powered neutron detectors used for the 2016 pulse was different than that of the 2011 pulses, and the sensitivities of some of the detectors appears to have been decreased.[7]

Lastly, it is noted that the deviations for the 3xFWHM yields for the $1.50 pulses may be related to the values used for rod drop delay time, as the peak of the pulse occurs about 40 ms after the RHU time is reached. Thus, downward rod motion may be occurring during the post-peak portion of the pulse.

[7] Refer to the PDS Data Sheet excerpts in Appendix B.

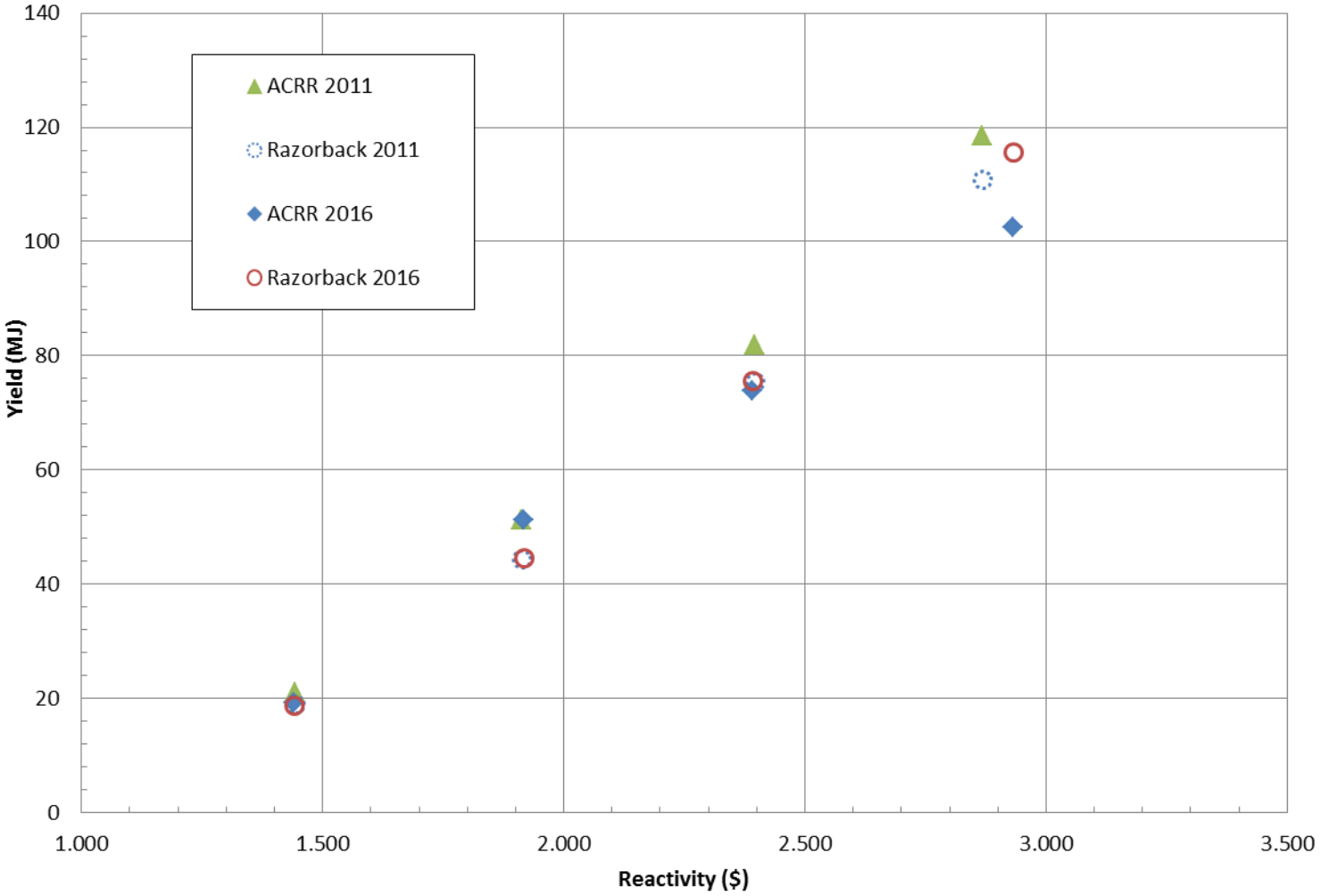

Figure 58. Comparison of Predicted and ACRR Reactor Yield at Pulse Peak for Several Pulses.

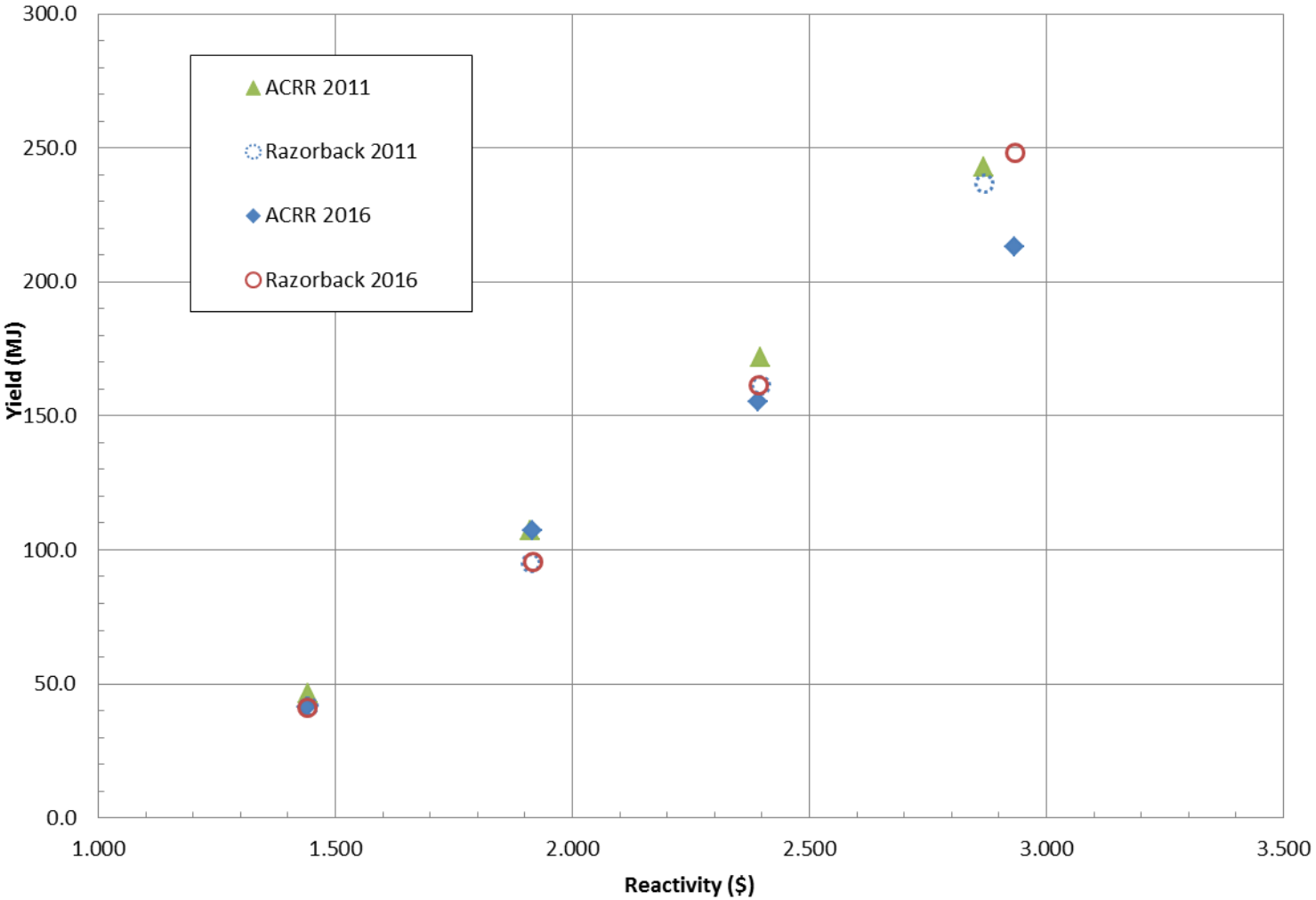

Figure 59. Comparison of Predicted and ACRR Reactor Yield at Peak+3FWHM for Several Pulses.

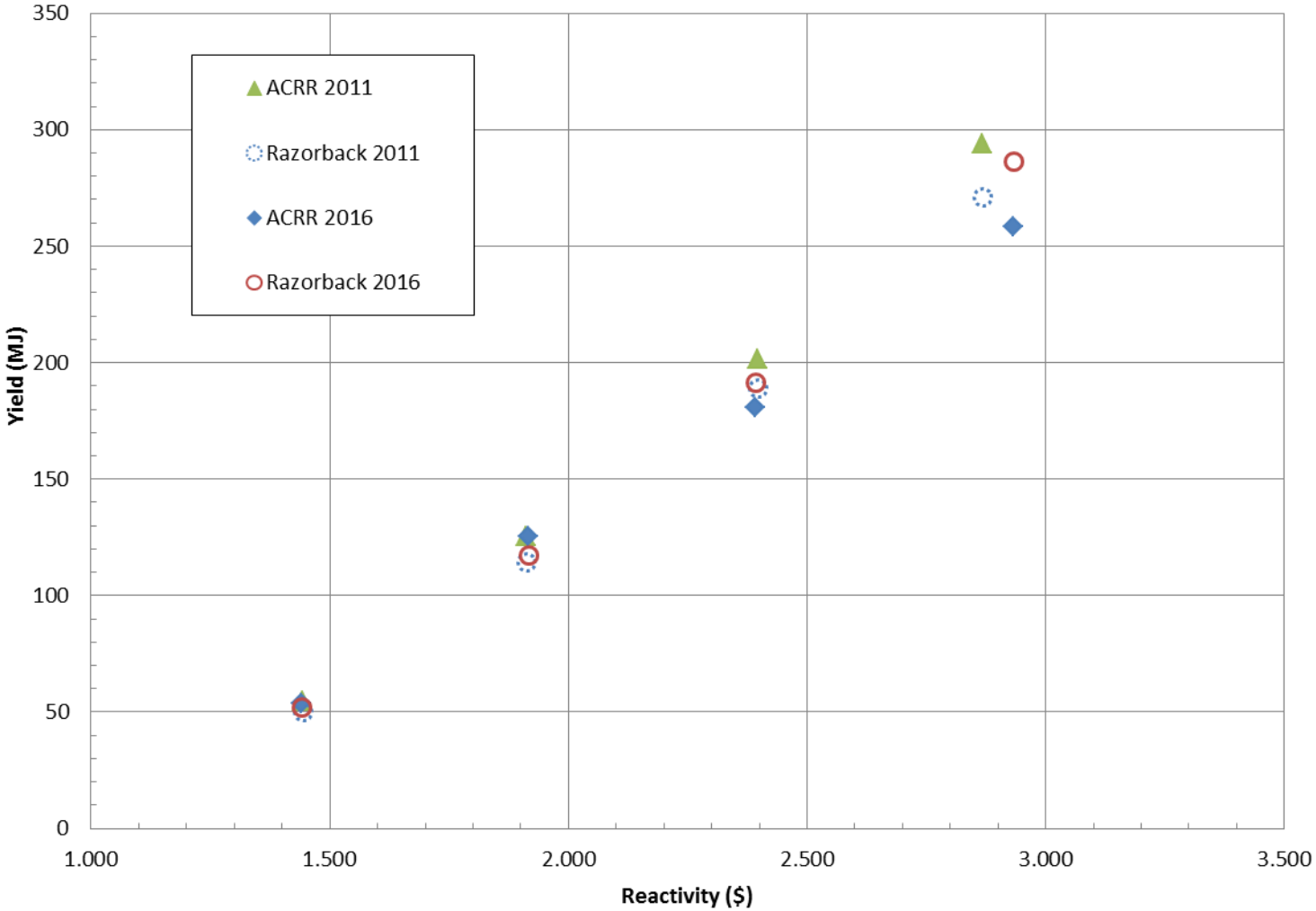

Figure 60. Comparison of Predicted and ACRR Total Reactor Yield for Several Pulses.

Table 17. Reactor Yield Comparison for Pulse Operations.

RUN #	9720	9719	9718	9716	11705	11704	11703	11694
Pulse Size ($) (nominal)	1.50	2.00	2.50	3.00	1.50	2.00	2.50	3.00
Pulse Size ($)	1.443	1.912	2.396	2.867	1.440	1.916	2.392	2.932
ACRR Diagnostic System								
Yield @ Peak (MJ)	20.9	51.2	81.8	118.5	19.1	51.2	73.9	102.4
Yield @ 3xFWHM (MJ)	46.3	107.3	171.7	242.9	41.2	107.3	155.2	213
Yield @ Total (MJ)	54.9	125.3	201.7	294.1	53.8	125.3	180.8	258.6
Razorback								
Yield @ Peak (MJ)	18.9	44.4	75.5	110.9	18.8	44.7	75.6	115.8
Yield @ 3xFWHM (MJ)	41.9	95.2	161.8	236.8	41.4	95.8	161.6	248.3
Yield @ Total (MJ)	49.3	112.2	186.8	268.4	52.0	118.7	191.1	284.5
Deviation								
Deviation @ Peak	-9.6%	-13.3%	-7.7%	-6.4%	-1.6%	-12.7%	2.3%	13.1%
Deviation @ 3xFWHM	-9.5%	-11.3%	-5.8%	-2.5%	0.5%	-10.7%	4.1%	16.6%
Deviation @ Total	-10.2%	-10.5%	-7.4%	-8.7%	-3.3%	-5.3%	5.7%	10.0%

In addition to the use of the ACRR PDS to determine pulse yield parameters (at power peak, at power peak + 3FWHM, and total), passive neutron dosimetry is installed in the ACRR's central cavity. The post-exposure specific activity of nickel foils and sulfur tablets can be related back to the total yield of the reactor pulse by means of a thorough characterization of the neutron energy spectrum in the central cavity, and detailed neutron transport calculations with a code such as MCNP. Parma (Ref. 27) has recently performed such a characterization of the free field ACRR central cavity neutron energy spectrum, and has derived the necessary characterization parameters to relate ACRR total yield to Ni and S specific activity.

Dosimetry data from the 2011 and 2016 pulse calibration operations has been used with Ref. 27 conversion parameters to determine the total energy yield for the calibration pulses. The results are shown graphically in Fig. 61 (for the 2011 pulses) and Fig. 62 (for the 2016 pulses), and the data is also presented in Table 18. The Razorback results are seen to under predict the total yield by 10%-20% with respect to the Ni foil dosimetry, and 5%-15% with respect to the S tablet dosimetry. The deviations tend to improve with increasing pulse worth. A qualitative look at Figs. 40-55 indicates that a better match of the pulse tail occurs with increasing pulse worth. However, unlike the PDS data, the deviations based on dosimetry appear to remain consistent from 2011 to 2016.

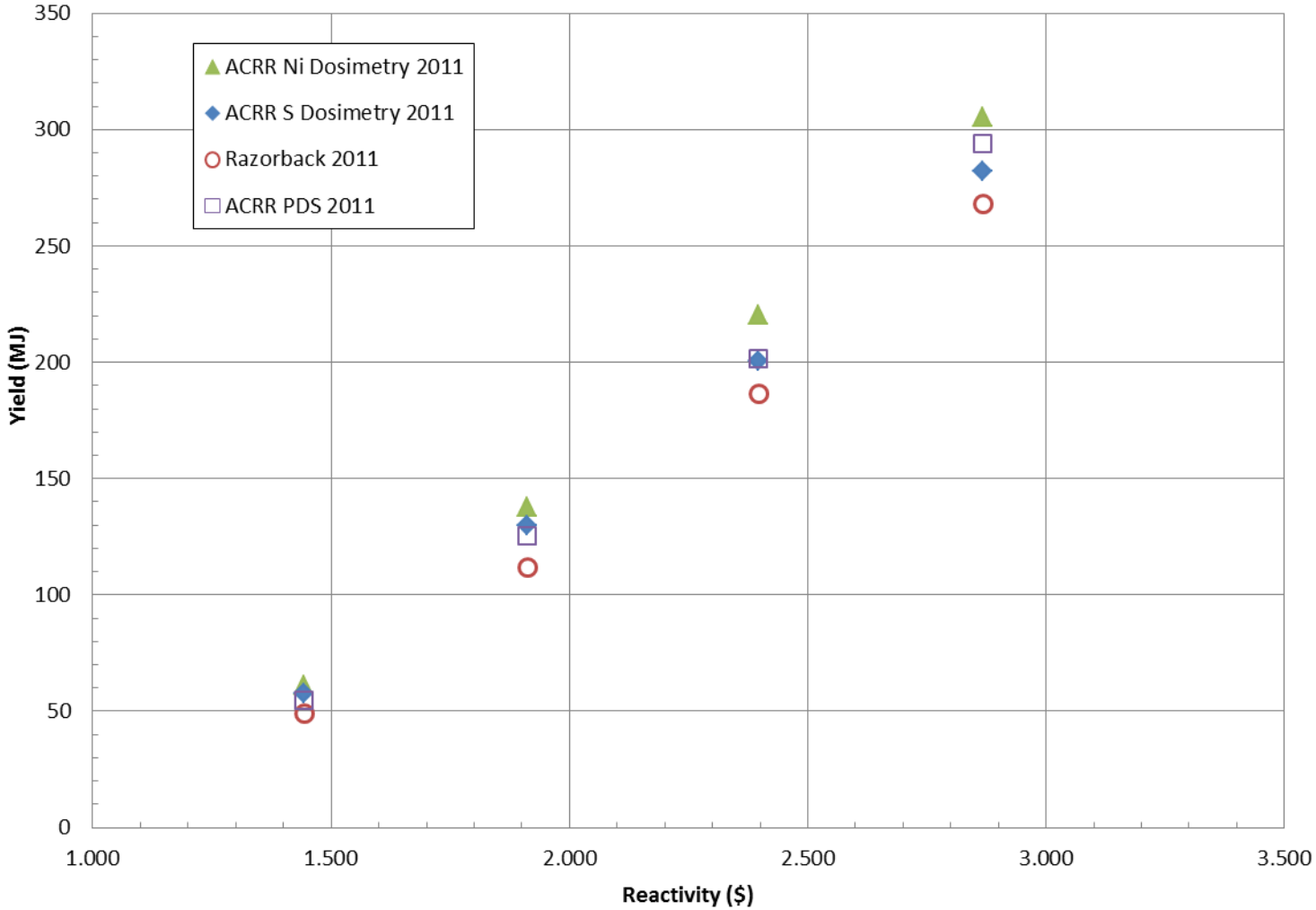

Figure 61. Predicted and ACRR Dosimetry-Based Total Reactor Yield for the Calibration Pulses of 2011.

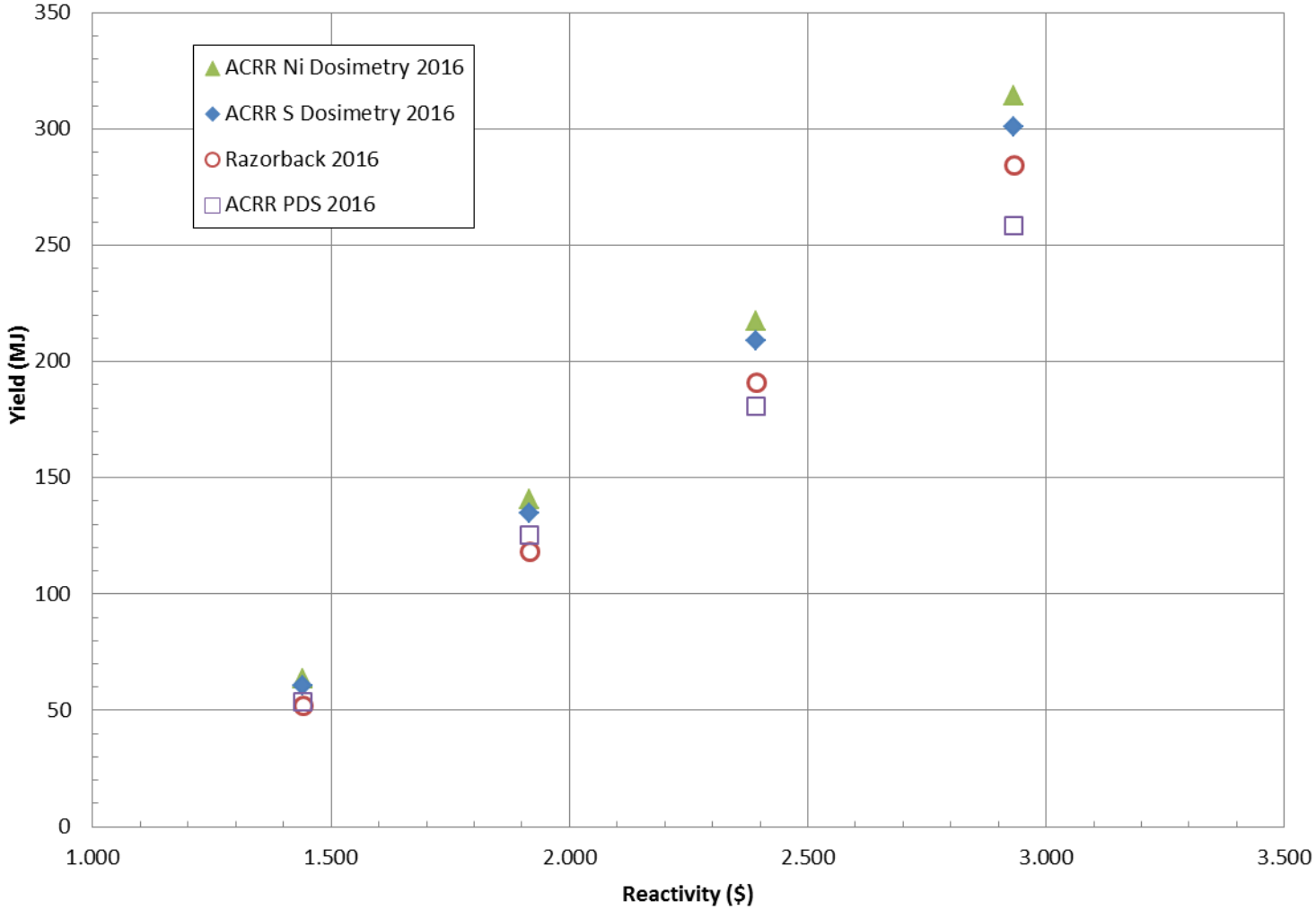

Figure 62. Predicted and ACRR Dosimetry-Based Total Reactor Yield for the Calibration Pulses of 2016.

Table 18. Total Reactor Yield Comparison for Pulse Operations and Dosimetry-Based Total Yield.

RUN #	9720	9719	9718	9716	11705	11704	11703	11694
Pulse Size ($) (nominal)	1.50	2.00	2.50	3.00	1.50	2.00	2.50	3.00
Pulse Size ($)	1.443	1.912	2.396	2.867	1.440	1.916	2.392	2.932
ACRR Diagnostic System								
Total Yield (MJ)	54.9	125.3	201.7	294.1	53.8	125.3	180.8	258.6
Nickel Dosimetry								
Total Yield (MJ)	61.3	137.9	220.1	305.3	63.6	141.0	217.2	314.2
Sulfur Dosimetry								
Total Yield (MJ)	57.6	129.9	200.5	282.0	60.6	134.6	209.0	301.0
Razorback								
Yield @ Total (MJ)	49.3	112.2	186.8	268.4	52.0	118.7	191.1	284.5
Deviation								
Nickel Dosimetry	-19.5%	-18.6%	-15.1%	-12.1%	-18.2%	-15.8%	-12.0%	-9.4%
Sulfur Dosimetry	-14.4%	-13.6%	-6.8%	-4.8%	-14.2%	-11.8%	-8.6%	-5.5%

4.3. Predicted Fuel Temperatures

A comparison of the peak measured fuel temperatures from the ACRR's Plant Protection System (PPS) and those predicted by Razorback for four pulse operations are shown in Table 19. The temperature input to the PPS is from one of two instrumented fuel elements, each having three thermocouple positioned to measure fuel temperature at the mid-plane of the fuel. The ACRR data below was from the PPS-1 instrumented element in core location 218.

The "measured" fuel temperature in the Razorback code was set so that the data output was equal to the average of six fuel material nodes about the radial center of the inner fuel pellet at the mid-plane of the simulated element. The results show Razorback predicting the peak fuel temperatures within 1 to 7.5% of the PPS instrumented element. Figure 63 displays the results in Table 19 graphically.

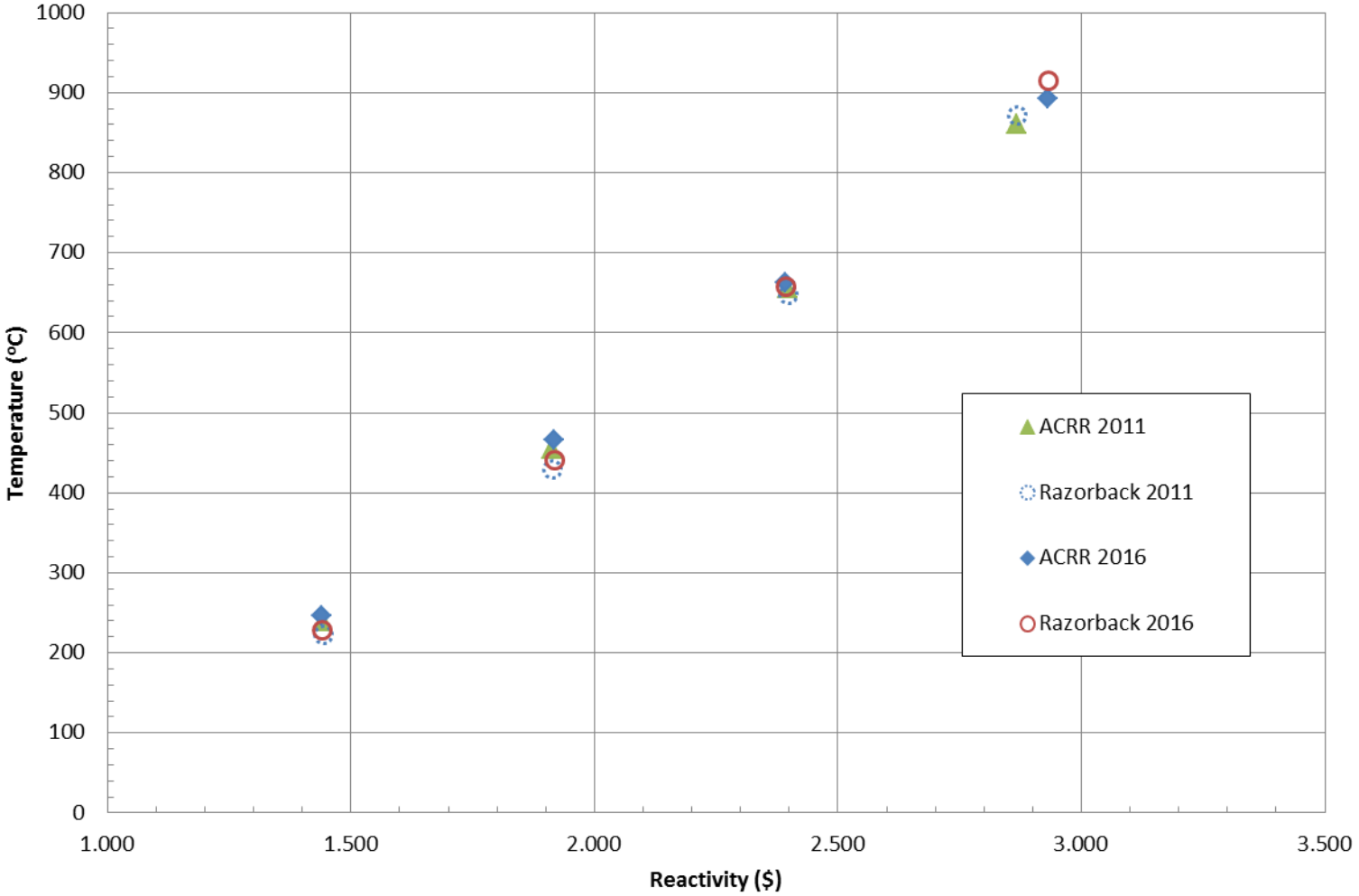

Figure 63. Comparison of Predicted and ACRR Peak Measured Fuel Temperatures for Several Pulses.

Table 19. PPS Peak Fuel Temperature Comparison for Pulse Operations.

RUN #	9720	9719	9718	9716	11705	11704	11703	11694
Pulse Size ($) (nominal)	1.50	2.00	2.50	3.00	1.50	2.00	2.50	3.00
Pulse Size ($)	1.443	1.912	2.396	2.867	1.440	1.916	2.392	2.932
ACRR Plant Protection System (PPS)								
Peak Fuel Temperature (°C) – PPS1/TC2*	239	454	656	860	247	466	663	892
Razorback								
Peak Fuel Temperature (°C)	219	423	641	865	228	443	654	905
Deviation	-8.2%	-6.9%	-2.3%	0.5%	-7.9%	-4.9%	-1.4%	1.4%

*TC2 refers to thermocouple channel #2 for the PPS drawer shown

4.4. Predicted Reactor Pulse Width Parameters

The pulse width parameters used to characterize a pulse are as follows:

- FWHM: Full Width at Half-Maximum. This parameter is determined by finding the time, before and after the pulse peak, when the power level is equal to one-half of the peak power.
- LEHM: Leading Edge (Width) at Half-Maximum. This parameter is the time difference between the one-half of peak power point before the pulse peak and the pulse peak. For a symmetrical pulse, this timespan would be one-half of the FWHM.
- TEHM: Trailing Edge (Width) at Half-Maximum. This parameter is the time difference between the one-half of peak power point after the pulse peak and the pulse peak. For a symmetrical pulse, this timespan would be one-half of the FWHM.
- LE/TE Ratio: Leading Edge/Trailing Edge Ratio. This parameter is simply the ratio of the LEHM to the TEHM. For a symmetrical pulse, this ratio would be 1. As such, this provides an indication of the asymmetry of the actual pulse. The impact of delayed neutrons on the pulse shape would lead to an LE/TE < 1.

Figure 64 illustrates these pulse width parameters.

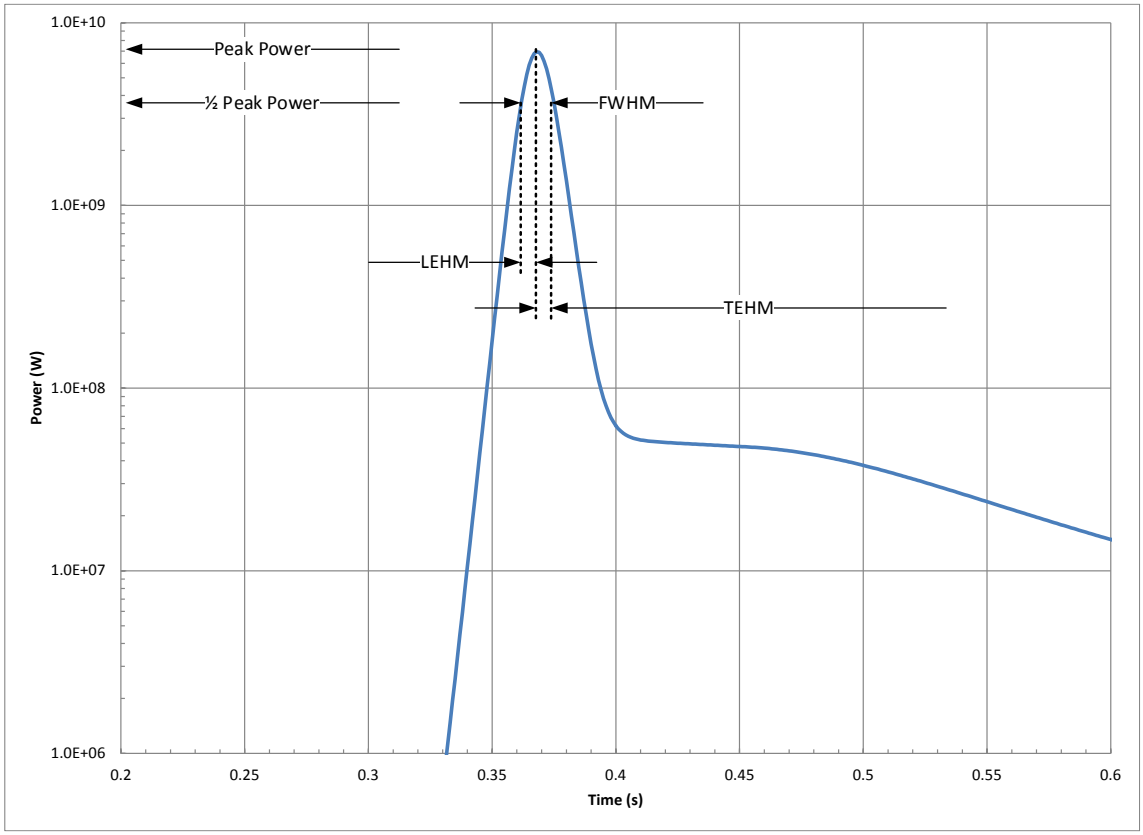

Figure 64. Depiction of Pulse Width Parameters.

A comparison of the measured pulse width parameters from the ACRR's Pulse Diagnostic System and those predicted by Razorback are shown in Table 20. Razorback tends to over predict the FWHM by as little as 1.5% to as much as 11.7%. Similar results are seen for the LEHM and TEHM. The ratio of LEHM to TEHM (LE/TE) is under predicted by 2% to 10%. Figure 65 displays the FWHM results in Table 20 graphically.

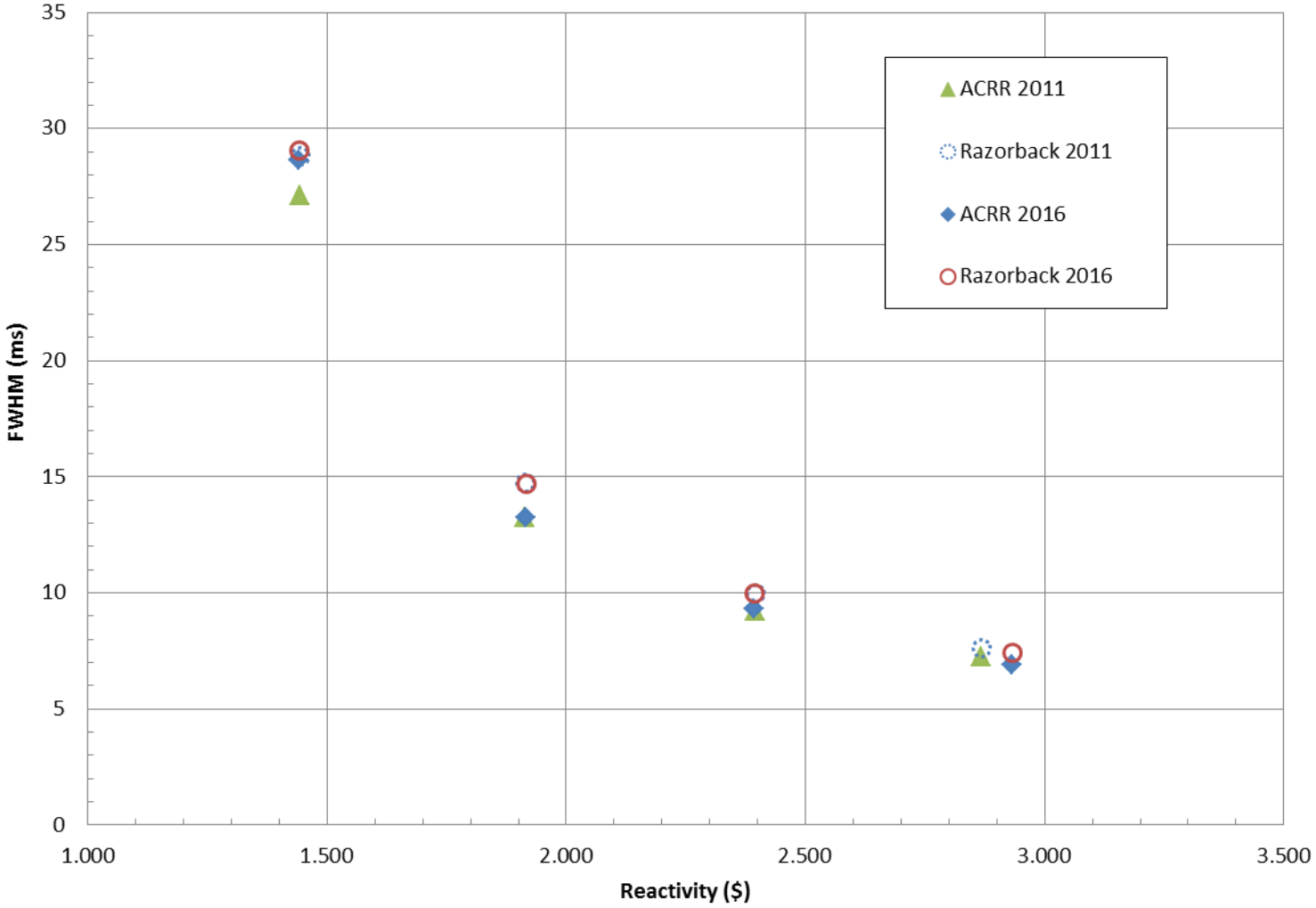

Figure 65. Comparison of Predicted and ACRR Pulse Widths for Several Pulses.

Table 20. Pulse Shape Comparisons for Pulse Operations.

RUN #	9720	9719	9718	9716	11705	11704	11703	11694
Pulse Size ($) (nominal)	1.50	2.00	2.50	3.00	1.50	2.00	2.50	3.00
Pulse Size ($)	1.443	1.912	2.396	2.867	1.440	1.916	2.392	2.932
ACRR FWHM (ms)	27.12	13.24	9.20	7.24	28.64	13.24	9.32	6.92
Razorback FWHM (ms)	28.84	14.79	10.02	7.62	28.84	29.06	14.71	10.00
Deviation	6.4%	11.7%	9.0%	5.3%	6.4%	1.5%	11.1%	7.3%
ACRR LEHM (ms)	12.88	6.44	4.48	3.60	14.12	6.44	4.52	3.36
Razorback LEHM (ms)	13.80	7.08	4.77	3.63	13.97	7.03	4.77	3.53
Deviation	7.1%	10.0%	6.4%	0.8%	-1.1%	9.2%	5.6%	5.0%
ACRR TEHM (ms)	14.24	6.88	4.72	3.64	14.52	6.88	4.80	3.56
Razorback TEHM (ms)	15.04	7.71	5.26	3.99	15.09	7.67	5.23	3.89
Deviation	5.6%	12.1%	11.4%	9.7%	3.9%	11.5%	8.9%	9.3%
ACRR Ratio LE/TE	0.904	0.936	0.949	0.989	0.972	0.936	0.942	0.944
Razorback Ratio LE/TE	0.917	0.919	0.907	0.909	0.926	0.916	0.913	0.907
Deviation	1.4%	-1.9%	-4.5%	-8.1%	-4.8%	-2.1%	-3.0%	-3.9%

4.5. Predicted Reactor Minimum Period

A comparison of the minimum reactor period determined from the ACRR's Pulse Diagnostic System (PDS) and those predicted by Razorback are shown in Fig. 66 and Table 21. The minimum period value selected from the PDS data report was the "average" minimum period, as opposed to selecting the minimum period from one of the individual channels. The "average" minimum period is the minimum period of the power trace formed by averaging the power traces of the individual channels of the PDS. As shown in Table 21, except for the \$2.00 case, Razorback predictions for minimum period are quite good (within 5%)

The interest in this parameter is that the minimum reactor period provides a means, assuming no appreciable delayed neutron effects or reactivity feedback effects, to determine the reactivity addition of the pneumatically-ejected transient rods, given a value for Λ/β.[8] As shown in Table 22, except for the \$2.00 case, the reactivity addition derived from the minimum period align better with the pulse size determined using the Ref. 20 control rod calibration curve rather than the nominal pulse worth.

[8] The Diagnostic System appears to utilize a value of 0.003288 s^{-1} (Λ=24 μs, β=0.0073).

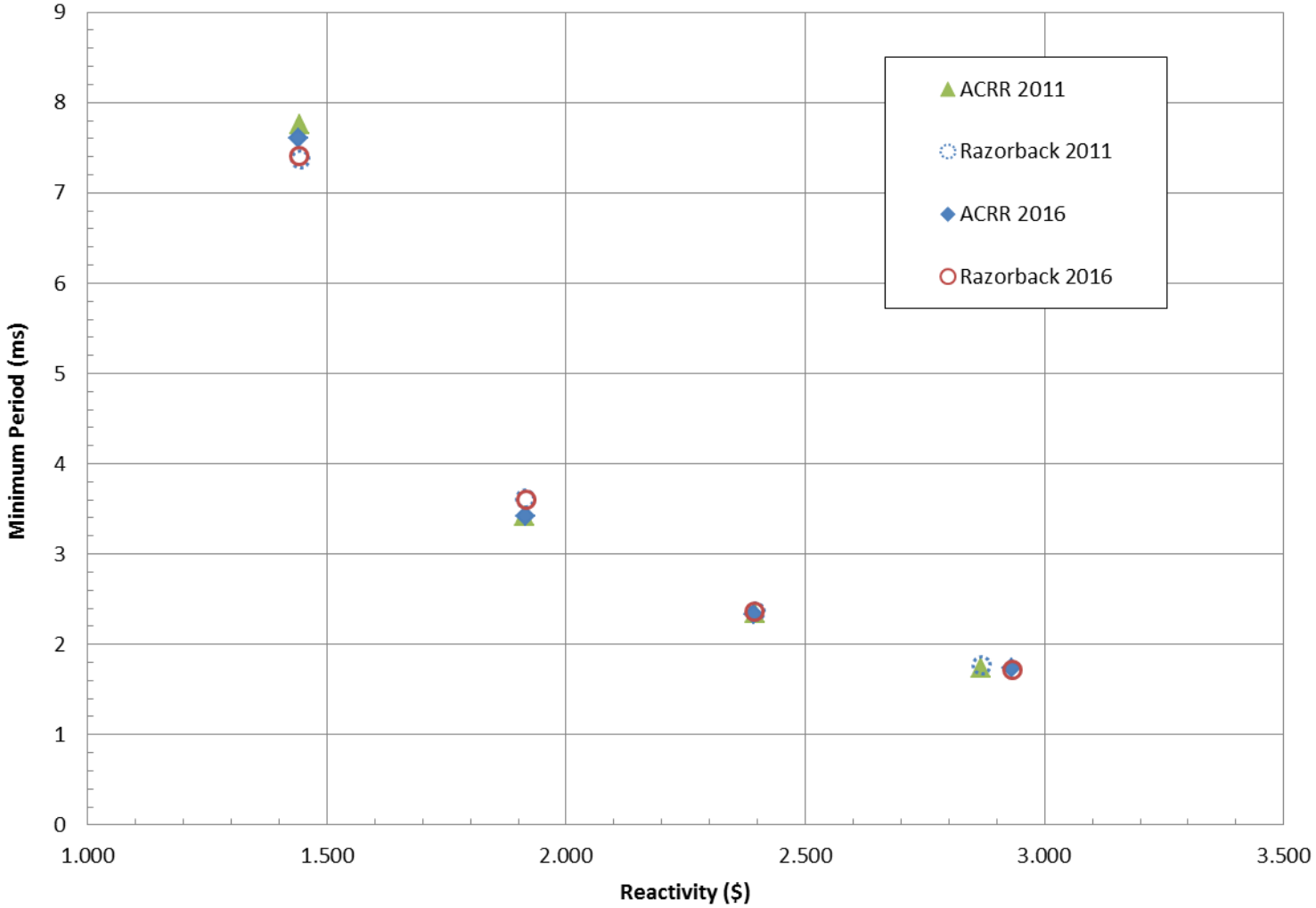

Figure 66. Comparison of Predicted and ACRR Minimum Period for Several Pulses.

Table 21. Minimum Period Comparison for Pulse Operations.

RUN #	9720	9719	9718	9716	11705	11704	11703	11694
Pulse Size ($) (nominal)	1.50	2.00	2.50	3.00	1.50	2.00	2.50	3.00
Pulse Size ($)	1.443	1.912	2.396	2.867	1.440	1.916	2.392	2.932
Minimum Period								
ACRR (ms)	7.76	3.42	2.34	1.74	7.61	3.42	2.33	1.74
Razorback (ms)	7.38	3.62	2.37	1.78	7.42	3.60	2.37	1.72
Deviation	-4.9%	5.9%	1.3%	2.1%	-2.5%	5.4%	1.8%	-1.2%

Table 22. Estimation of Reactivity Addition Using the Minimum Period.

RUN #	9720	9719	9718	9716	11705	11704	11703	11694
Pulse Size ($) (nominal)	1.50	2.00	2.50	3.00	1.50	2.00	2.50	3.00
Pulse Size ($)	1.443	1.912	2.396	2.867	1.440	1.916	2.392	2.932
Minimum Period-Based Reactivity Addition								
ACRR ($)[a]	1.424	1.961	2.405	2.889	1.432	1.961	2.411	2.889
Razorback ($)[a]	1.446	1.908	2.387	2.851	1.443	1.912	2.387	2.913

a. Using Λ=24 μs and β_{eff}=0.0073

[This page intentionally left blank.]

5. COMPARISON TO AN ACRR PULSE WITH LONG-TERM COOLDOWN DATA

A Razorback simulation of ACRR pulse operation 11277 was performed. Operation 11277 was a "maximum" pulse operation of ~$3.04 performed on February 2, 2015. In addition to the ACRR Pulse Diagnostic System (which is normally operative during a pulse operation), two other instruments were deployed: (1) a spare ACRR instrumented element (IE-603) was installed in core location 208 to provide a measurement of fuel temperature during the pulse, and (2) a flowmeter tube with an entry funnel (with an internal thermocouple) was placed over the top of the fuel element at core location 225 to provide a measurement of coolant channel outlet temperature. These signals were recorded using a Yokogawa digital oscilloscope/recorder. In addition to these, data for the ACRR's Plant Protection System (PPS) instrumented fuel elements (IE-602 and IE-603) was obtained from the ACRR's LogMaster computer. Figure 67 shows the instrument locations in the ACRR core, and the associated element peaking factor with the control rods at 27.50 cm.

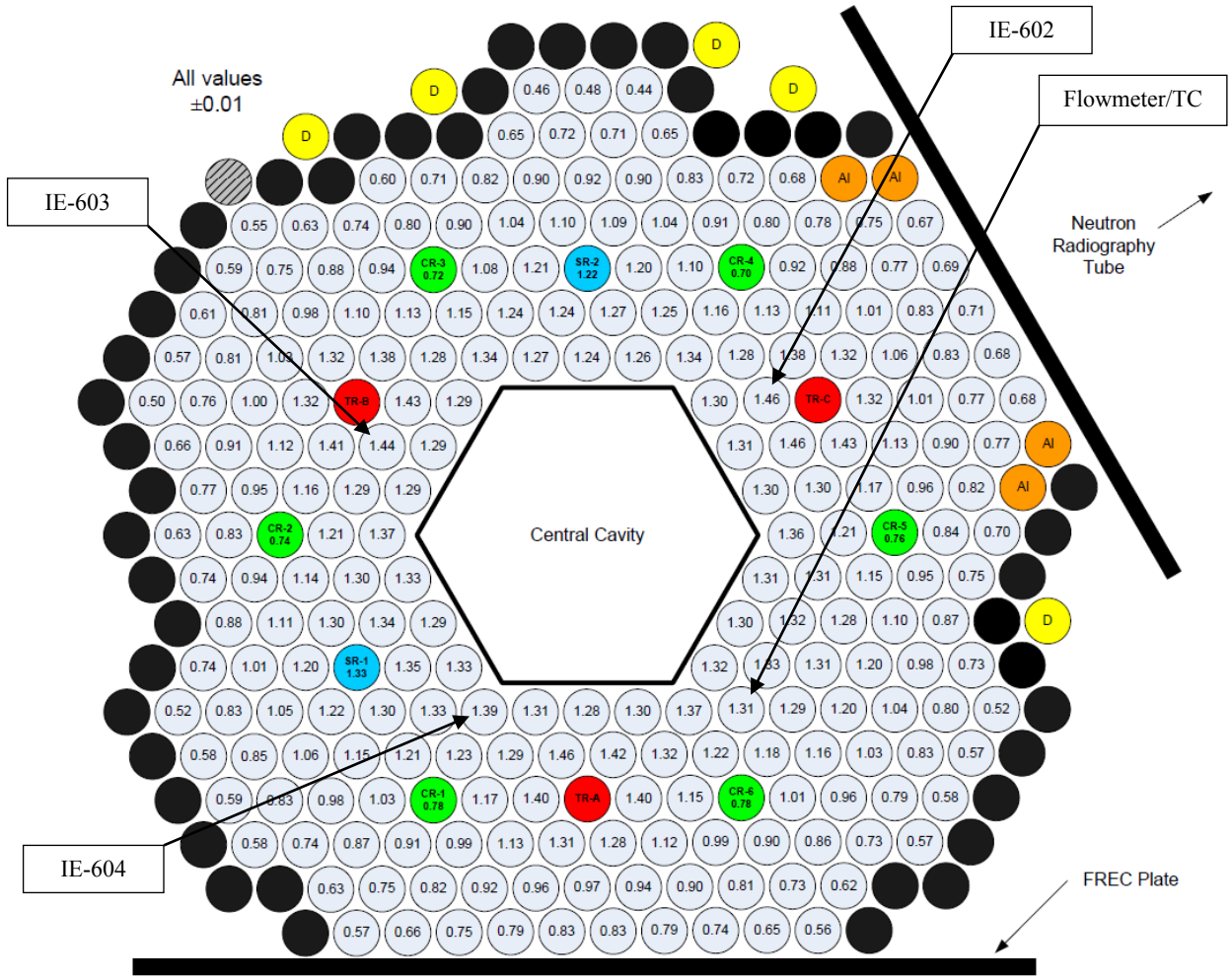

Figure 67. Instrumentation locations for Operation 11277 and 11278.

Figure 68 shows the flowmeter/thermocouple fixture. In the upper left photo in Fig. 68, the flowmeter can be seen at the center of the fixture between the two end flow funnels. The flowmeter itself failed during initial testing of the device installed at the core upper grid, presumably due to radiation exposure. The thermocouple, however, remained operable. The flow funnel on the left (which is enlarged somewhat in the upper right photo) is the portion of the fixture which is seated over an ACRR fuel element at the upper grid plate. The bottom photo shows the inside of this flow funnel, and the thermocouple which was used to obtain the outlet temperature for a fuel element.

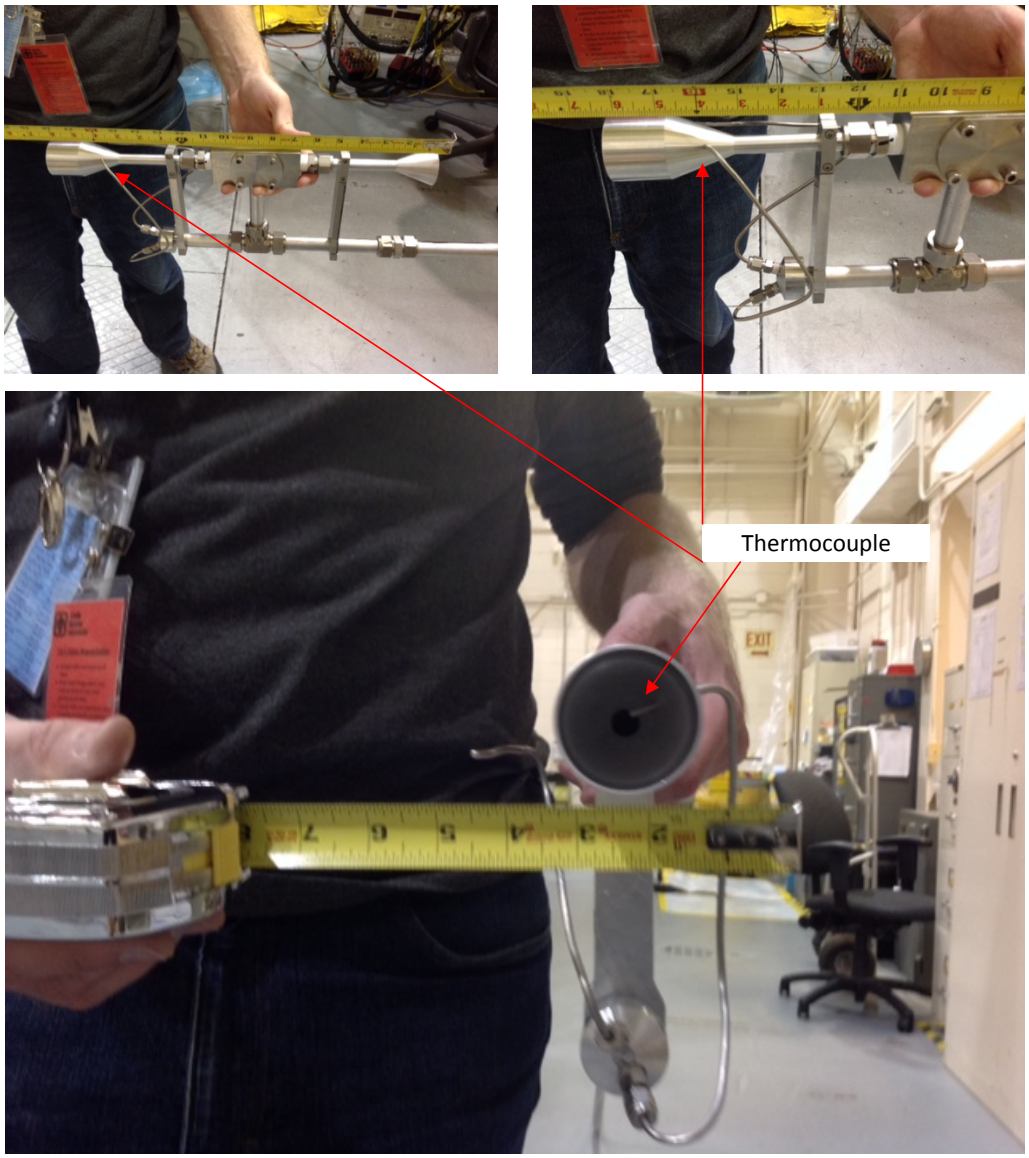

Figure 68. Flowmeter fixture with thermocouple at flowmeter inlet.

The pulse diagnostic system power history for Operation 11277 is shown in Figs. 69 and 70, along with the Razorback simulation of the operation. The fidelity of the simulation is seen in the figures to be similar to that of the pulse operations considered in Section 4.

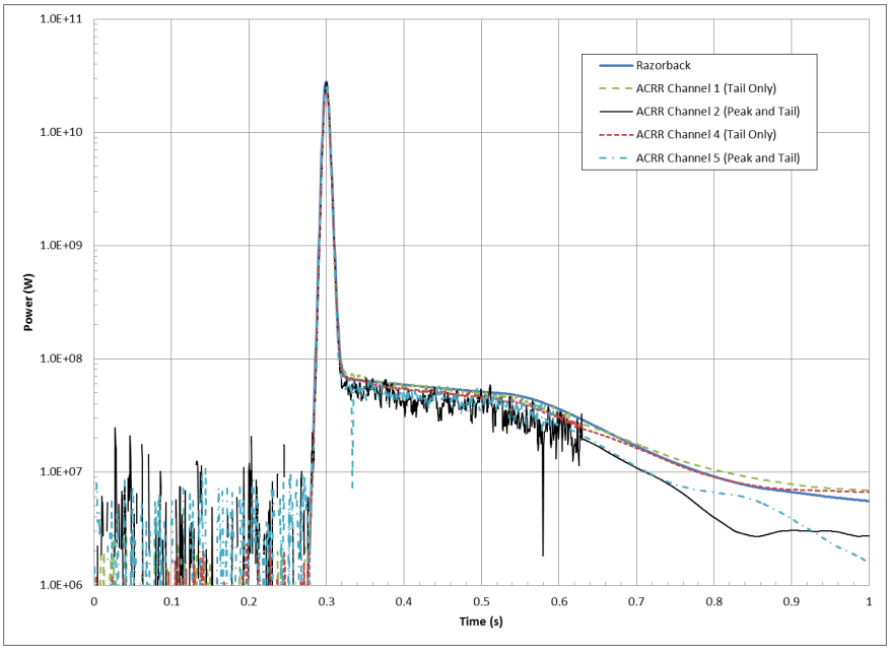

Figure 69. Razorback Simulation of a Pulse #11277 for the first second of the transient.

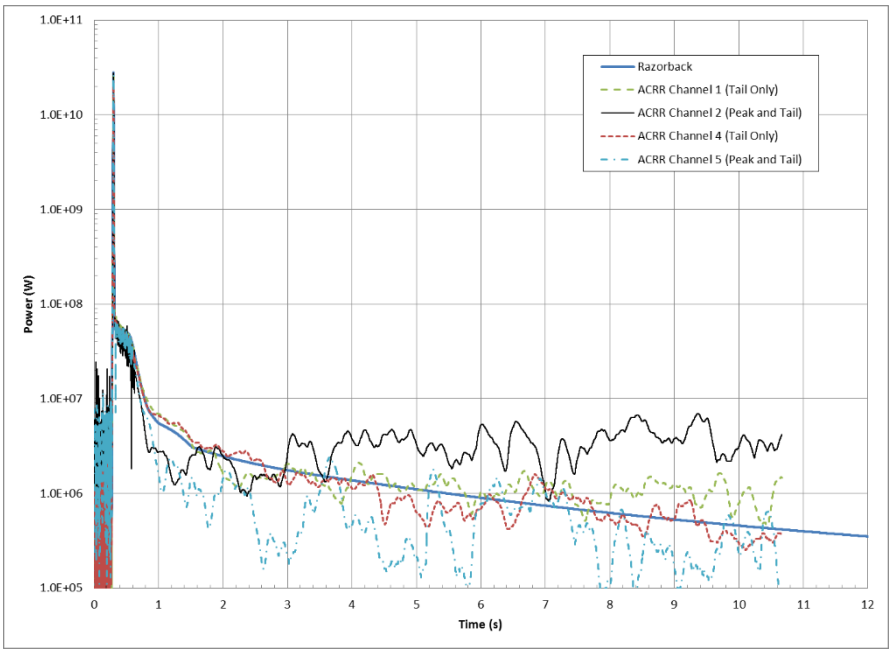

Figure 70. Razorback Simulation of a Pulse #11277 for the first 12 s of the transient.

Figure 71 shows the IE-603 fuel temperature trace from Operation 11277, along with the Razorback measured fuel temperature prediction for an element with a peaking factor of 1.44 (i.e., the peaking factor associated with the IE-603 location). Note first the near instantaneous rise in the IE-603 temperature to ~410°C at the beginning of the transient. This initial temperature rise is due to gamma radiation heating of the IE-603 fuel thermocouple itself, which is made of a W/Re alloy. There is then an initial cooling of the thermocouple until the heat transfer from the BeO-UO_2 fuel begins to heat the thermocouple. The subsequent time evolution of the increase in the measured temperature is due to the thermal time constant of the thermocouple. Note especially that the Razorback measured temperature peaks between 10 and 12 seconds, while the thermocouple has still not attained equilibrium with the surrounding fuel. In this case, the result is that the thermocouple "misses" the peak of the temperature history. This indicates that the maximum PPS measured fuel temperature for a pulse may underestimate the actual maximum fuel temperature. The difference seen in Fig. 71 is ~30°C, but the magnitude of the difference seen here should only be taken qualitatively due to uncertainty in the actual element peaking factor.

Figure 72 shows the Razorback prediction of the long-term fuel cooldown for an element with a peaking factor of 1.46 to simulate the response of IE-602 for the PPS1 fuel temperature. The PPS1 fuel temperature recorded by the Logmaster computer was sampled at a rate of ~ 1 sample per minute. The results show reasonable success early in the transient, and late in the transient. Discrepancies on the order of 70-80°C are seen at intermediate times. The discrepancies may be due to underestimating the clad-to-coolant heat transfer coefficient due to choice of heat transfer coefficient correlation parameters or due to underestimating the local coolant flow rate.

Figure 73 shows the flowmeter funnel thermocouple temperature trace from Operation 11277, along with the Razorback measured fuel temperature prediction for an element with a peaking factor of 1.31 (i.e., the peaking factor associated with the location of the flowmeter/thermocouple fixture). Note first the near instantaneous rise in the flowmeter funnel thermocouple temperature to ~33°C at the beginning of the transient. This initial temperature rise is due to gamma radiation heating of the thermocouple itself, which is Type K chromel/alumel. There is then an initial cooling of the thermocouple until the heat transfer from the coolant begins to heat the thermocouple. The subsequent time evolution of the increase in the measured temperature is due to the thermal time constant of the thermocouple. Note especially that the Razorback-predicted outlet temperature peaks at about 5 seconds, while the thermocouple has still not attained equilibrium with the flowing water. In this case, the result is that the thermocouple "misses" the peak of the outlet temperature history. At about 12 seconds, the thermocouple appears to have reached equilibrium with the flowing water. However, the Razorback result under predicts the measured outlet temperature by about 5°C. A second Razorback prediction, with an element peaking factor of 1.46 is also shown in Fig. 73. This prediction matches better with the measured data. The reason for the under prediction is presumed to be due to underestimating the heat transfer rate to the coolant. The better match with the 1.46 peaking factor results may indicate that the heat transfer rate to the coolant should be ~11% higher than Razorback is predicting.

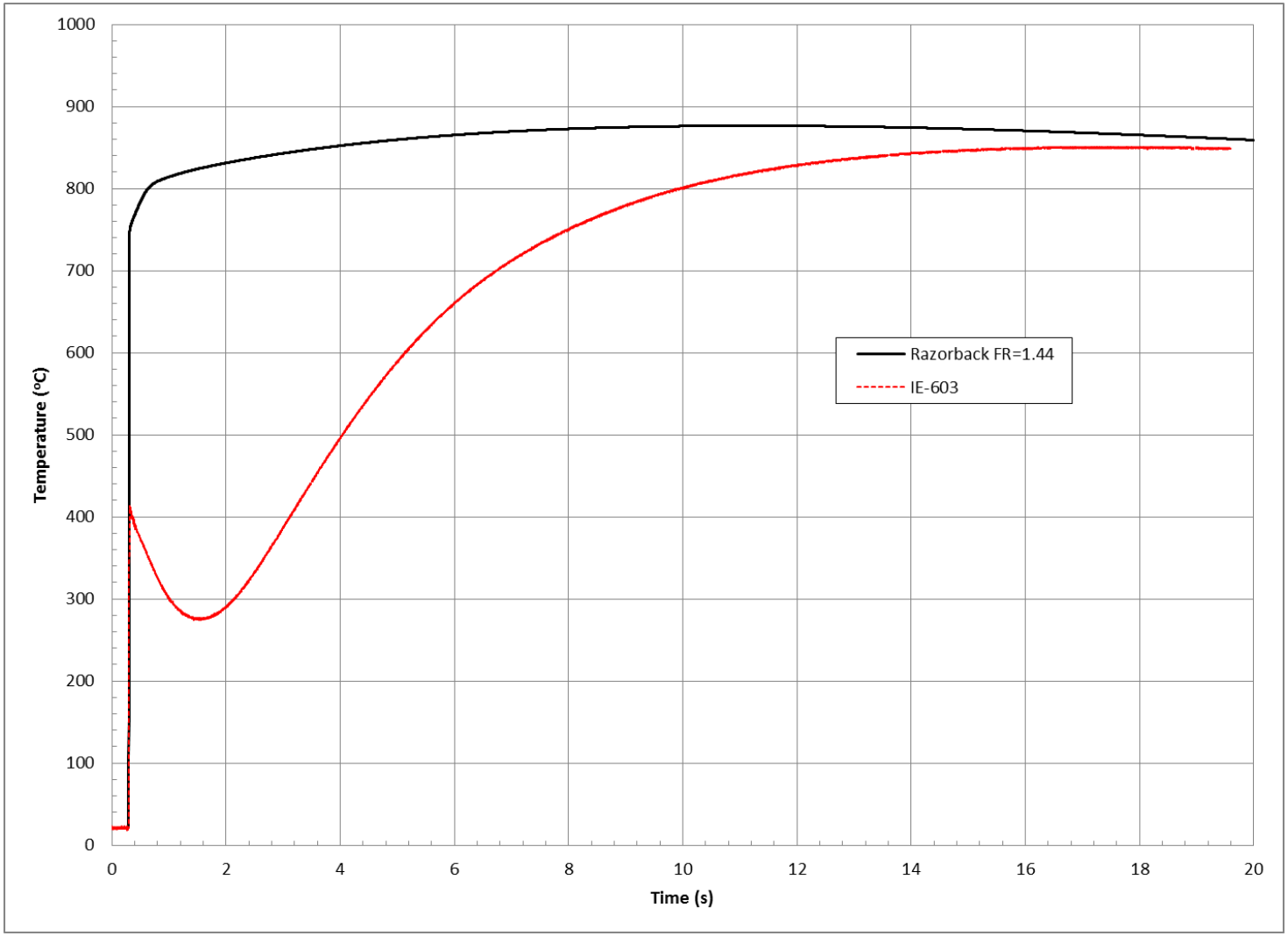

Figure 71. Instrumented Element (IE-603) fuel temperature history for Pulse #11277.

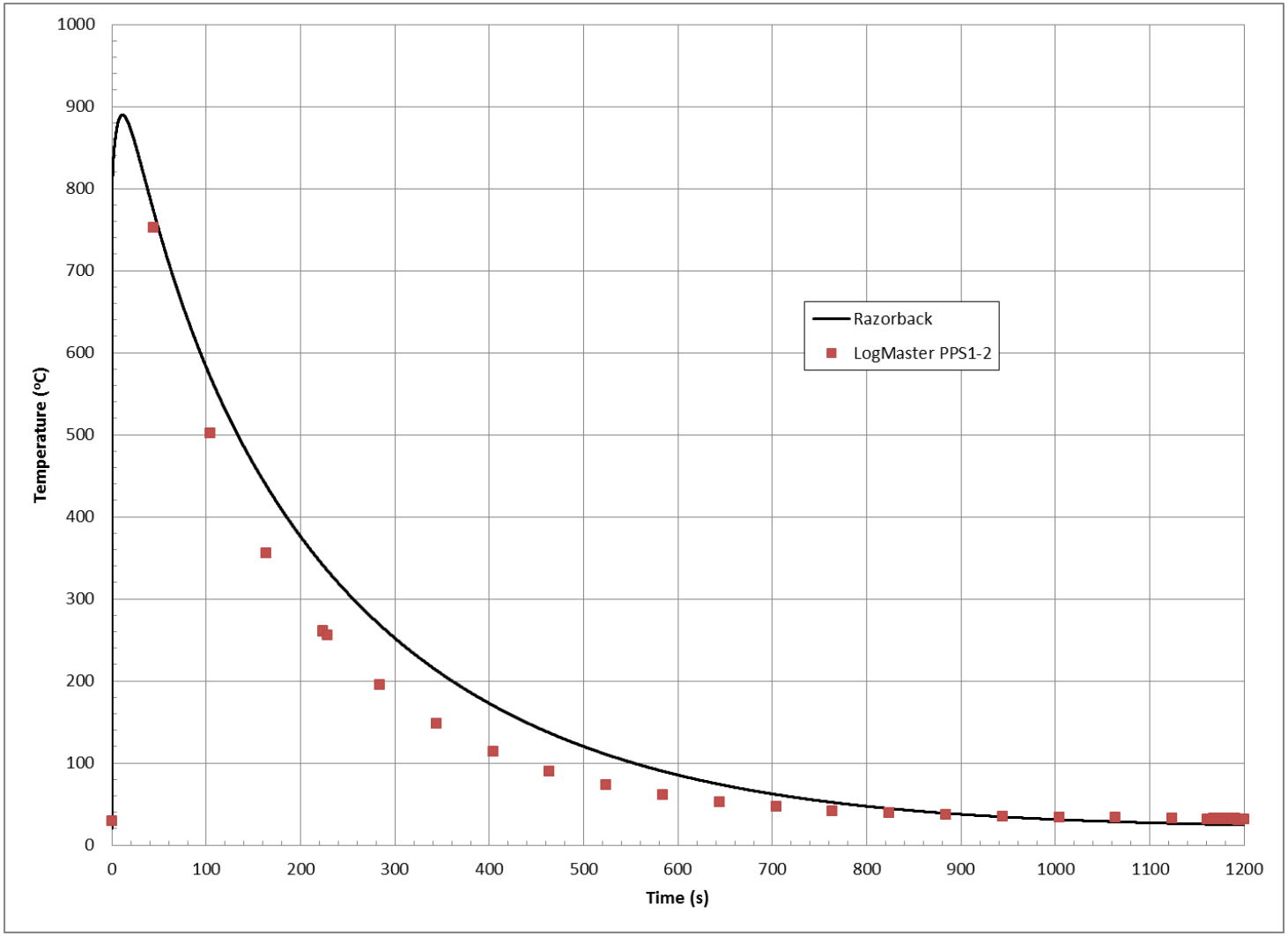

Figure 72. Long term cooldown of the PPS1 instrumented fuel element for Pulse #11277.

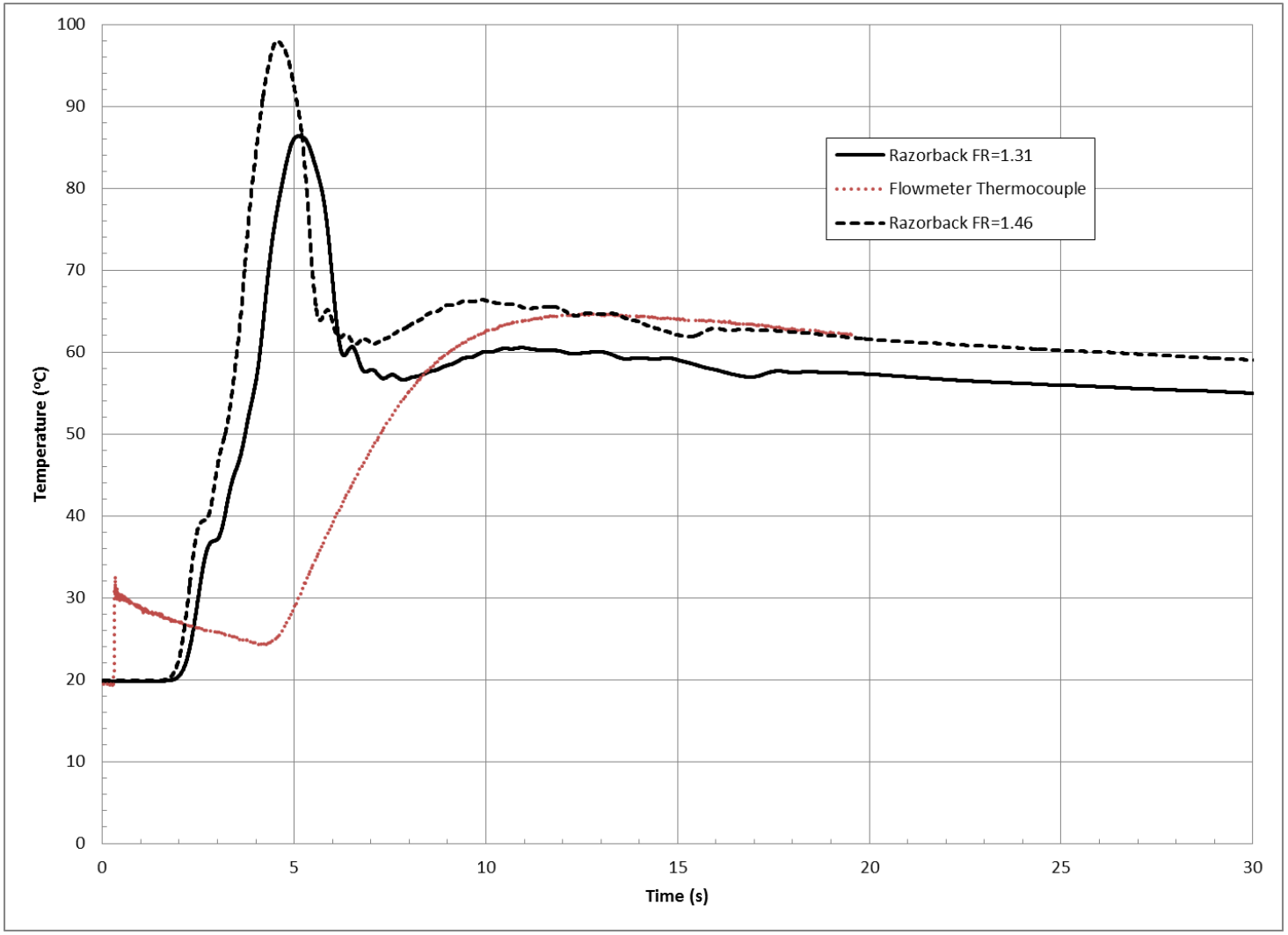

Figure 73. Channel outlet coolant temperature history for Pulse #11277.

The results of the Razorback simulation of a pulse as compared to the longterm cooldown are favorable, but indicate that the fuel-to-coolant heat transfer rate may be underestimated. As noted earlier, this may be due to the heat transfer coefficient correlation, or due to an underestimated coolant flow rate. However, comparison of the predicted coolant outlet temperature with measured results show that the coolant flow rate is likely not underestimated, as this would tend to further decrease the discrepancy between the predicted and measured outlet temperature. The outlet temperature results do appear to indicate that the fuel-to-coolant heat transfer rate is under predicted. Ultimately, however, additional testing and evaluation is needed to confirm these hypotheses. In particular, steady-state operation coolant outlet temperature data is needed to ensure that the discrepancy is limited to transient heat transfer situations such as this post-pulse cooldown.

6. COMPARISON TO ACRR TRANSIENT ROD WITHDRAWAL OPERATIONS

Simulations using Razorback were performed for ACRR Runs 9022 and 9023. These were both TRW operations, with relatively similar TRW programs beginning from a position of 3500 units (1 unit = 0.01 cm). The Console Logs are included as Appendix C. An initial power level of 1.2 kW (0.05% of full power) was assumed for both simulations, and the pool water was assumed to be at 20°C. These assumptions are typical for ACRR operations. However, an assumption regarding the core radial peaking factor was necessary because of the nature of a TRW vs. a pulse or control rod driven power transient.

Since the TRW begins with the TR bank inserted to the 35 cm location, the TR poison section covers just over three-fourths of the fuel. The core radial peaking factor (F_R) for the peak element upon which a Razorback analysis is typically based is 1.46. This peak location is directly adjacent to a TR, which is normally fully withdrawn in steady-state mode, or rapidly withdrawn (~80 ms) for a pulse operation. Since much of the TRW to be modeled occurs with the TR bank position between one-half and three-fourths inserted, a new estimate of the peaking factor is needed. The need for estimating a new peaking factor may also be seen by examining the peak fuel temperature results shown in the Console Logs in Appendix C. The peak measured fuel temperatures associated with PPS1 (measured by an instrumented fuel element directly adjacent to a TR) are normally higher than those for PPS2 (measured by an instrumented fuel element at a corner of the central cavity) because the F_R is larger at the PPS1 location. However, the Console Log results show PPS1 temperatures to be less than PPS2 temperatures. This is due to a reduction in the TR-adjacent fuel element F_R because of the inserted position of the TRs during the operation.

An initial simulation of TRW 9022 with an F_R of 1.46 resulted in a peak measured fuel temperature of ~920°C, compared to the PPS1 peak measured fuel temperature of ~720°C (see Appendix C). If the F_R is multiplied by the ratio of the measured temperature change to the simulated temperature change, a reduced F_R of 1.135 results (which can be set as 1.15, simply for the sake of having a "round" number). By consulting Ref. 7, one can see that the peaking factors near a one-half to three-fourths inserted control rod are reasonably close to 1.15. Thus, an F_R of 1.15 was selected and the TRW simulations were executed again.

Figure 74 shows the TR bank movements and resulting power traces in the Razorback simulations of TRWs 9022 and 9023. The initial movement for TRW 9022 is from 3500 units to 4428 units in 1.0 s and dwelling until t = 1.6 s, while the initial movement for TRW 9023 is from 3500 units to 4428 units in 1.6 s. From t = 1.6 s onward, the TR bank movements are exactly the same. While the TRW 9022 TR movement dwells from t = 1.0 s to t = 1.6 s, the initial pulse is allowed to be turned over by fuel temperature feedback. For TRW 9023, TR bank movement does not dwell after reaching 4428 units, but rather continues withdrawal. Therefore, the initial pulse for TRW 9023 has a higher peak power than that for TRW 9023. However, since both TRWs initially proceed to the same point (4428 units), and are the same from this point on, we would expect that the peak fuel temperature attained would be essentially the same. Figure 75 shows that the predicted temperature traces for both TRWs are indeed essentially the same,

peaking at a measured temperature of ~720°C (compared to 718°C and 723°C for the actual TRW results shown in Appendix C.

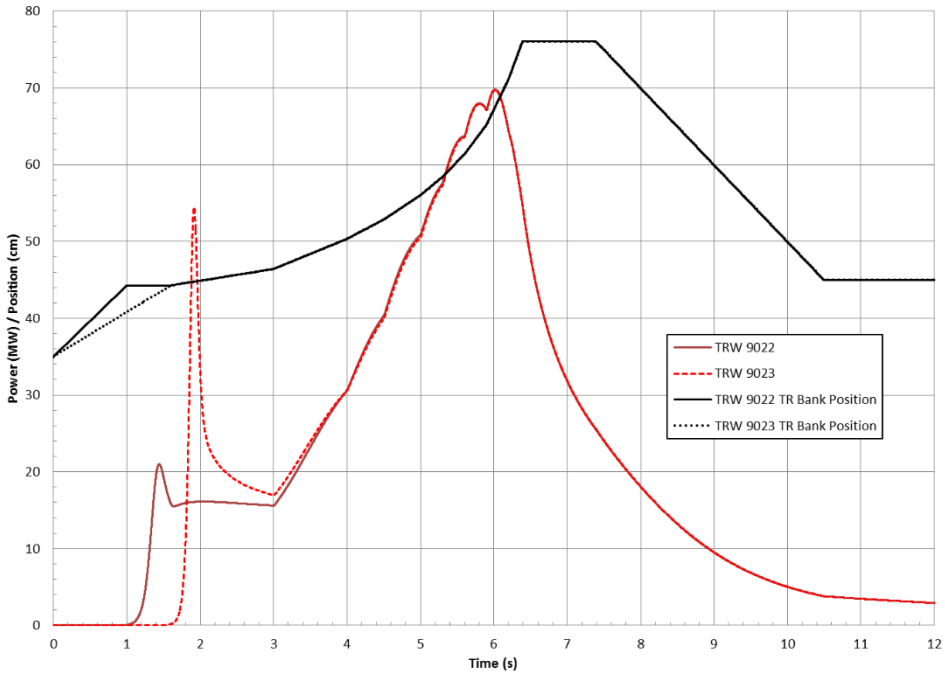

Figure 74. Transient rod bank movement and reactor power response for Razorback simulations of TRWs 9022 and 9023.

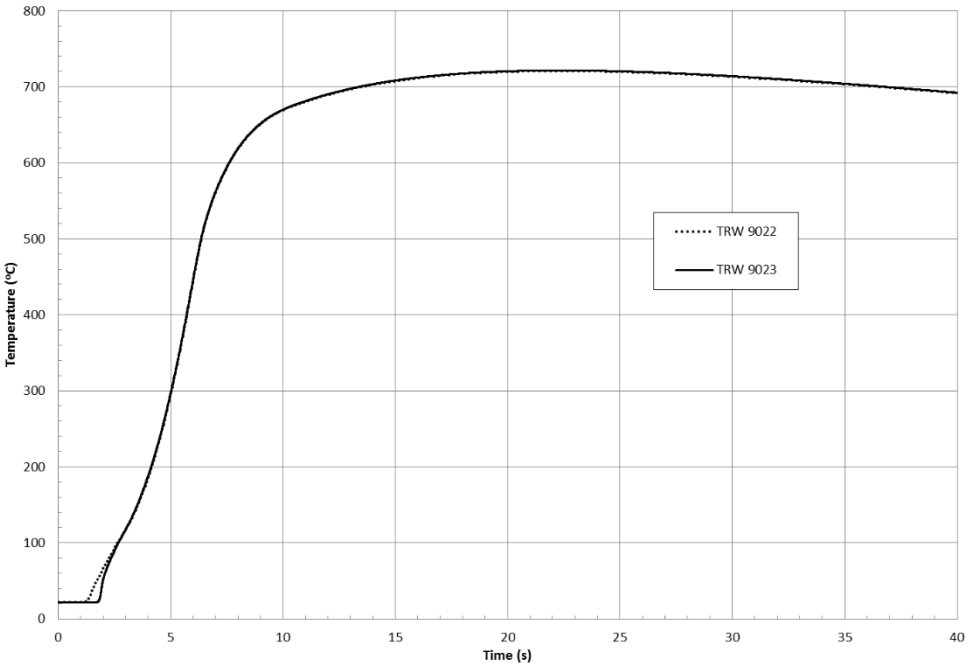

Figure 75. Measured temperature response for Razorback simulations of TRWs 9022 and 9023.

The results of the simulations are shown in Figs. 76 and 77, which show ACRR power levels as measured by Channels 1, 2, and 3 of the Diagnostic System, the power level determined in the Razorback simulations, and the position of the TR bank during the TRW. Razorback achieves a good match with the timing of the initial pulse for TRW operation 9022, but the initial peak power is lower than that for all three ACRR Diagnostic System channels. The initial peak power is low and the timing of the initial pulse peak is off for TRW operation 9023. It should also be noted that Operation 9023 was initiated approximately one hour and twenty minutes after Operation 9022, which would leave an elevated photoneutron source level in the fuel. Thus, the assumption of an initial power of 0.05% for 9023 (as was used for 9022) may not be valid.

The comparison of the simulations with the second higher power peak is qualitatively good (with respect to matching the shape of the profile response to the TR bank movements), but the Razorback predicted power profile is higher than the measured profile. This could be due to the non-ideal fit of the TR differential worth curve using an assumed $\sin^2(z)$ relationship. It may also be due to differences in the as-programmed and actual TR bank movement history resulting from the inertia of the drive system components. Also, the response of Channel 1 of the Diagnostic System is troubling in that its response sensitivity appears to have autonomously increased to the level of Channel 2 between the two TRW operations.

In general, the Razorback results demonstrate reasonable agreement with the TRW operations. Because of the non-rigorous means of estimating the proper F_R to be used in the simulations, it is best to simply conclude that Razorback is capable of modeling TRW operations in conjunction with experience-based selection of inputs. The reasonable agreement is considered to be noteworthy given the interplay of the various reactivity feedback mechanisms (i.e., fuel temperature, fuel and cladding expansion, coolant density and temperature).

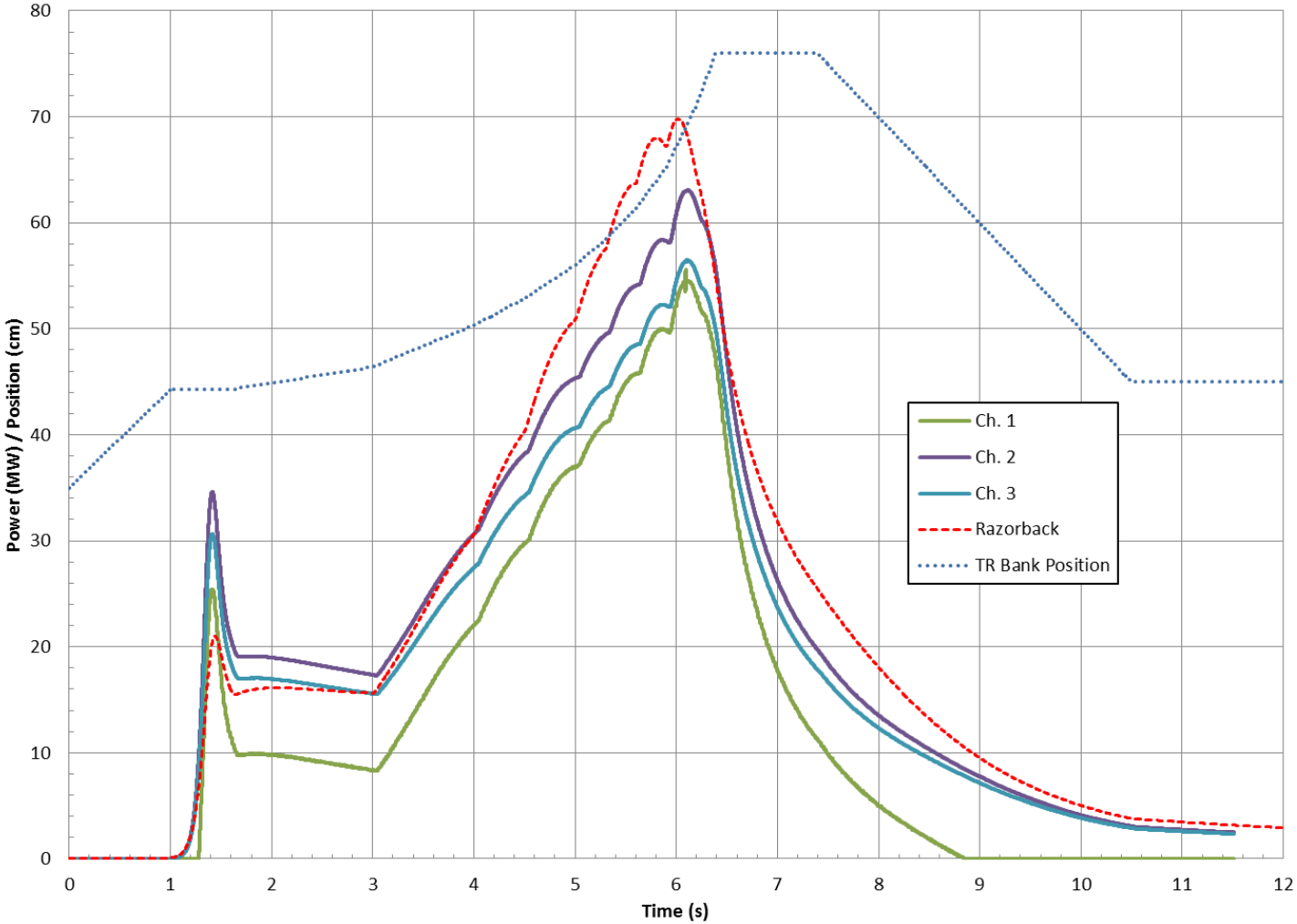

Figure 76. Razorback Simulation of TRW Operation 9022.

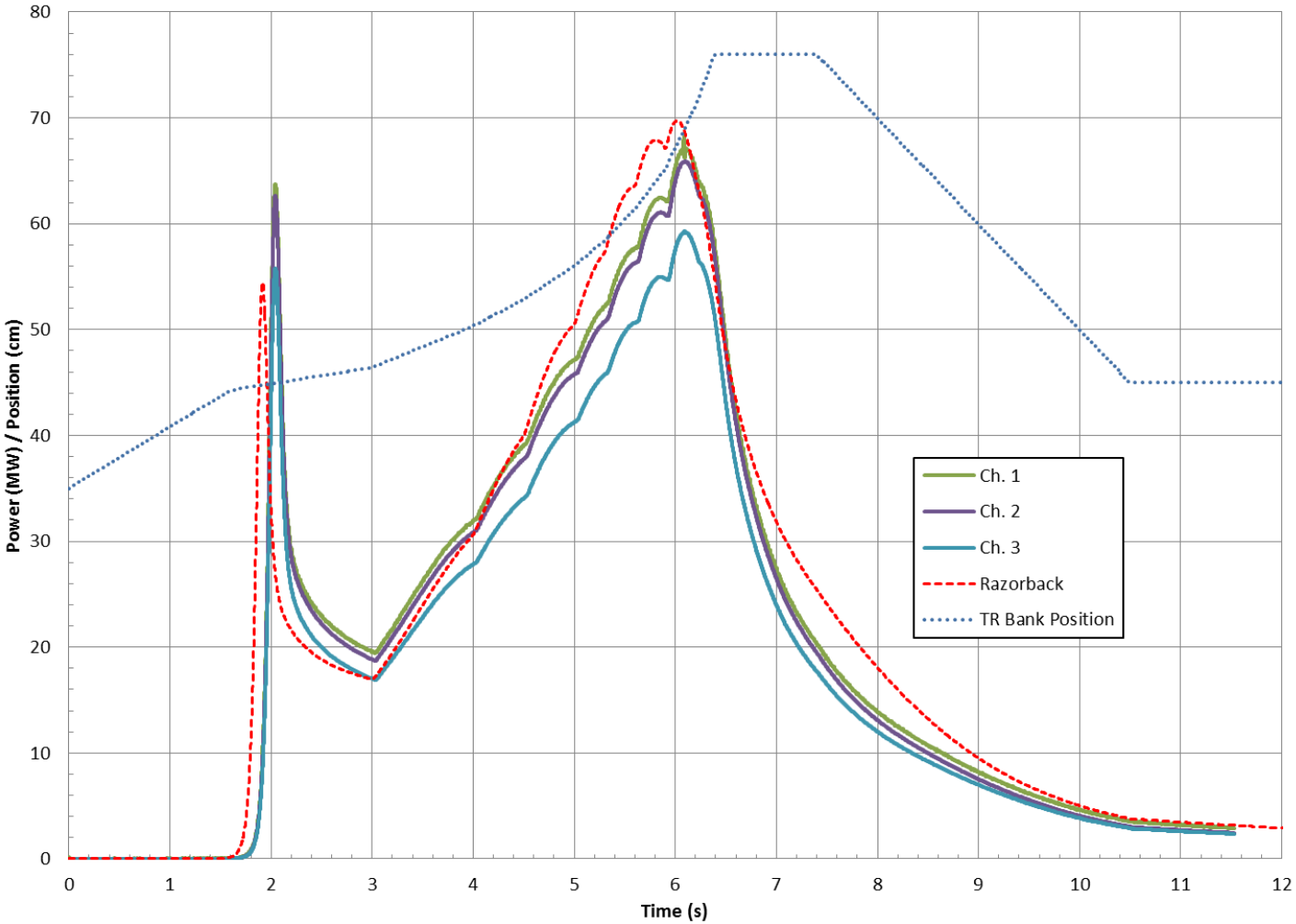

Figure 77. Razorback Simulation of TRW Operation 9023.

[This page intentionally left blank.]

7. COMPARISON TO A SLOW REACTOR TRANSIENT OPERATION

On February 2, 2015, a planned slow reactor transient was conducted with the intent of stepping down in reactor power in controlled increments, attaining a steady power level for a few minutes after each step down. Specifically, the following operation plan was followed:

- Achieve steady-state at ~90% of full power.
- Drive the control rod bank in 50 units (0.50 cm)[9], and allow the reactor to attain a new steady power level.
- Drive the control rod bank in 100 units (1.00 cm), and allow the reactor to attain a new steady power level.
- Drive the control rod bank in 150 units (1.50 cm), and allow the reactor to attain a new steady power level.
- Drive the control rod bank in 200 units (2.00 cm), and allow the reactor to attain a new steady power level.
- Drive the control rod bank in 200 units (2.00 cm), and allow the reactor to attain a new steady power level.
- Drive the control rod bank to full down, and allow the reactor to attain a new steady power level.

This operation was simulated in Razorback by constructing a set of control rod operation commands to match the actual control rod motion of the ACRR as recorded by the Logmaster computer. The control rod commands input to Razorback were as follows:

Control Rod Bank Control (1=on w/curve, 0=off, 2=ramp)	Number of CR Bank Commands (up to 20)	
1	12	
CR Start Time (s)	CR End Time (s)	CR Speed (cm/s) or Ramp ($/s)
0.0	5.3	-0.10
5.3	204.0	0.00
204.0	213.9	-0.10
213.9	453.0	0.00
453.0	467.9	-0.10
467.9	738.0	0.00
738.0	758.2	-0.10
758.2	1108.0	0.00
1108.0	1128.2	-0.10
1128.2	1558.0	0.00
1558.0	1754.4	-0.10
1754.4	3600.0	0.00

[9] 1 unit = 0.01 cm.

The comparison of the Razorback rod motion due to this input with the ACRR control rod motion is shown in Figure 78.

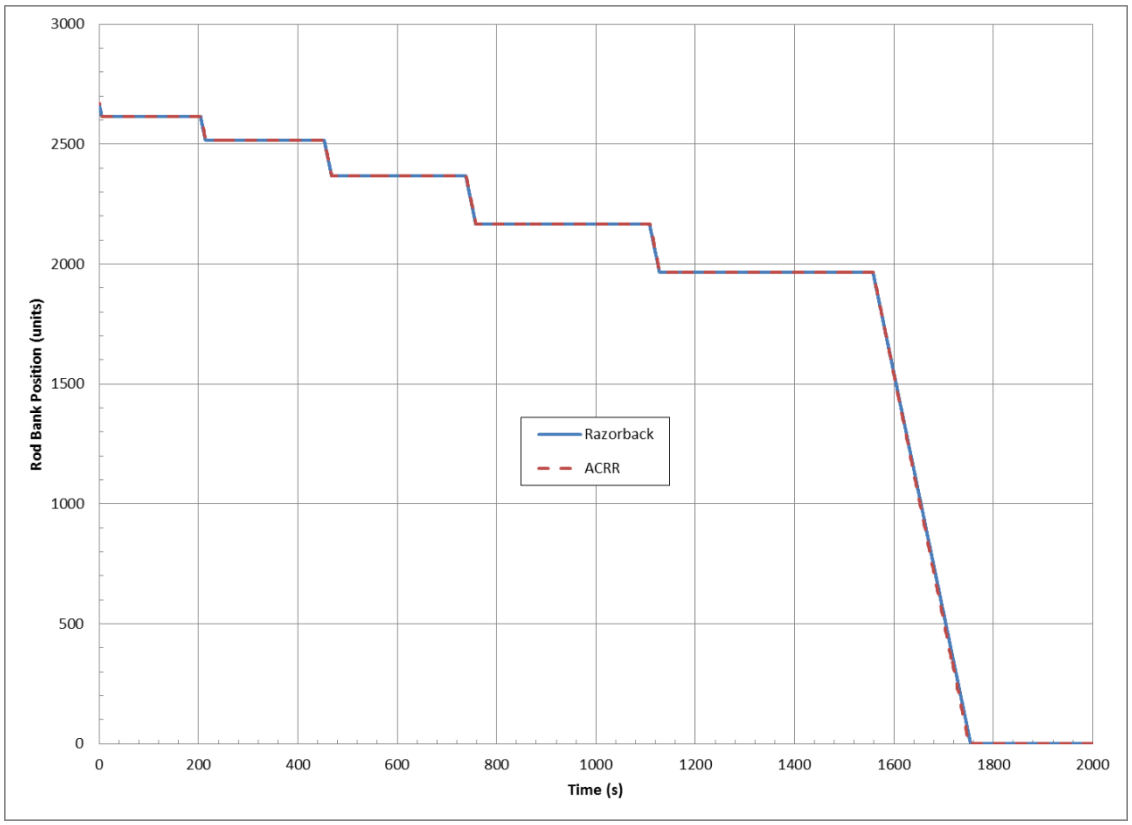

Figure 78. Comparison of ACRR and Razorback Control Rod Bank Motion During Operation 11278.

Figures 79 and 80 show the results for the power and "measured" fuel temperature history of the Razorback simulation compared to the ACRR power (Wide Range Log Power, Channel 1) and temperature (PPS1-TC2) history. The power history results match reasonably well, with better agreement at power levels above about 20-30 %Full Power (%FP). A significant discrepancy arises around 10-20%FP. The temperature history matches well in general shape, but there is clearly an offset in the magnitude of the predicted temperature which is on the order of 150-200°C. This offset is similar in magnitude to that seen in the comparison of steady-state fuel temperatures (see Section 8), and is likely due to the same factors discussed in Section 8.

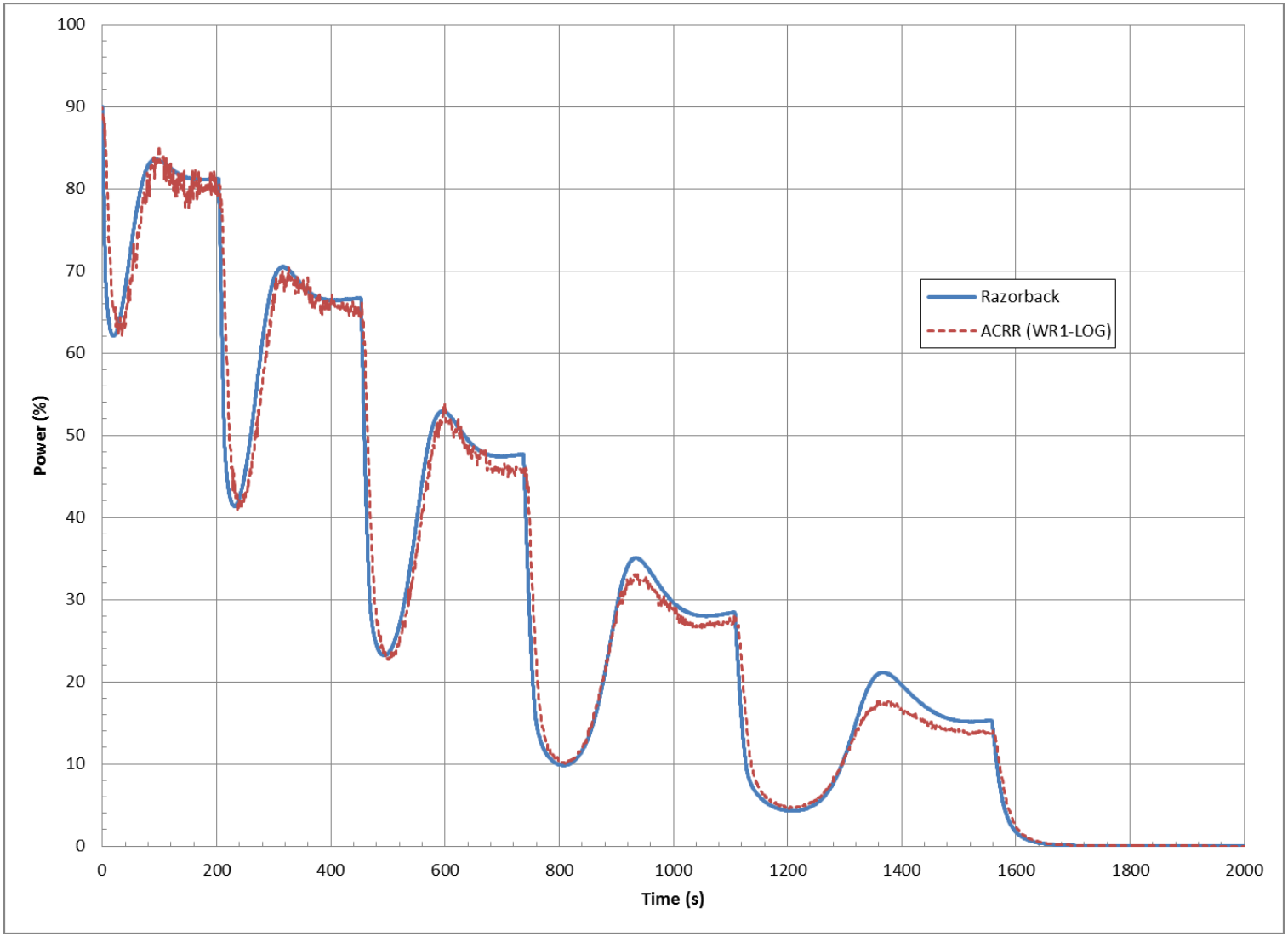

Figure 79. Comparison of Razorback Predicted Power History to Operation 11278.

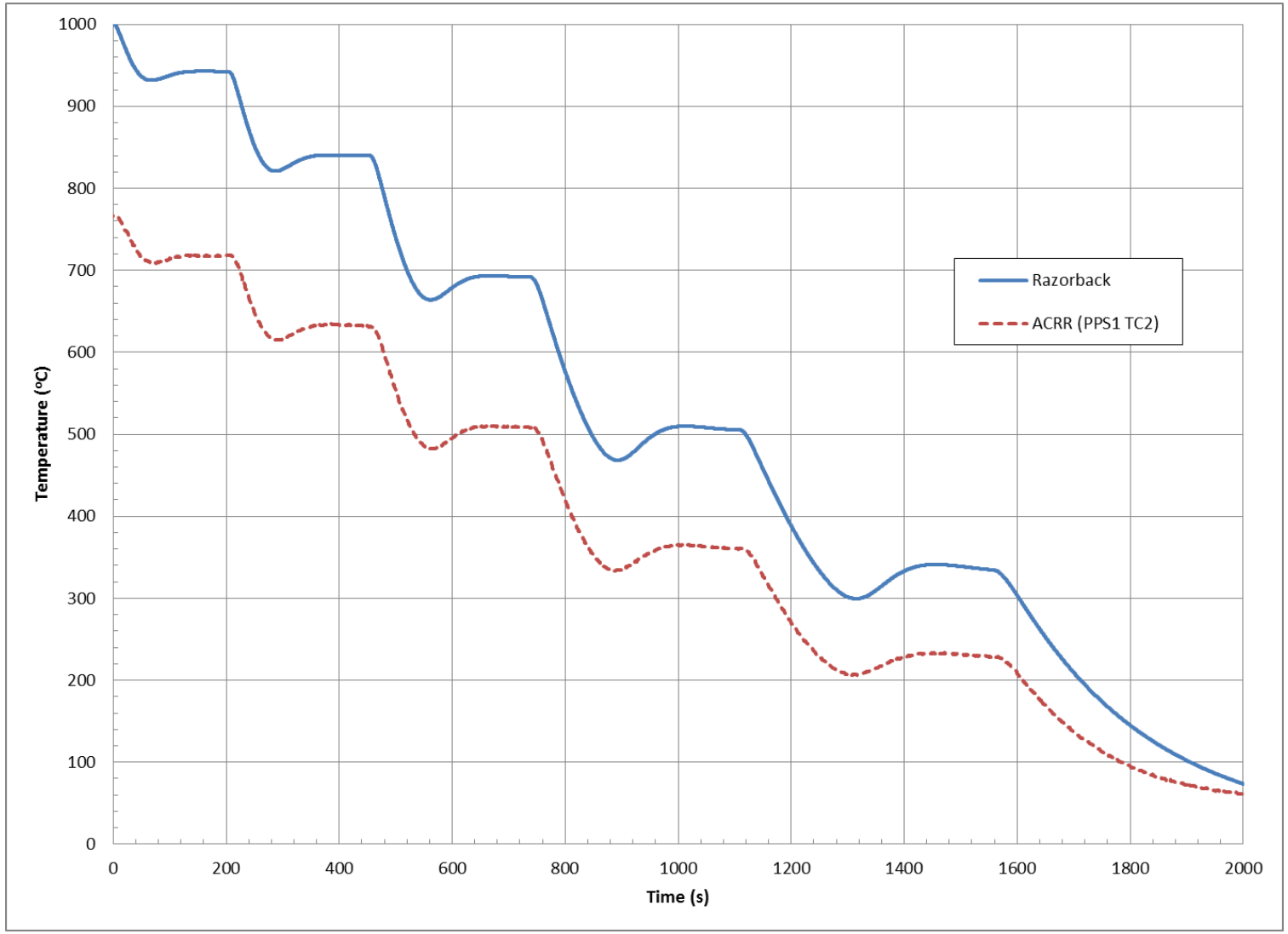

Figure 80. Comparison of Razorback Predicted Fuel Temperature for Operation 11278.

8. COMPARISON TO ACRR STEADY STATE OPERATION

The Razorback code was run in steady-state mode to compute estimates of the measured fuel temperature in the ACRR for various element power levels. The results are shown in Fig. 81. There are three temperature vs. power data sets also presented in Fig. 81 for comparison with the Razorback results. The first is referred to as "Parma 1998," and uses a correlation[10] intended to predict ACRR measured temperature for a given ACRR fuel element power level (Ref. 21). The analyses in Ref. 21 which were used to produce the correlation were performed using the CYLSS code (Ref. 22), which is similar in function to Razorback, but developed independently. The second is referred to as "ACRR IP Measurements," and is a correlation (Ref. 12) based on ACRR fuel temperatures measured while operating the ACRR in its Isotope Production configuration.[11] The third data is a set of temperatures corresponding to the power plateaus for Operation 11278 (see Section 7).

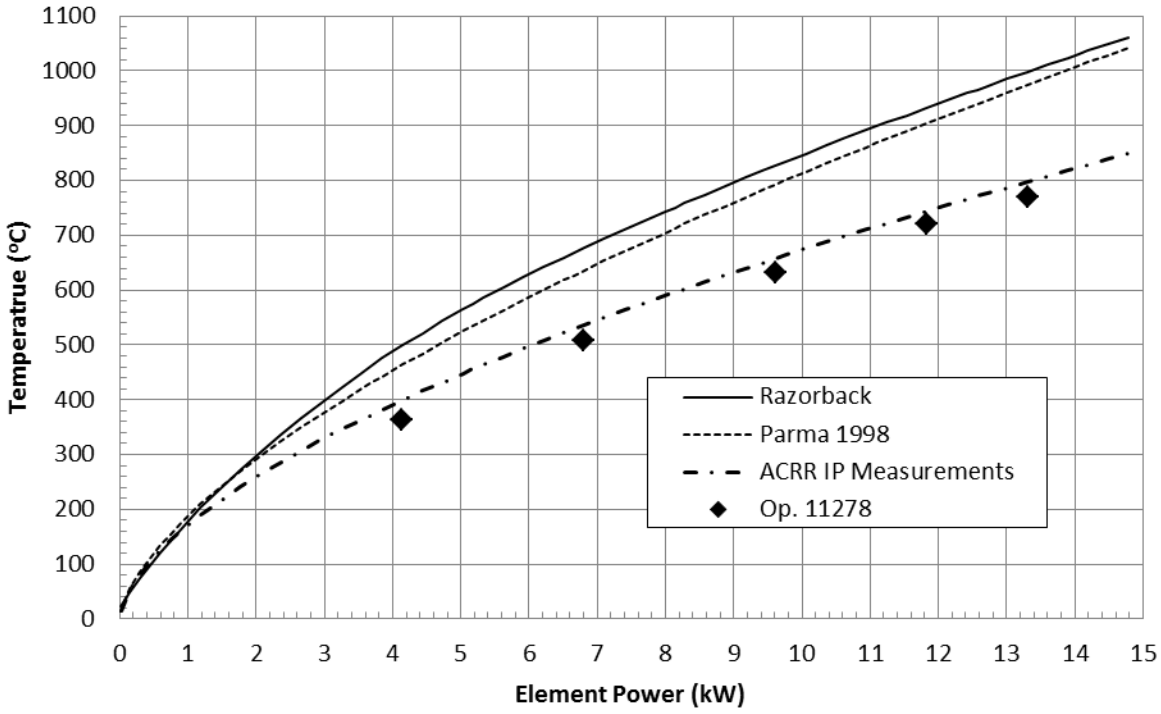

Figure 81. Comparison of Predicted Fuel Temperatures with Various References.

Figures 82 and 83 show the error in the predicted temperatures (absolute and relative, respectively) as a function of reactor power level. The comparison to Parma's CYLSS code provides additional evidence of the proper implementation and solution of the governing heat transfer equations in the Razorback code. The differences are within ±10% for element powers above ~1 kW, with larger relative differences only for lower powers where fuel temperatures are decreasing. The differences fall below 5% after ~9 kW.

[10] This power law correlation was $T(°C) = 187.9[P(kW)]^{0.636}$.

[11] This power law correlation was $T(°C) = 171.9[P(kW)]^{0.593}$.

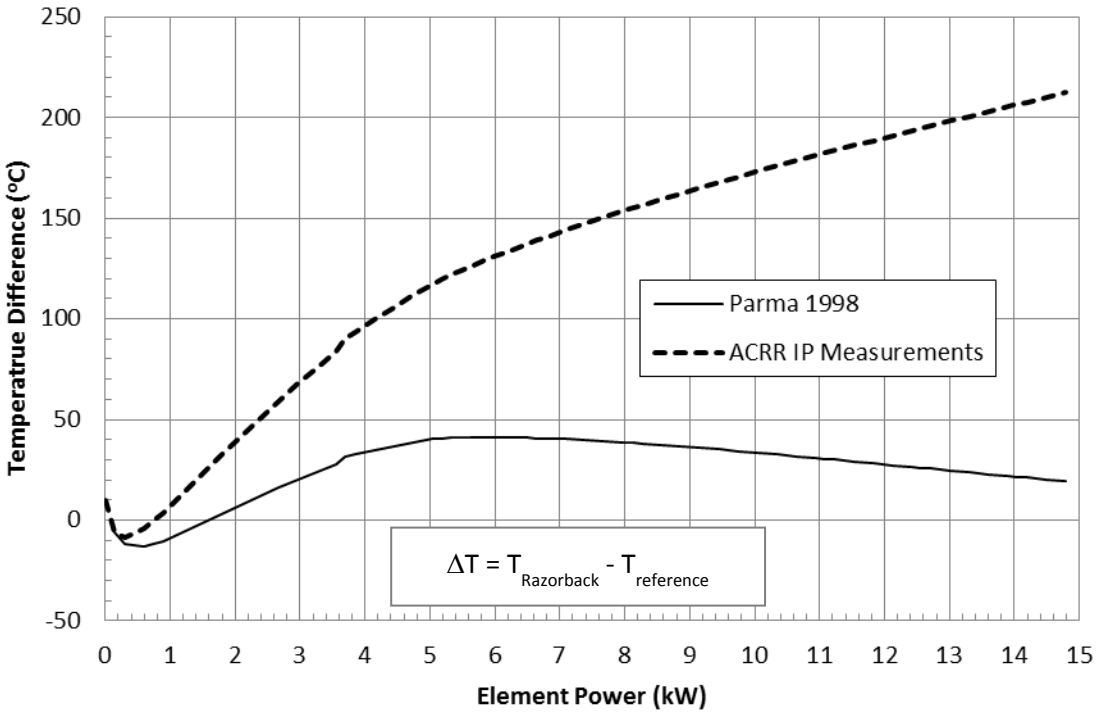

Figure 82. Difference in Predicted vs. Reference ACRR Fuel Temperatures.

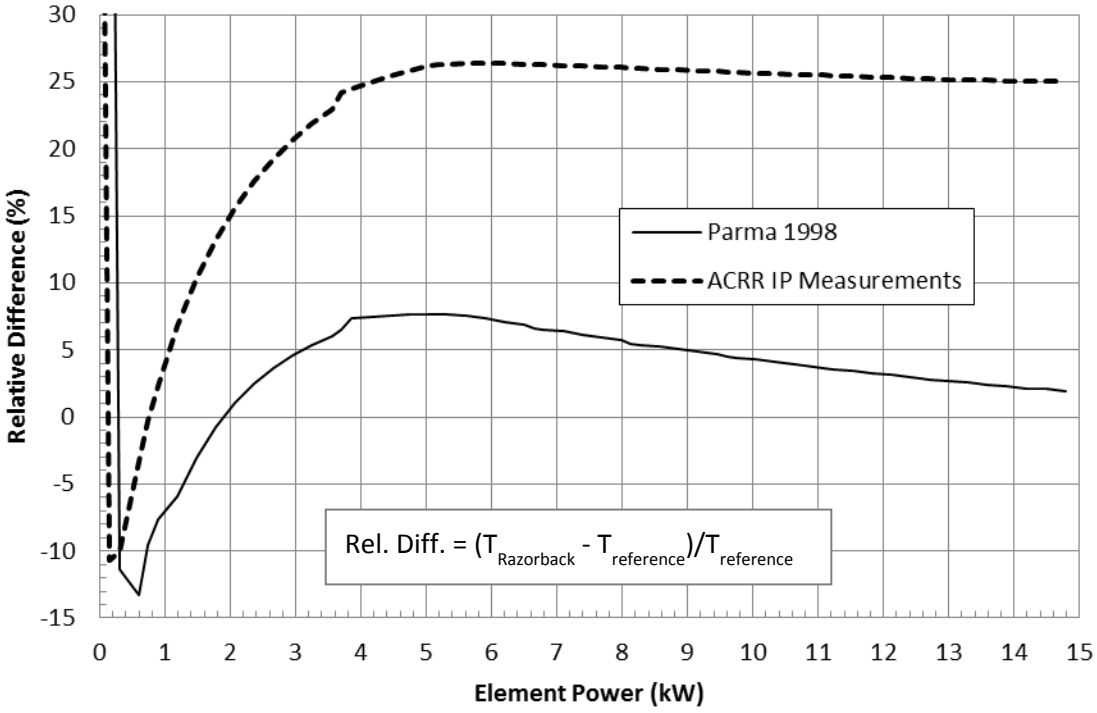

Figure 83. Relative Difference in Predicted vs. Reference ACRR Fuel Temperatures.

Comparison to the ACRR Isotope Production fuel temperature measurements are not favorable, other than that the predictions are generally conservative (i.e., higher than the reference). Differences are greater than 100°C for element powers above 4 kW, and monotonically increasing to over 200°C at element powers of ~15 kW. The relative difference is seen to rise to above 25% at 4 kW and remain relatively constant up to 15 kW.

Potential causes for the predicted fuel temperatures being much higher than actual include:

- Fuel pellet dimensions are greater than specified in design drawings.
    - The actual fuel pellet dimensions may be such that the gaps between the fuel pellets and the niobium fuel cup are smaller than indicated on drawings, which would lead to lower predicted fuel temperatures. The outer radius would have to be 180% out of tolerance to decrease the temperature to ~850°C at 2.39 MW. This degree of out-of-tolerance is not likely.
- Thermal expansion of the fuel relative to the niobium can is underestimated.
    - The linear thermal expansion coefficient for the fuel may be underestimated. However, the actual thermal expansion coefficient would need to be a factor of three higher to yield fuel temperatures of ~850°C.
- The vertical fluting of the niobium can is impacting the overall heat transfer.
    - The niobium fuel cans have vertical fluting which alternately extends into the gap between the fuel and the can wall, and into the gap between the can wall and the cladding. It is possible that the local heat transfer across the gaps is enhanced, which could lead to lower-than-predicted fuel temperatures (if these features are not modeled).
- The smaller inner fuel pellets in the Instrumented Fuel Elements may be impacting the internal fuel temperature.
    - The inner fuel pellets of the upper half of the Instrumented Fuel Elements have 40° segments removed to form a path for two thermocouple guide tubes to be placed on either side of the central thermocouple tube. The "missing" fuel and/or resultant geometry may be affecting the temperature distribution within these elements.
- The Instrumented Fuel Element thermocouple tube end plate may be affecting local heat transfer and temperature distributions.
    - The three thermocouple tubes in the Instrumented Fuel Elements are welded to a thin molybdenum disk at the fuel element mid-plane. This end plate may be altering the local heat transfer and temperature distributions within these elements.

There is evidence that the power levels determined during ACRR pool heatup calibrations may be conservatively lower than the actual power levels. Appendix D presents this evidence.

At this point we must conclude that the Razorback steady-state fuel temperature predictions are conservatively high. As such, the analyst should take this into account when performing work with Razorback. In general, conservatively high fuel temperature prediction is favorable for safety analyses.

As a post-script here, it is noted that a different set of reactor power detectors is utilized for ACRR steady-state operation vs. pulse operation. The steady-state mode power detectors are calibrated using the pool heatup power determination method. The Pulse Diagnostic System (PDS) uses different detectors which are periodically adjusted to correlate with dosimetry measurements. Thus, the actual-to-indicated power ratio issue discussed here would not necessarily apply to the PDS results, as periodic dosimetry adjustments would most likely eliminate much of the potential discrepancy.

9. CONCLUSIONS

In Section 3, it is seen that the agreement of the code results with analytical solution data is excellent (with relative errors on the order of 0.1%) for the reactor kinetics model (covering a wide variety of reactivity inputs), the model for heat transfer within a fuel element, and the model for thermal expansion of the fuel element materials. The agreement of code results with analytical solution data for mechanical stress is good (within ±10% for von Mises stresses). Stresses are computed from gradients of the displacement results. Thus, we note: (1) stress computations involve numerical differentiation of the discrete numerical displacement results, and (2) stress computations are independent of the reactor kinetics and thermal-hydraulics.

The pulse operation simulations agree well with the Pulse Diagnostic System (PDS) data. Maximum measured fuel temperatures during a simulated pulse are within 2% for pulses above $2, and within 5%-10% for pulses below $2. Predicted peak power is generally low by ~10%-15%, although the predicted peak power for both $2 pulses used for comparison about 20% low. The reason for this particular discrepancy is unknown. Prediction of peak power is improved when better estimates of the initial reactor power are available. Predicted pulse energy yield is generally within ~±10%-15%. Predicted FWHMs are 1%-12% high. The author is not aware of a documented evaluation of the measurement error associated with the PDS, but an estimate of ±10% for overall accuracy would not be unreasonable.

The total energy yields of the pulse operation simulations were also compared with total energy yields determined via neutron dosimetry activation via the methodology of Ref. 27. Under this comparison, Razorback under predicts the total yield from 5%-20%, with the predictions improving as the pulse size increases. The uncertainty of the dosimetry method is expected to be on the order of ±10%. The under prediction of total energy yield may be related to the prediction of the post-pulse decay power tail.

The TRW operation simulations agree reasonably well with the PDS data. The discrepancies in initial pulse peak power and timing may be attributable to actual vs. demanded Transient Rod bank position for the TRW operation. TRW mode is not currently available, but new TRW operations should be run when it becomes available in order to obtain additional and more complete data for V&V comparison. Further work is needed to determine if better Transient Rod bank worth curves improve the accuracy of the simulations in the later time portion of the TRW operations.

Simulation of the longterm cooldown of a fuel element after a pulse indicates that Razorback may be underestimating the fuel-to-coolant heat transfer rate. Likewise, a comparison with coolant outlet temperature measurements made during the same pulse indicates possible underestimation of the fuel-to-coolant heat transfer rates.

The power stepdown transient operation simulation agrees well with the ACRR reactor power history data. However, there is a clear offset (~30-40%) in the prediction of the ACRR measured fuel temperatures for that power history. Razorback predictions of ACRR fuel temperature in a steady-state mode also appear to be high (~25% for appreciable element power levels). Further

work is needed to determine the reason[12] for this offset in predicted fuel temperatures for steady-state and quasi-steady-state operation. The fuel temperature results are, in general, conservative.

The Version 1.0 release of the Razorback code is considered adequately verified and validated for use in the simulation of ACRR transient and steady-state operation.

[12] See Appendix D for a possible reason for the offset.

10. RECOMMENDATIONS FOR FURTHER WORK

The following areas for additional work have been identified over the course of developing and evaluating the results presented herein:

- A means of providing a documented calibration basis for the Pulse Diagnostic System is needed.
- A means of reducing the Pulse Diagnostic System power trace noise in order to better estimate the minimum reactor period should be pursued.
- A 3-D finite element model of a fuel element and an Instrumented Fuel Element needs to be developed to address important issues:
    - The temperature distribution within a fuel element using a better representation of the niobium fuel can fluting and its impact on the gap heat transfer rates.
    - The temperature distribution within a fuel element due to the impact of fuel pellet shifting.
    - The temperature distribution within an Instrumented Fuel Element using a detailed representation of the modified inner fuel pellets, the thermocouple guide tubes, and the molybdenum thermocouple end plate.
    - Relating the measured temperature in an Instrumented Fuel Element to the maximum fuel temperature within a fuel element.
- The methodology and assumptions for the ACRR pool heatup calorimetric power determination need to be re-examined, and other methods of power calibration need to be considered.
    - A 3-D model of the ACRR pool should be developed to determine the flow patterns within the pool during a pool heatup power determination.
    - The ACRR's bulk cooling system should be used to determine the heat rejection rate from the ACRR pool and relate this to reactor power.
- Obtain channel outlet temperature measurements for use in V&V of steady-state and transient simulations.
- Obtain channel flowrate measurements for use in V&V of steady-state and transient simulations.

[This page intentionally left blank.]

11. REFERENCES

1. Talley, D. G., "Initial Verification and Validation of RAZORBACK – A Research Reactor Transient Analysis Code," SAND2015-8336, Sandia National Laboratories, September 2015.
2. Duderstadt, J. J. and L. J. Hamilton, Nuclear Reactor Analysis, John Wiley & Sons, Inc., 1976.
3. Coats, R. L., et. al., "Prompt-Period Measurement of the Annular Core Research Reactor Prompt Neutron Generation Time," SAND91-0501, Sandia National Laboratories, July 1994.
4. Pickard, P. S., and J. P. Odom, "Reactor Physics Design Calculations for the ACPR Upgrade," SAND80-0764, Sandia National Laboratories, February 1982.
5. Spriggs, G. D., et. al., "An 8-Group Delayed Neutron Model Based on a Consistent Set of Half-Lives," *Progress in Nuclear Energy*, Vol. 41, No. 1-4, 2002, pp. 223-251.
6. Pickard, P. S., and J. P. Odom, "Sandia Reactor Kinetics Codes: SAK and PK1D," SAND77-1211, Sandia National Laboratories, January 1978.
7. Internal SNL Technical Area V Calculation Document, CALC-ACRR-2014-003, "ACRR Peaking Factor Distributions," December 19, 2014.
8. Internal SNL Technical Area V Evaluation Document, EE-TAV-2013-001, "Evaluation of RAZORBACK's Point Kinetic Model Against Numerical Benchmarks," July 25, 2103
9. Ganapol, B. D., "A highly accurate algorithm for the solution of the point kinetics equations," *Annals of Nuclear Energy,* 62 (2013), pp. 564-571.
10. Internal SNL Memorandum, K. R. Boldt to F. M. McCrory, "ACRR SPND Detector Currents for NV/NVT Systems," dated December 22, 1999.
11. Martin, L. E., and L. L. Lippert, "Technical Safety Requirements (TSRs) for the Annular Core Research Reactor Facility (ACRRF)," SAND2008-5637, CN7, Sandia National Laboratories, April 22, 2014.
12. Internal SNL Memorandum, J. S. Philbin to J. W. Bryson, "ACRR Committee Meeting Minutes for December 6, 1999," dated December 7, 1999 (TA-V Record ID#10537).
13. Maestas, B. A., "Annular Core Research Reactor Pulse Diagnostics' Performance Assessment – A Comparison of Nickel & Sulfur Activation to Diagnostics Energy Yield," unpublished internal report, dated Spring 2008.
14. Timoshenko, S. P. and J. N. Goodier, Theory of Elasticity, 3rd Edition, McGraw-Hill Book Company, 1970.
15. Internal SNL Technical Area V Calculation Document, CALC-ACRR-2015-001, "ACRR Core and Rod Bank Reactivity Evaluations," February 19, 2015.
16. Internal SNL Technical Area V Calculation Document, CALC-ACRR-2015-006, "ACRR Fuel Temperature and Expansion Reactivity Coefficients," December 18, 2015.

17. Internal SNL Technical Area V Calculation Document, CALC-ACRR-2015-008, "ACRR Cladding Expansion Reactivity Coefficients," December 18, 2015.

18. Internal SNL Technical Area V Calculation Document, CALC-ACRR-2015-007, "ACRR Coolant Reactivity Coefficients," December 18, 2015.

19. Internal SNL Technical Area V Calculation Document, CALC-ACRR-2015-009, "ACRR Fuel Element Energy Deposition Fractions," December 18, 2015.

20. Depriest, K. R., et. al., "Control Rod Reactivity Curves for the Annular Core Research Reactor," SAND2011-2453C, Sandia National Laboratories, April 2011.

21. Parma, E. J., "Safety Analysis for Operating the Annular Core Research Reactor with the Central Cavity Liner Removed," SAND98-0769, Sandia National Laboratories, April 1998.

22. E.J. Parma, Memorandum to Moly-99 Project File, "CYLSS Rev 1 – A steady-state R-Z or R-Phi heat transfer computer program for solving fuel element and target temperature distributions," dated January 7, 1998.

23. Kim, Sung-Ho., and M. S. El-Genk, "Heat Transfer Experiments for Low Flow of Water in Rod Bundles," *International Journal of Heat and Mass Transfer*, Vol. 32, No. 7, 1989, pp. 1321-1336.

24. Incropera, F. P. and D. P. DeWitt, Fundamentals of Heat and Mass Transfer, John Wiley & Sons, Inc., 1985.

25. Jens, W. H., and P. A. Lottes, "Analysis of Heat Transfer, Burnout, Pressure Drop and Density Data for High-Pressure Water," ANL-4627, Argonne National Laboratory, Chicago, IL, May 1, 1951.

26. Bergles, A. E., and W. M. Rohsenow, "The Determination of Forced-Convection Surface-Boiling Heat Transfer," Transactions of the ASME, *Journal of Heat Transfer*, Vol. 86, No. 3, 1964, pp. 365-372.

27. Parma, E. J., et. al., "Radiation Characterization Summary: ACRR Central Cavity Free-Field Environment with the 32-Inch Pedestal at the Core Centerline (ACRR-FF-CC-32-cl)," SAND2015-6483, Sandia National Laboratories, November 2015.

APPENDIX A: SAMPLE RAZORBACK INPUT FILE

```
**************************************************************************
*                      RAZORBACK Input File
*  Note: an "*" in the first column denotes a comment statement
**************************************************************************
*                   CALCULATION AND PRINTING CONTROLS
**************************************************************************
*------------------|------------------|-------------|------------------|
* Calculation Type | Rx Kinetics (0)  |    Total    |    Number of     |
* (1=steady-state, | or Power History |  Transient  |   Title Cards    |
*  0=transient)    | Data File (1)    |   Time (s)  |    (up to 20)    |
*------------------|------------------|-------------|------------------|
        1                  0              20.0             5
*-------------------------------------------------------------------------|
*                          Title Cards                                    |
*-------------------------------------------------------------------------|
  Steady-State power run file for validation
   - Standard ACRR model
   - 20 C inlet temperature
   - Core radial peaking factor 1.46
   - CR at 27.50 cm
*
*------------------------------|-----------------------------------------|
*  Number of Time Step Ranges  |   Initial Condition Stabilization       |
*       (up to 20)             |     Duration (s) | Time Step (s)        |
*------------------------------|------------------|----------------------|
             1                          0.0                 0.05
*-----------------|-----------------|-----------------------------------|
*                 |                 |      Time Step Control (TSC)      |
*                 |                 |       (If TSC is off, then        |
*                 |                 |    dt = max time step of range)   |
*   Time Range    |    Time Step    |   T/H        TSC     |    TSC     |
* Begin(s)/End(s) | max(s) / min(s) |  dt(s)    | "Error"   | (1=y/0=n)  |
*-----------------|-----------------|----------|-----------|------------|
   0.0 10000.00      1.0d-3  1.0d-9     1.0d-3      1.0d-3        1
*
*-----------------------------------|-----------------------------------|
*  Number of Print Increment Ranges  |                                   |
*           (up to 20)               |                                   |
*-----------------------------------|-----------------------------------|
              2
*-------------------------------|------------|------------|------------|
*                               |   screen   |   plot     |   file     |
*     Print Time Range          |   print    |   print    |   print    |
*      Begin(s)/End(s)          |   incr.(s) |  incr.(s)  |  incr.(s)  |
*-------------------------------|------------|------------|------------|
       0.0    1.0                  1.0e-3      1.0e-3       5.0e-2
       1.0  10000.0                1.0e-2      1.0e-3       5.0e-1
*-------------------------------|-----------------------------------------|
* pulse parameter file print    |     fuel rod screen/file print          |
*     (1=yes, 0=no)             |          (1=yes, 0=no)                  |
*-------------------------------|-----------------------------------------|
             1                                  1
*
**************************************************************************
*               REACTOR POWER AND INITIAL CONDITIONS
**************************************************************************
*-------------------|--------------|----------------|------------------|
*  Initial Reactor  | 100% Reactor |   Number of    |     Element      |
*    Power (%)      |  Power (W)   | Fuel Elements  | Peak-to-Average  |
*-------------------|--------------|----------------|------------------|
```

```
    100.0e-00          2.39e+06           236                1.46
*-------------------------------------------------------------------------|
*
**************************************************************************
*                  REACTIVITY ADDITION SYSTEM CONTROLS
**************************************************************************
*
*-----------------------------------|-----------------------------------|
*     Control Rod Bank Control      |   Number of CR Bank Commands      |
*  (1=on w/curve, 0=off, 2=ramp)    |          (up to 20)               |
*-----------------------------------|-----------------------------------|
             0                                    1
*
*----------------------|----------------------|-------------------------|
*      CR Start        |       CR End         |     CR Speed (cm/s)     |
*      Time (s)        |      Time (s)        |     or Ramp ($/s)       |
*----------------------|----------------------|-------------------------|
          0.0                   55.0                    1.00
*-------------------------------------------------------------------------|
*
*  Note: 0.1 cm/s CR Speed = slow speed; 2.0 cm/s CR Speed = fast speed
*
*----------------------|----------------------|-------------------------|
*      CR Start        |       CR down        |        CR Up            |
*    Position (cm)     |    Position (cm)     |     Position (cm)       |
*----------------------|----------------------|-------------------------|
       24.00                   0.0                    55.00
*-------------------------------------------------------------------------|
*
*-------------------|-----------------------------------------------------|
*    CR Bank        |      CR Bank Differential Reactivity Curve          |
*     Total         |           drho/dz = A sin2[ B(z) + C]               |
*   Worth ($)       |       A        |       B        |       C           |
*-------------------|----------------|----------------|-------------------|
      11.57           0.03003581      0.0463939        0.425066
*-------------------------------------------------------------------------|
*
*-----------------------------------|-----------------------------------|
*       Safety Rod Bank Control     |   Number of SR Bank Commands      |
*  (1=on w/curve, 0=off, 2=ramp)    |          (up to 20)               |
*-----------------------------------|-----------------------------------|
              0                                    2
*
*----------------------|----------------------|-------------------------|
*      SR Start        |       SR End         |     SR Speed (cm/s)     |
*      Time (s)        |      Time (s)        |     or Ramp ($/s)       |
*----------------------|----------------------|-------------------------|
         0.0                   1.0                     0.0
         1.0                10000.0                    0.0
*-------------------------------------------------------------------------|
*
*  Note: 0.24 cm/s CR Speed = slow speed, 7.26 cm/s = fast speed
*
*----------------------|----------------------|-------------------------|
*      SR Start        |       SR down        |        SR Up            |
*    Position (cm)     |    Position (cm)     |     Position (cm)       |
*----------------------|----------------------|-------------------------|
        55.00                   0.0                    55.00
*-------------------------------------------------------------------------|
*
*-------------------|-----------------------------------------------------|
*    SR Bank        |      SR Bank Differential Reactivity Curve          |
*     Total         |           drho/dz = A sin2[ B(z) + C]               |
```

```
*   Worth ($)       |       A        |       B        |       C        |
*-------------------|----------------|----------------|----------------|
      2.22            0.03003581        0.0463939        0.425066
*
*-----------------------------------|---------------------------------|
*    Transient Rod Bank Control     |   Number of TR Bank Commands    |
*      (0=off, 1=on w/curve)        |          (up to 20)             |
*        (2=pulse, 3=ramp)          |                                 |
*-----------------------------------|---------------------------------|
               2                                    1
*
*----------------------|----------------------|-------------------------|
*      TR Start        |       TR End         |     TR Speed (cm/s)     |
*      Time (s)        |      Time (s)        |     or Ramp ($/s)       |
*----------------------|----------------------|-------------------------|
         0.165               1.000                    0.00
*
*----------------------|----------------------|-------------------------|
*      TR Start        |       TR down        |        TR Up            |
*    Position (cm)     |    Position (cm)     |     Position (cm)       |
*----------------------|----------------------|-------------------------|
        43.70                 43.69                    90.00
*-------------------------------------------------------------------------|
*   Note:  TR full down = 22.00 cm    TR pedestal down = 43.70 cm
*
*------------|------------------------------------------------------------|
*  TR Bank   |          TR Bank Differential Reactivity Curve             |
*  Total     |            drho/dz = A sin2[ B(z - z0) + C]                |
*  Worth($)  |      A      |      B      |      C      |      z0         |
*------------|-------------|-------------|-------------|-----------------|
  4.454         0.0282943     0.0423011      0.634055        26.0
*
*-------------------------------------------------------------------------|
*     Range of Validity for TR Bank Differential Reactivity Curve         |
*             lower end (cm)       |      upper end (cm)                  |
*----------------------------------|--------------------------------------|
                25.0                              85.0
*-------------------------------------------------------------------------|
*               Transient Rod Pulse Pneumatic System                      |
*  N2 Valve |   N2      | N2 Accum. |     Piston      |      TR           |
*  opening  | Pressure  |  Volume   |   Effective     |   Mass (kg)       |
*  time (s) | (psig)    |  (cm3)    |   Area (cm2)    |                   |
*-----------|-----------|-----------|-----------------|-------------------|
   78.0e-3      65.0       2.00d+5       28.96              13.75
*-------------------------------------------------------------------------|
*
*  Pulse Rod Holdup (= time after pulse when rods drop back into core)
*  Time begins from t=0
*  PRT submode all rods drop
*  Pulse submode TRs and SRs drop (CRs do not)
*-----------------------------------|---------------------------------|
*         Transient Rod Pulse       |        Pulse Submode            |
*         Rod Holdup Time (s)       |      (Pulse=0 or PRT=1)         |
*-----------------------------------|---------------------------------|
              0.4e0                                 1
*
*---------------------------------|-------------|----------------------|
*  Functional Reactivity Addition | Number of   |  Time to Turn        |
*  (0=off, 1=polynomial,  2=sine) | Terms(</=5) |  Addition Off (s)    |
*---------------------------------|-------------|----------------------|
               0                              1                 1e10
*************************************************************************
*                    REACTOR KINETICS PARAMETERS
```

```
*************************************************************************
*
*----------------------|----------------------|------------------------|
*  Neutron Generation  |  Effective Delayed   |     No. of Delayed     |
*      Time (s)        |  Neutron Fraction    |     Neutron Groups     |
*----------------------|----------------------|------------------------|
       24.0e-06               0.0073                     8
*
*-----------------------------------------------------------------------|
*                          Delayed Neutron                              |
*             Group Decay Constants (1/s) - lambda i's                  |
*       (up to 18 groups allowed -- up to 6 lambdas per line)           |
*----------|----------|----------|----------|----------|----------|
  1.25e-02    2.83e-02    4.25e-02    1.33e-01   2.92e-01    6.66e-01
  1.63e-00    3.55e-00
* (Campbell and Spriggs 8 groups)
*-----------------------------------------------------------------------|
*
*-----------------------------------------------------------------------|
*                          Delayed Neutron                              |
*                    Group Fractions - beta i's                         |
*         (up to 18 groups allowed -- up to 6 betas per line)           |
*----------|----------|----------|----------|----------|----------|
  2.409e-04  1.1242e-03  6.643e-04  1.4381e-03  2.4163e-03  6.570e-04
  5.913e-04  1.679e-04
* (Campbell and Spriggs 8 groups)
*-----------------------------------------------------------------------|
*
*-------------------------------------|--------------------------------|
*     Fuel Temperature Feedback       |       Coolant Reactivity       |
*     drho/dT = c1 + c2/(T**0.5)      |       Feedback Coefficients    |
*        c1     |         c2          |    Density      |   Spectral   |
*      ($/K)    |     ($/K^1/2)       |   ($/%void)     |    ($/K)     |
*---------------|---------------------|-----------------|--------------|
    -0.000988       -0.079422            -0.382           -0.00116
*
*-----------------------------------------------------------------------|
*            Fuel Expansion Reactivity Feedback Coefficients            |
*       Outer Radius     |      Inner Radius     |       Density        |
*          ($/cm)        |        ($/cm)         |     [$/(g/cm)]       |
*------------------------|-----------------------|----------------------|
           47.50                 -6.31                    11.26
*
*-----------------------------------------------------------------------|
*        Cladding Expansion Reactivity Feedback Coefficients            |
*       Outer Radius     |      Inner Radius     |       Density        |
*          ($/cm)        |        ($/cm)         |     [$/(g/cm)]       |
*------------------------|-----------------------|----------------------|
          -122.51                104.46                -0.71
*
*-----------------------------------------------------------------------|
*          Reactivity Feedback Scaling and Adjustment Factors           |
* -------------- Scaling ------------------|--------------------------|
*  Fuel T | Fuel Exp |  Clad  |  Coolant   |     PLA      Exp         |
*---------|----------|--------|------------|--------------------------|
    1.00     1.00      1.00       1.00         0.9247     2.0
*
*************************************************************************
*                   REACTOR PROTECTION SYSTEM SETTINGS
*************************************************************************
*
*----------------------|----------------------|------------------------|
*       Percent        |       Reactor        |        Element         |
```

```
*      Power (%)       |      Power (W)       |       Power (W)        |
*----------------------|----------------------|------------------------|
      115.0e+40               20.0e+49                25.00e+43
*
*----------------------|----------------------|------------------------|
*       Reactor        |      Rod Block       |       Rod Block        |
*     Period (s)       |    (1=on,0=off)      |      Rate  (dpm)       |
*----------------------|----------------------|------------------------|
       8.50e-20                  0                     4.0e10
*
*------------------------------|---------------------------------------|
*       Reactor Yield (J)      |         Fuel Temperature (C)          |
*------------------------------|---------------------------------------|
          300.0e46                                 1250.0e20
*
*------------------------------|---------------------------------------|
*      Pool Level Scram        |           Inlet Temperature           |
*    (cm below tank top)       |               Scram (C)               |
*------------------------------|---------------------------------------|
          100.0e20                                 40.0e20
*
*----------------------|----------------------|------------------------|
*   Scram Mode         |             Specified Scram Parameters        |
*    0=normal          |     Scram            |     Scram              |      Scram          |
*   1=specified        | Reactivity ($) | Delay Time (s) | Addition Time (s) |
*--------------------|----------------|----------------|-------------------|
        0                  -6.25              0.500              2.000
*
*----------------|-----------------------|-----------------------------|
*    Scram       |   Rod Fall Times (s)  |      Stuck Rod Factors      |
* Delay Time (s) |  CRs  |  SRs  |  TRs  |   CRs   |   SRs   |   TRs   |
*----------------|-----------------------|-----------------------------|
     0.050           0.5     0.5     0.5      1.0       1.0       1.0
*
*------------------------------|---------------------------------------|
*        Scram Failure         |             Manual Scram              |
*      (1 = yes, 0 = no)       |             Delay Time (s)            |
*------------------------------|---------------------------------------|
               0                                  10.0
*
**************************************************************************
*             POOL TANK/WATER AND POOL WATER COOLING SYSTEM
*                 INITIAL CONDITIONS AND TRANSIENT(S)
**************************************************************************
*
*-------------------------------------------------------------------------|
*                            |  Pool Tank    |                            |
*   Pool Tank  | Pool Tank  |  Displaced    | Maximum Water Height       |
*  Height (cm) | Area (cm2) | Volume (cm3)  | Above Reactor Core (cm)    |
*--------------|------------|---------------|----------------------------|
      857.25      72965.88      0.0d+00              700.0
*
*-------------------------------------------------------------------------|
*                     |                                    | Cooling System  |
* Initial Pool Water | Initial Pool Water Level (cm) |  Heat Removal   |
*  Temperature (C)   | (Distance Below Tank Lip)     | (% of Rx Power) |
*--------------------|-------------------------------|-----------------|
       20.0                    100.0                         0.0
*
*-------------------------------------------------------------------------|
*                           Pool Heatup                                   |
*   Flag = 0 -> no pool heatup (constant Tpool = Tinlet)                  |
*   Flag = 1 -> pool heatup by reactor/cooling system (Tpool = Tinlet)    |
```

```
*   Flag = 2 -> pool temperature ramp (Tpool = Tinlet)                  |
*   Flag = 3 -> inlet temperature ramp (constant Tpool <> Tinlet)       |
*                                                                       |
*      Flag        |  Ramp (degC/s)  | Start Time (s)  |  End Time (s) |
*------------------|-----------------|-----------------|---------------|
       0                 0.0             0.0               0.0
*
*-----------------------------------------------------------------------|
*                    Loss of Coolant Accident                           |
*      Flag     |    Start     |      Break     |  Effective Reactor    |
* (1=on, 0=off) |   Time (s)   |   Size (cm2)   |      Power (W)        |
*---------------|--------------|----------------|-----------------------|
        0            0.1              40.64             2.0e6
*
*-----------------------------------------------------------------------|
*                     Loss of Heat Sink Accident                        |
*        Flag          |      Start Time      |   Flowrate Coastdown    |
*   (1=on, 0=off)      |         (s)          |       Time  (s)         |
*-----------------------|----------------------|-------------------------|
          0                     5.0                      1.00
*
*-----------------------------------------|
*    Decay Heat Option (1=on,0=off)        |
*-----------------------------------------|
                   0
*
************************************************************************
*                      NUMERICAL SOLUTION SETTINGS
************************************************************************
*-------------------------------------|
*     Implicit Formulation Factors    |
*-------------------------------------|
*    Theta    |     Phi     |    Psi   |
*-------------------------------------|
     1.00          1.00         1.00
*-------------|-------------|----------|
*
*-----------------------------------------------------------------------|
*                       Iteration Error Limits                          |
*                  Steady-State                 |       Transient       |
*----------------------|---------------------|-----------------------|
*     Temperature      |        Flow         |      Temperature      |
*----------------------|---------------------|-----------------------|
         1.0e-4               1.0e-3                  1.0e-3
*
************************************************************************
*                         FUEL ELEMENT MODEL
************************************************************************
*
*               Standard ACRR Thermal-Hydraulics Model
*----------|----------|-------------------------------------------------|
*  Number  |   Fuel   |        Fuel Coordinate System Geometry          |
*  of Fuel |  R_inner |            0 = plate geometry                   |
*  Zones   |   (cm)   |            1 = cylindrical geometry             |
* (10 max) |          |                                                 |
*----------|----------|-------------------------------------------------|
      8      0.00000                          1
*
*------------|----------|----------|---------|--------------|----------|
* Zone Outer |  Number  | Material |   Gap?  | Fiss. Energy | Th. Exp. |
* Radius (cm)| of nodes |   Type   |(0=n/1=y)| Dep. Frac.   | Option   |
*------------|----------|----------|---------|--------------|----------|
  0.24130         10         3         1        0.0              1
```

```
  1.09982         30         1         0        0.97846          1
  1.11760         10         3         1        0.0              1
  1.68402         10         1         0        0.97846          1
  1.73228         10         3         1        0.0              1
  1.77038         10         2         0        0.00400          1
  1.82245         10         3         1        0.0              1
  1.87325         10         4         0        0.00456          1
*------------|----------|----------|---------|-------------------------|
*
*-----------------------------------------------------------------------|
*                      Fuel Element Geometry                            |
*-----------------------------------------------------------------------|
*              |          |   Pitch or   |     Pitch/Flow Geometry     |
*     Fuel     |  Number  | Channel O.D. | (1=square pitch,2=hex pitch |
*  Length (cm) | of Nodes |    (cm)      |    3=annulus, 4=tube)       |
*--------------|----------|--------------|-----------------------------|
     52.25         104        4.171                  2
*
*------------|--------------|--------------|--------------|------------|
*  Fissile   | Internal     | External     |    Allow     | Allow Gap  |
*   Mat. #   | Element      | Element      | Thermal Exp. | Rad HX     |
* (only one) | Press (psia) | Press (psia) | (0=no,1=yes) |(0=no,1=yes)|
*------------|--------------|--------------|--------------|------------|
      1           0.0            0.0             1            1
*
*-----------------------------------|-----------------------------------|
*  Center radial node of fuel "TC"  |  # of radial nodes to average     |
*       (at half fuel height)       | on each side of the center node   |
*-----------------------------------|-----------------------------------|
           25                                    6
*
*-----------------------------------------------------------------------|
*        Fuel Pellet Radial Fission Density Peaking Distribution        |
*                         f(r) = A*exp(B*r) + C                         |
*-----------------------|-----------------------|-----------------------|
*          A            |           B           |          C            |
*-----------------------|-----------------------|-----------------------|
        0.0157                   1.9370                 0.8211
*
*----------------|------------------------------------------------------|
*  # of Axial    |                                                      |
*  Peaking       |   Control Rod Positions (cm)for each Distribution    |
*  Distributions |   (at least one entry is required, but arbitrary,    |
*  (max of 5)    |      if only one distribution)                       |
*----------------|------------------------------------------------------|
      5                0.00  13.75  27.50  41.25  55.00
*
*-----------------------------------------------------------------------|
*        Fuel Element Axial Fission Density Peaking Distribution        |
*               f(z) = SUM{a(i)*(z/H)^(i)} for i = 0 to 6               |
*----------|---------|---------|---------|---------|---------|---------|
   0.6899   -0.6649    21.1255  -75.0610  121.2574   -98.9146  32.2021
   0.7368    0.4815    13.2107  -55.3610   95.7562   -81.6327  27.3933
   0.7721   -0.6252    24.0903  -89.6026  141.5383  -108.8048  33.1631
   0.7003   -0.2774    19.7349  -72.5156  117.7643   -96.6116  31.7668
   0.6470   -0.0999    18.6886  -70.3298  116.8484   -96.9372  31.7967
*
************************************************************************
*                       COOLANT CHANNEL MODEL
************************************************************************
*
*------------------------------|--------------|----------------------|
*   Coolant Channel Option     | Coolant Type |       Flow Type      |
```

```
* (0 = fuel coupled to coolant) | (1 = water)  |   (1=Natural Conv.)   |
* (1 = channel only)            |              |   (0=Forced Conv.)    |
*--------------------------------|--------------|-----------------------|
            0                          1                 1
*
*----------------|-------------|--------------------------|------------|
* Two-Phase Flow |   Boiling   | (Forced Conv.-Not Active) | Artificial |
* Drift Velocity |  Expansion  |  Inlet   |   Inlet       | Viscosity  |
* Nominal Value  | Suppression | Pressure | Mass Flow     | Constant   |
*    (cm/s)      |   Factor    | (psia)   |  (g/sec)      |            |
*----------------|-------------|----------|---------------|------------|
      50.0            30.0        22.0        100.0            0.0
*
*-------------------------------------------------------------------|
*                      Atmospheric Pressure                         |
*                     Above Pool Water (psia)                       |
*-------------------------------------------------------------------|
                              12.5
*
*-----------------|-----------------|--------------|-----------------|
*                    Channel Inlet Node Definition                   |
* Node Inlet      | Node Exit       |                                |
* Flow Area (cm2) | Flow Area (cm2) |     Minor Loss Coefficient     |
*-----------------|-----------------|--------------------------------|
     4.042398          4.042398                   1.50
*
*-------------------------------------------------------------------|
*            Unheated Channel Length (Lower and Upper)              |
*-------------------------------------------------------------------|
*    Number of Lower Nodes      |       Number of Upper Nodes        |
*-------------------------------|------------------------------------|
             12                                  9
*-------------------------------------------------------------------|
*                   Lower Unheated Length Description               |
*-------------------------------------------------------------------|
* Node Height | Exit Flow  | Wetted Perimeter |        Exit          |
*    (cm)     | Area (cm2) |       (cm)       |  Loss Coefficient    |
*-------------|------------|------------------|----------------------|
 1.0048076923      4.042398         11.76998              0.0
 1.0048076923      4.042398         11.76998              0.0
 1.0048076923      4.042398         11.76998              0.0
 1.0048076923      4.042398         11.76998              0.0
 1.0048076923      4.042398         11.76998              0.0
 1.0048076923      4.042398         11.76998              0.0
 1.0048076923      4.042398         11.76998              0.0
 1.0048076923      4.042398         11.76998              0.0
 1.0048076923      4.042398         11.76998              0.0
 1.0048076923      4.042398         11.76998              0.0
 1.0048076923      4.042398         11.76998              0.0
*
*-------------------------------------------------------------------|
*
*-------------------------------------------------------------------|
*                   Upper Unheated Length Description               |
*-------------------------------------------------------------------|
* Node Height | Exit Flow  | Wetted Perimeter |        Exit          |
*    (cm)     | Area (cm2) |       (cm)       |  Loss Coefficient    |
*-------------|------------|------------------|----------------------|
 1.0048076923      4.042398         11.76998              0.0
 1.0048076923      4.042398         11.76998              0.0
 1.0048076923      4.042398         11.76998              0.0
 1.0048076923      4.042398         11.76998              0.0
```

```
 1.0048076923      4.042398         11.76998               0.0
 1.0048076923      4.042398         11.76998               0.0
 1.0048076923      4.042398         11.76998               0.0
 1.0048076923      4.042398         11.76998               0.0
 1.0048076923      4.042398         11.76998               0.0
*
*
*-----------------------------------------------------------------------|
*                    Channel Outlet Node Definition                     |
*     Node Exit Flow Area (cm2)     |     Minor Loss Coefficient       |
*-----------------------------------|-----------------------------------|
              4.042398                            1.50
*
************************************************************************
*  Test Options (only the "Reactor Only" option is currently available)
************************************************************************
*
*-----------------------------------------------------------------------|
*                             Test Mode                                 |
*-----------------------------------------------------------------------|
*   0 = Normal (no test; next 3 cards not required, so comment out)     |
*   1 = Specify BCs and/or Conductivities (next 2 cards required)       |
*-----------------------------------------------------------------------|
                               0
*
*  Fuel Element Surface BC  1=convection / 2=constant T --> BC Temp
*            2                                                 120.0
*
*-----------------------------------------------------------------------|
*                     Reactor Only Test Option                          |
*-----------------------------------------------------------------------|
*   Reactor Only (1=y/0=no)     |   Energy Yield Feedback ($/J-Rx)      |
*-------------------------------|---------------------------------------|
                0                           -3.87597e-4
*
************************************************************************
*********************************************************************************
*  Begin Material Property Entries
*********************************************************************************
4  # of materials
*----------------------------------------BeO-UO2--------------------------------
3.500000d+00  BeO-UO2
 2  # of temperature ranges for k (</= 3)
 273.15d0  2423.15d0
 6  0.00d0   1.000000d+00
 7.388187d+00 -2.472780-02  3.932623d-05 -3.484550d-08  1.742192d-11
-4.576267d-15  4.902442d-19
 2423.15d0  3273.15d0
 0  0.00d0   1.000000d+00
 0.178994d+00    assume constant after eutectic melt
*
 3  # of temperature ranges for k (</= 3)
 273.15d0  2423.15d0
6  0.00d0   1.000000d+00
-6.988880d-01  8.637336d-03 -1.476482d-05  1.390025d-08 -7.220731d-12
1.947498d-15 -2.126275d-19
 2423.15d0  2623.15d0
6 -2400.00d0   1.000000d+00
2.684542d+00 -6.808448d-03 3.586942d-04 -5.392987d-06 4.553262d-08
-1.882605d-10  3.243747d-13
 2623.15d0  3273.15d0
6 -2600.00d0   1.000000d+00
2.154782d+02 -2.532661d+01  1.239674d+00 -3.122766d-02  4.305744d-04
```

```
-3.087149d-06 9.072820d-09
*
0.8d0  0.0d0
*
2  0.00d0   1.000000d+00
4.380929d-06  6.667636d-09 -8.749789d-13
*
0  0.00d0   1.000000d+00
345.0000d+09
*
0.26d0
*-------------------------------------------------------------------------------
*---------------------------------------Niobium---------------------------------
8.570000d+00  Niobium
1  # of temperature ranges for k (</= 3)
 273.15d0  3273.15d0
2  0.00d0   1.000000d+00
0.48705456d+00  1.6410260d-04 -6.1258996d-09
*
1  # of temperature ranges for k (</= 3)
 273.15d0  3273.15d0
5  0.00d0   1.000000d+00
2.145847d-01  2.429998d-04 -3.253767d-07  2.386227d-10 -8.133768d-14
1.102552d-17
*
0.8d0  0.0d0
*
2  0.00d0   1.000000d+00
6.696000d-06  2.191880d-09 -3.141264d-13
*
0  0.00d0   1.000000d+00
105.0000d+09
*
0.4d0
*-------------------------------------------------------------------------------
*----------------------------------------Helium---------------------------------
3.328d-04    Helium
1  # of temperature ranges for k (</= 3)
 273.15d0  3273.15d0
2  0.00d0   1.000000d+00
5.259485d-04  3.333698d-06 -2.484752d-10
*
1  # of temperature ranges for cp (</= 3)
 273.15d0  3273.15d0
0  0.00d0   1.000000d+00
5.193122d+00
*
1.0d0  1.0d0
*
0  0.00d0   1.000000d+00
0.00000d-00
*
0  0.00d0   1.000000d+00
1.00000d-20
*
0.3d0
*-------------------------------------------------------------------------------
*---------------------------------------Stainless Steel-------------------------
7.950000d+00  Stainless_Steel
1  # of temperature ranges for k (</= 3)
 273.15d0  3273.15d0
1  0.00d0   1.000000d+00
0.08116d+00  0.0001618d+00
```

```
*
1  # of temperature ranges for cp (</= 3)
 273.15d0  3273.15d0
1  0.00d0   1.000000d+00
0.46287d+00   1.3289d-04
*
0.3d0  0.0d0
*
0  0.00d0   1.000000d+00
1.730000d-05
*
0  0.00d0   1.000000d+00
190.0000d+09
*
0.3d0
*-------------------------------------------------------------------------------
*******************************************************************************
*  Begin Heat Transfer Coefficient Correlation Entries
*******************************************************************************
*
*----------------------------Natural Convection---------------------------------
*      C          Ra exp
   0.2720d+00    0.250d-00
*
*----------------------Laminar Forced Convection--------------------------------
*      C          Re exp        Pr exp        visc ratio exp     Re Transition
*   1.061d+00    0.3400d-00    0.3333d-00          0.0d-00         4137.47d-00
   1.061d+00    0.3400d-00    0.3333d-00          0.0d-00         3000.0d-00
*
*---------------------Turbulent Forced Convection-------------------------------
*      C          Re exp        Pr exp        visc ratio exp
   0.0230d+00   0.800d-00      0.4000d-00         0.0d-00
*
*-----------------Boiling Heat Transfer Coefficent Option-----------------------
*            i_bht                    |
*  (1 = Jens-Lottes/Thom, 2 = Chen)  |
               1
*
*-----------------Post-CHF Heat Transfer Coefficent Option----------------------
*         MCHFR Limit               |     Post-CHF HT Coefficient (W/cm2/K)
             -2.0                                      0.001
*-------------------------------------------------------------------------------
*******************************************************************************
```

APPENDIX B: PULSE LOG SHEET EXCERPTS

Operation 9716 Console Log

```
DATE  01-05-11
TIME  16:56
RUN NO      09716

PPS1

NV    33310
NVT   312
TEMPERATURE 1 PEAK      37
TEMPERATURE 2 PEAK      860
TEMPERATURE 3 PEAK      860


PPS2

NV    34240
NVT   330
TEMPERATURE 1 PEAK      819
TEMPERATURE 2 PEAK      842
TEMPERATURE 3 PEAK      815


FREC

TEMPERATURE 1 PEAK      28
TEMPERATURE 2 PEAK      207


      CR Bank Position (RU)   CR Bank Worth (cents)
TR UP DC          1488        1020.5
Free Field DC     1501        1016.8
Experiment Worth        3.7

TR Down DC        2410        717.0
TR Bank Worth           303.5

Setup DC          2400        720.6
Pulse Size        299.9

      TR Bank Position (RU)   TR Bank Worth (cents)
Setup Pulse Size  4185        309.8
```

Operation 9716 Diagnostic System Report (Excerpt)

Shot Information			Predicted Values		
Run Number	9716		**Expected MW**		35500
Operator	Dave Clovis		**Expected TTP**		0.3125
Date \ Time	1/5/2011 16:52		**Expected MJ**		286.26
Experimenter Name	ACRR		**Expected Fuel Temp**		837.2
Experiment Plan #	MP 11		**Dialed In MW**		32285.51
Package Worth $	0.037				
Shot Worth $	3.035				
Rod Hold Up (sec)	0.4				
FREC Mode	Decoupled				
FREC RODS	DOWN				

Comments

	Average	CH-1	CH-2	CH-3	CH-4
Detector		DE2-3	DE4-9	DE5-1	
Detector Calibration		42.6	40.2	40.6	
Channel Type		PXI Amp	SR570 Amp	SR570 Amp	
Average Used		Both	Both	Both	
Period Used		Yes	Yes	Yes	
PEAK DATA:					
Peak (MW)	**29605.9**	27216.3	31278.5	30395.7	
TTP (sec)	0.34356	0.34208	0.34352	0.34356	
FWHM (sec)	0.00724	0.00768	0.00708	0.00708	
LEHM (sec)	0.0036	0.00252	0.0034	0.0034	
TEHM (sec)	0.00364	0.00516	0.00368	0.00368	
Ratio (LE/TE)	0.989	0.488	0.924	0.924	
Shot Worth	2.851	3.179	3.068	3.029	
YIELD DATA:					
Total Yield (MJ)	**294.132**	266.532	350.252	270.045	
TTP+3fwhm (MJ)	242.895	236.182	249.605	242.814	
Yield @ Peak (MJ)	118.517	80.292	118.256	115.563	
Min Period (sec)	0.001738	0.001474	0.001554	0.001584	

Operation 9718 Console Log

```
DATE  01-06-11
TIME  13:39
RUN NO      09718

PPS1

NV    17867
NVT   229
TEMPERATURE 1 PEAK      36
TEMPERATURE 2 PEAK      656
TEMPERATURE 3 PEAK      654


PPS2

NV    18347
NVT   242
TEMPERATURE 1 PEAK      618
TEMPERATURE 2 PEAK      635
TEMPERATURE 3 PEAK      612


FREC

TEMPERATURE 1 PEAK      27
TEMPERATURE 2 PEAK      160


      CR Bank Position (RU)   CR Bank Worth (cents)
TR UP DC          1484        1021.6
Free Field DC     1481        1022.5
Experiment Worth        -0.9

TR Down DC        2408        717.8
TR Bank Worth           303.8

Setup DC          2257        771.5
Pulse Size        250.1

      TR Bank Position (RU)   TR Bank Worth (cents)
Setup Pulse Size  4561        260.5
```

Operation 9718 Diagnostic System Report (Excerpt)

Shot Information			Predicted Values		
Run Number	9718		Expected MW		18000
Operator	Kraig Deike		Expected TTP		0.3208
Date \ Time	1/6/2011 13:35		Expected MJ		209.34
Experimenter Name	ACRR Staff		Expected Fuel Temp		618.5
Experiment Plan #	OP-2/OP AID 29		Dialed In MW		16398.82
Package Worth $	-0.009				
Shot Worth $	2.501				
Rod Hold Up (sec)	0.4				
FREC Mode	Decoupled				
FREC RODS	DOWN				

Comments ACRR Cal pulse per MP-11

	Average	CH-1	CH-2	CH-3	CH-4
Detector		DE2-3	DE4-9	DE5-1	
Detector Calibration		42.6	40.2	40.6	
Channel Type		PXI Amp	SR570 Amp	SR570 Amp	
Average Used		Both	Both	Peak	
Period Used		Yes	Yes	Yes	
PEAK DATA:					
Peak (MW)	**16393**	16256	16659.8	16292.5	
TTP (sec)	0.34928	0.34904	0.34932	0.34936	
FWHM (sec)	0.0092	0.00916	0.00924	0.0092	
LEHM (sec)	0.00448	0.0044	0.00444	0.00444	
TEHM (sec)	0.00472	0.00476	0.0048	0.00476	
Ratio (LE/TE)	0.949	0.924	0.925	0.933	
Shot Worth	2.378	2.665	2.875	2.839	
YIELD DATA:					
Total Yield (MJ)	**201.706**	203.771	202.722	189.433	
TTP+3fwhm (MJ)	171.709	170.027	174.429	170.663	
Yield @ Peak (MJ)	81.805	80.265	82.363	80.856	
Min Period (sec)	0.002343	0.001935	0.001716	0.00175	

Operation 9719 Console Log

```
DATE  01-10-11
TIME  15:56
RUN NO      09719

PPS1

NV    7755
NVT   144
TEMPERATURE 1 PEAK      39
TEMPERATURE 2 PEAK      454
TEMPERATURE 3 PEAK      458


PPS2

NV    7962
NVT   155
TEMPERATURE 1 PEAK      432
TEMPERATURE 2 PEAK      444
TEMPERATURE 3 PEAK      424


FREC

TEMPERATURE 1 PEAK      30
TEMPERATURE 2 PEAK      113


      CR Bank Position (RU)   CR Bank Worth (cents)
TR UP DC          1485        1021.4
Free Field DC     1481        1022.5
Experiment Worth        -1.1

TR Down DC        2405        718.8
TR Bank Worth           302.6

Setup DC          2115        821.2
Pulse Size        200.2

      TR Bank Position (RU)   TR Bank Worth (cents)
Setup Pulse Size  4946        210.9
```

Operation 9719 Diagnostic System Report (Excerpt)

Shot Information			Predicted Values		
Run Number	9719		**Expected MW**		7000
Operator	Lance Lippert		**Expected TTP**		0.3395
Date \ Time	1/10/2011 15:54		**Expected MJ**		136.15
Experimenter Name	ACRR STAFF		**Expected Fuel Temp**		413.8
Experiment Plan #	MP-11		**Dialed In MW**		6528.42
Package Worth $	-0.011				
Shot Worth $	2.002				
Rod Hold Up (sec)	0.4				
FREC Mode	Decoupled				
FREC RODS	DOWN				

Comments

	Average	CH-1	CH-2	CH-3	CH-4
Detector		DE2-3	DE4-9	DE5-1	
Detector Calibration		42.6	40.2	40.6	
Channel Type		PXI Amp	SR570 Amp	SR570 Amp	
Average Used		Both	Both	Both	
Period Used		Yes	Yes	Yes	
PEAK DATA:					
Peak (MW)	**7092.1**	6991.4	7227.2	7061.9	
TTP (sec)	0.36816	0.36788	0.36816	0.3682	
FWHM (sec)	0.01324	0.01324	0.01324	0.0132	
LEHM (sec)	0.00644	0.00636	0.00636	0.00636	
TEHM (sec)	0.0068	0.00688	0.00688	0.00684	
Ratio (LE/TE)	0.947	0.924	0.924	0.93	
Shot Worth	1.947	2.082	2.215	2.398	
YIELD DATA:					
Total Yield (MJ)	**125.349**	122.929	129.803	125.204	
TTP+3fwhm (MJ)	107.281	105.702	109.316	106.807	
Yield @ Peak (MJ)	51.18	49.785	51.56	50.518	
Min Period (sec)	0.003415	0.002989	0.00266	0.002309	

Operation 9720 Console Log

```
DATE  01-13-11
TIME  11:04
RUN NO      09720

PPS1

NV    1560
NVT   68
TEMPERATURE 1 PEAK      35
TEMPERATURE 2 PEAK      239
TEMPERATURE 3 PEAK      236


PPS2

NV    1616
NVT   71
TEMPERATURE 1 PEAK      227
TEMPERATURE 2 PEAK      233
TEMPERATURE 3 PEAK      223


FREC

TEMPERATURE 1 PEAK      27
TEMPERATURE 2 PEAK      68


      CR Bank Position (RU)   CR Bank Worth (cents)
TR UP DC          1491        1019.6
Free Field DC     1481        1022.5
Experiment Worth        -2.9

TR Down DC        2419        713.8
TR Bank Worth           305.8

Setup DC          1973        869.5
Pulse Size        150.1

      TR Bank Position (RU)   TR Bank Worth (cents)
Setup Pulse Size  5404        156.5
```

Operation 9720 Diagnostic System Report (Excerpt)

Shot Information			Predicted Values		
Run Number	9720		**Expected MW**		1500
Operator	Lonnie Martin		**Expected TTP**		0.4085
Date \ Time	1/13/2011 11:03		**Expected MJ**		62.57
Experimenter Name	ACRR staff		**Expected Fuel Temp**		207.1
Experiment Plan #	MP-11		**Dialed In MW**		1300.77
Package Worth $	-0.029				
Shot Worth $	1.5				
Rod Hold Up (sec)	0.4				
FREC Mode	Decoupled				
FREC RODS	DOWN				

Comments TRW Worth Determination

	Average	CH-1	CH-2	CH-3	CH-4
Detector		DE2-3	DE4-9	DE5-1	
Detector Calibration		42.6	40.2	40.6	
Channel Type		PXI Amp	SR570 Amp	SR570 Amp	
Average Used		Both	Both	Both	
Period Used		Yes	Yes	Yes	
PEAK DATA:					
Peak (MW)	**1429.8**	1412.8	1457.8	1419.1	
TTP (sec)	0.43896	0.43888	0.43944	0.43904	
FWHM (sec)	0.02712	0.02716	0.02712	0.02708	
LEHM (sec)	0.01288	0.013	0.01328	0.01284	
TEHM (sec)	0.01424	0.01416	0.01384	0.01424	
Ratio (LE/TE)	0.904	0.918	0.96	0.902	
Shot Worth	1.416	1.732	1.702	2.077	
YIELD DATA:					
Total Yield (MJ)	**54.787**	55.594	57.937	51.656	
TTP+3fwhm (MJ)	46.28	45.804	47.2	45.856	
Yield @ Peak (MJ)	20.892	20.829	21.879	20.667	
Min Period (sec)	0.007756	0.004422	0.004615	0.003002	

Operation 11694 Console Log

```
DATE  01-12-16
TIME  10:18
RUN NO      11694

PPS1

NV    37875
NVT   360
TEMPERATURE 1 PEAK      33
TEMPERATURE 2 PEAK      892
TEMPERATURE 3 PEAK      893


PPS2

NV    32746
NVT   307
TEMPERATURE 1 PEAK      850
TEMPERATURE 2 PEAK      856
TEMPERATURE 3 PEAK      847


FREC

TEMPERATURE 1 PEAK      186
TEMPERATURE 2 PEAK      206


      CR Bank Position (RU)   CR Bank Worth (cents)
TR UP DC          1499        1017.3
Free Field DC     1512        1013.6
Experiment Worth              3.7

TR Down DC        2428        710.7
TR Bank Worth                 306.6

Setup DC          2428        710.7
Pulse Size                    306.6

      TR Bank Position (RU)   TR Bank Worth (cents)
Setup Pulse Size  4210        306.6
```

Operation 11694 Diagnostic System Report (Excerpt)

Shot Information			Predicted Values			
Run Number	11694		**Expected MW**		40000	
Operator	Krista Kaiser		**Expected TTP**		0.3122	
Date \ Time	1/12/2016 10:14		**Expected MJ**		290.79	
Experimenter Name	ACRR Staff		**Expected Fuel Temp**		849.9	
Experiment Plan #	MP-11		**Dialed In MW**		33491.5	
Package Worth $	0.037					
Shot Worth $	3.066					
Rod Hold Up (sec)	0.4					
FREC Mode	Decoupled					
FREC RODS	DOWN					
Comments	Cal Pulse - Max					

	Average	CH-1	CH-2	CH-3	CH-4	CH-5
Detector		DE5-1	DE4-9		DE5-8	DE2-98
Detector Calibration		44.1	45.3		52.29	53.6
Channel Type		PXI Amp	SR570 Amp		PXI Amp	Terminated
Average Used		Tail Only	Both		Tail Only	Both
Period Used		Yes	Yes		Yes	Yes
PEAK DATA:						
Peak (MW)	**27087.8**	25870.1	28899.3		22066.5	25352.7
TTP (sec)	0.31024	0.3086	0.31032		0.30792	0.31004
FWHM (sec)	0.00692	0.00784	0.00696		0.00868	0.00696
LEHM (sec)	0.00336	0.00228	0.00332		0.002	0.00336
TEHM (sec)	0.00356	0.00556	0.00364		0.00668	0.0036
Ratio (LE/TE)	0.944	0.41	0.912		0.299	0.933
Shot Worth	2.819	2.937	3.216		2.952	3.032
YIELD DATA:						
Total Yield (MJ)	**258.572**	271.715	281.067		255.194	252.2
TTP+3fwhm (MJ)	213.021	230.832	227.272		216.181	198.777
Yield @ Peak (MJ)	102.439	71.297	107.218		54.77	94.905
Min Period (sec)	0.00177	0.001661	0.001449		0.001647	0.001582

Operation 11703 Console Log

```
DATE  01-15-16
TIME  10:52
RUN NO      11703

PPS1

NV    19150
NVT   252
TEMPERATURE 1 PEAK      34
TEMPERATURE 2 PEAK      663
TEMPERATURE 3 PEAK      654


PPS2

NV    16260
NVT   208
TEMPERATURE 1 PEAK      624
TEMPERATURE 2 PEAK      649
TEMPERATURE 3 PEAK      622


FREC

TEMPERATURE 1 PEAK      143
TEMPERATURE 2 PEAK      159


      CR Bank Position (RU)   CR Bank Worth (cents)
TR UP DC    1539  1005.8
Free Field DC     1512  1013.6
Experiment Worth        -7.8

TR Down DC  2460  699.0
TR Bank Worth           306.8

Setup DC    2301  755.8
Pulse Size        250.0

      TR Bank Position (RU)   TR Bank Worth (cents)
Setup Pulse Size  4601  255.3
```

Operation 11703 Diagnostic System Report (Excerpt)

Shot Information			Predicted Values			
Run Number	11703		**Expected MW**		25000	
Operator	Dave Clovis		**Expected TTP**		0.3208	
Date \ Time	1/15/2016 10:48		**Expected MJ**		210.66	
Experimenter Name	ACRR Staff		**Expected Fuel Temp**		618.5	
Experiment Plan #	11703		**Dialed In MW**		15829.39	
Package Worth $	-0.078					
Shot Worth $	2.5					
Rod Hold Up (sec)	0.4					
FREC Mode	Decoupled					
FREC RODS	DOWN					
Comments	MP-11 Cal Pulse					

	Average	CH-1	CH-2	CH-3	CH-4	CH-5
Detector		DE5-1	DE4-9	DE5-1	DE5-8	DE2-98
Detector Calibration		44.1	45.3	47	52.29	53.6
Channel Type		PXI Amp	SR570 Amp	SR570 Amp	PXI Amp	Terminated
Average Used		Both	Peak	None	Both	Peak
Period Used		Yes	Yes	Yes	Yes	Yes
PEAK DATA:						
Peak (MW)	**14580.1**	15504.8	14496.6	59078.3	15637.5	12712.2
TTP (sec)	0.3178	0.31772	0.31796	0.3104	0.31772	0.31764
FWHM (sec)	0.00932	0.00936	0.00936	0.02044	0.00932	0.00932
LEHM (sec)	0.00452	0.00452	0.00448	0.00192	0.00448	0.00448
TEHM (sec)	0.0048	0.00484	0.00488	0.01852	0.00484	0.00484
Ratio (LE/TE)	0.942	0.934	0.918	0.104	0.926	0.926
Shot Worth	2.386	2.905	2.783	2.64	2.509	3.156
YIELD DATA:						
Total Yield (MJ)	**180.786**	193.777	246.203	1902.597	189.826	155.976
TTP+3fwhm (MJ)	155.236	164.712	154.864	1348.629	165.971	135.407
Yield @ Peak (MJ)	73.948	78.001	73.212	154.816	78.512	63.86
Min Period (sec)	0.002329	0.001689	0.001805	0.001965	0.002137	0.001489

Operation 11704 Console Log

```
DATE  01-18-16
TIME  12:06
RUN NO      11704

PPS1

NV    8155
NVT   173
TEMPERATURE 1 PEAK      34
TEMPERATURE 2 PEAK      466
TEMPERATURE 3 PEAK      463


PPS2

NV    7003
NVT   134
TEMPERATURE 1 PEAK      441
TEMPERATURE 2 PEAK      458
TEMPERATURE 3 PEAK      439


FREC

TEMPERATURE 1 PEAK      104
TEMPERATURE 2 PEAK      115


      CR Bank Position (RU)   CR Bank Worth (cents)
TR UP DC    1536  1006.9
Free Field DC     1512  1013.6
Experiment Worth        -6.7

TR Down DC  2458  699.7
TR Bank Worth           307.2

Setup DC    2156  807.0
Pulse Size        199.9

      TR Bank Position (RU)   TR Bank Worth (cents)
Setup Pulse Size  4993  205.1
```

Operation 11704 Diagnostic System Report (Excerpt)

Shot Information			Predicted Values			
Run Number	11704		**Expected MW**		10000	
Operator	Dave Clovis		**Expected TTP**		0.3397	
Date \ Time	1/18/2016 12:01		**Expected MJ**		136.47	
Experimenter Name	ACRR Staff		**Expected Fuel Temp**		412	
Experiment Plan #	MP-11		**Dialed In MW**		6131.55	
Package Worth $	-0.067					
Shot Worth $	1.999					
Rod Hold Up (sec)	0.4					
FREC Mode	Decoupled					
FREC RODS	DOWN					

Comments MP-11 $2.00 calibration pulse. DE5-1 reset to 40.2 nA/MW prior to pulse.

	Average	CH-1	CH-2	CH-3	CH-4	CH-5
Detector		DE5-1	DE4-9	DE5-1	DE5-8	DE2-98
Detector Calibration		44.1	45.3	40.2	52.29	53.6
Channel Type		PXI Amp	SR570 Amp	SR570 Amp	PXI Amp	Terminated
Average Used		Both	Peak	None	Both	Peak
Period Used		Yes	Yes	Yes	Yes	Yes
PEAK DATA:						
Peak (MW)	**6216.9**	6588	6220.1	1471.7	6650.4	5410.8
TTP (sec)	0.33712	0.33696	0.33716	0.3374	0.337	0.33704
FWHM (sec)	0.01348	0.01348	0.01348	0.01352	0.01348	0.01344
LEHM (sec)	0.00656	0.00644	0.00636	0.0066	0.00648	0.00656
TEHM (sec)	0.00692	0.00704	0.00712	0.00692	0.007	0.00688
Ratio (LE/TE)	0.948	0.915	0.893	0.954	0.926	0.953
Shot Worth	1.943	2.642	2.63	2.556	2.605	7.228
YIELD DATA:						
Total Yield (MJ)	**119.012**	124.284	127.669	37.129	127.467	132.357
TTP+3fwhm (MJ)	96.133	101.836	96.218	22.972	102.712	83.749
Yield @ Peak (MJ)	45.871	47.832	44.886	11.094	48.46	40.272
Min Period (sec)	0.003432	0.001963	0.001977	0.002073	0.002009	0.0005

Operation 11705 Console Log

```
DATE  01-19-16
TIME  10:03
RUN NO      11705

PPS1

NV    1711
NVT   77
TEMPERATURE 1 PEAK      34
TEMPERATURE 2 PEAK      247
TEMPERATURE 3 PEAK      243


PPS2

NV    1374
NVT   60
TEMPERATURE 1 PEAK      234
TEMPERATURE 2 PEAK      242
TEMPERATURE 3 PEAK      231


FREC

TEMPERATURE 1 PEAK      59
TEMPERATURE 2 PEAK      65


      CR Bank Position (RU)   CR Bank Worth (cents)
TR UP DC    1528  1009.0
Free Field DC     1512  1013.6
Experiment Worth        -4.6

TR Down DC  2452  701.9
TR Bank Worth           307.1

Setup DC    2004  859.0
Pulse Size        150.0

      TR Bank Position (RU)   TR Bank Worth (cents)
Setup Pulse Size  5418  154.9
```

Operation 11705 Diagnostic System Report (Excerpt)

Shot Information			Predicted Values			
Run Number	11705		**Expected MW**		2000	
Operator	Lance Lippert		**Expected TTP**		0.4085	
Date \ Time	1/19/2016 10:00		**Expected MJ**		62.67	
Experimenter Name	ACRR Staff		**Expected Fuel Temp**		206.7	
Experiment Plan #	MP-11		**Dialed In MW**		733.7	
Package Worth $	-0.046					
Shot Worth $	1.5					
Rod Hold Up (sec)	0.4					
FREC Mode	Decoupled					
FREC RODS	DOWN					
Comments	MP-11 Cal Pulse					

	Average	CH-1	CH-2	CH-3	CH-4	CH-5
Detector		DE5-1	DE4-9	DE5-1	DE5-8	DE2-98
Detector Calibration		44.1	45.3	40.2	52.29	53.6
Channel Type		PXI Amp	SR570 Amp	SR570 Amp	PXI Amp	Terminated
Average Used		Both	Both	None	Both	Peak
Period Used		Yes	Yes	Yes	Yes	No
PEAK DATA:						
Peak (MW)	**1195.7**	1272.9	1191.9	565.9	1283.1	1045.6
TTP (sec)	0.40356	0.40356	0.40348	0.40344	0.40336	0.40244
FWHM (sec)	0.02864	0.0286	0.0288	0.02876	0.02872	0.02848
LEHM (sec)	0.01412	0.01416	0.01392	0.0138	0.014	0.01304
TEHM (sec)	0.01452	0.01444	0.01488	0.01496	0.01472	0.01544
Ratio (LE/TE)	0.972	0.981	0.935	0.922	0.951	0.845
Shot Worth	1.424	2.093	1.763	1.751	1.697	7.211
YIELD DATA:						
Total Yield (MJ)	**53.776**	56.153	51.588	23.754	59.357	78.081
TTP+3fwhm (MJ)	41.191	43.5	40.901	19.412	44.1	36.223
Yield @ Peak (MJ)	19.117	20.196	18.598	8.779	20.196	15.962
Min Period (sec)	0.007612	0.002959	0.004241	0.004309	0.004647	0.000501

[This page intentionally left blank.]

APPENDIX C: TRANSIENT ROD WITHDRAWAL CONSOLE LOGS

Operation 9022 Console Log

```
DATE  05-30-08
TIME  11:27
RUN NO      09022

PPS1

NV    65
NVT   311
TEMPERATURE 1 PEAK      37
TEMPERATURE 2 PEAK      718
TEMPERATURE 3 PEAK      723


PPS2

NV    98
NVT   306
TEMPERATURE 1 PEAK      732
TEMPERATURE 2 PEAK      769
TEMPERATURE 3 PEAK      752


FREC

TEMPERATURE 1 PEAK      213
TEMPERATURE 2 PEAK      195


      CR Bank Position (RU)   CR Bank Worth (cents)
TR UP DC          1514        1013.1
Free Field DC     1505        1015.6
Experiment Worth        -2.5

TR Down DC        2818        570.1
TR Bank Worth           443.0

Setup DC          2668        624.0
Pulse Size        389.1

      TR Bank Position (RU)   TR Bank Worth (cents)
Setup Pulse Size  3500        388.6
```

Operation 9023 Console Log

```
DATE  05-30-08
TIME  12:48
RUN NO      09023

PPS1

NV    44
NVT   308
TEMPERATURE 1 PEAK      35
TEMPERATURE 2 PEAK      722
TEMPERATURE 3 PEAK      726


PPS2

NV    98
NVT   307
TEMPERATURE 1 PEAK      730
TEMPERATURE 2 PEAK      767
TEMPERATURE 3 PEAK      749


FREC

TEMPERATURE 1 PEAK      214
TEMPERATURE 2 PEAK      195


      CR Bank Position (RU)   CR Bank Worth (cents)
TR UP DC          1504        1015.9
Free Field DC     1505        1015.6
Experiment Worth        0.3

TR Down DC        2818        570.1
TR Bank Worth           443.0

Setup DC          2654        629.1
Pulse Size        386.8

      TR Bank Position (RU)   TR Bank Worth (cents)
Setup Pulse Size  3500        388.6
```

[This page intentionally left blank.]

APPENDIX D: ON THE ACRR STEADY-STATE POWER

Introduction and Purpose

The validation results in Section 8 (and Section 7) of this report indicate that Razorback significantly overestimates the steady-state fuel temperature for a given ACRR power level. This appendix documents considerations which provide evidence that the actual ACRR power level may be lower than the current calibration process results indicate.

Full Power Temperature Now vs. Then

The memorandum[13] documenting the annual power calibration by pool heatup for 2016 includes a table with measured fuel temperature data from the 2013 through 2016 power calibrations. That data is presented in Table D-1 below. Note that the number 2 thermocouple of Plant Protection System Channel 1 (PPS1) measured fuel temperatures range from 776°C-813°C for ACRR pool heatup rate-determined power levels from 2.17 MW to 2.26 MW. If one were to extrapolate upward to 2.39 MW (100% power), the temperature should be ~866°C.

Table D-1. ACRR fuel temperature data for recent power calibration operations.

	2016	2015	2014	2013
Pool Heat Up Rate	37.08°C/h	37.6°C/h	36.1°C/h	36.2°C/h
Calculated True Power (%)	93.4%	94.7%	90.9%	90.86%
Calculated True Power (MW)	2.23 MW	2.26 MW	2.17 MW	2.17 MW
PPS1 Fuel Temperature #2	803°C	813°C	776°C	777°C
PPS2 Fuel Temperature #2	758°C	746°C	730°C	732°C

Operation logs for a 24 hour full power operation from February 2, 1995, at which time 100% power was 2 MW were examined. For this run, the steady-state fuel temperatures were ~885°C for PPS1 Fuel Temperature #2 and ~836°C for PPS2 Fuel Temperature #2.[14]

From this we may conclude that one or the other calibration is incorrect. Either the calibration results of 1990s yield an "actual" power that is too low, or the calibration results for the post 2000 era yield an "actual" power that is too high. The pool heatup calibration method was used in both eras.

[13] Memorandum from L. Martin and K. Kaiser, "Completion of the 2016 Annual Power Determination Calibration Procedure," dated January 6, 2016.

[14] Steady-State Power Operations Checklist for Run #95021, TAV Record #3100.

Pool Heatup Calibration Considerations

For the pool heatup calibration method, the reactor is operated at a steady power level, while pool temperatures at various heights above the core are recorded over time. The rate of change of the pool water temperatures (dT/dt) is used to determine the reactor power level (P) as follows

$$P = \rho V c_p \frac{dT}{dt}$$

The density (ρ) and specific heat capacity (c_p) variation over the pool heatup range (10°C to 40°C) is minimal. A least-squares fit of the pool temperature data is used to determine dT/dt, and the method assumes that the temperature measurement locations are representative of the overall dT/dt of the water volume (V).

It is this water volume that is perhaps the most crucial parameter in this method. It is determined by computing the pool volume and subtracting the volume displaced by the structures within the pool (e.g., reactor fuel and support structure, central experiment cavity, FREC-II and its experiment cavity, etc.). The currently used value is 13725 gal. with the FREC-II installed in the ACRR pool, or 14290 gal. if FREC-II is not installed. However, it is important to know if all of this water volume "participates" in the heatup. If not all of the water volume is determined to participate, then the power computed by the calibration method must be reduced by the percentage of the volume which is not participating

Figure D-1 shows a schematic not-to-scale diagram of the ACRR pool. The pool is 120" in diameter. The height of the water level above the top of the upper core grid is ~20'. This yields a volume of 11750 gal. The central cavity outer diameter is ~9.5", which results in ~74 gal. displaced above the core grid. The FREC-II cavity outer diameter is ~20.5", which results in ~340 gal. displaced above the core grid. The neutron radiography tube is ~2 ft^2, which results in ~300 gal. displaced above the core grid. The net result is ~11036 gal (11750 gal. – 714 gal.).

A 90° arc curved steel plate (48" radius and 10' tall) is aligned concentrically with the pool tank wall, serving as a flow diverter/baffle for water coming from the outlet of the pool's coolant system (a 16" pipe approximately 20" from the base of the pool tank). If the pool cooling system is not running (and it is not during the pool heatup calibration process), then it may be argued that this portion of the pool water is relatively stagnant and does not participate in the heatup. This plate extends ~4.5 ft above the upper core grid. The total volume above the upper core grid and behind this plate is ~238 gal. The net result is ~10798 gal (11036 gal. – 238 gal.).

The water entering the core at its bottom grid plate is drawn through the core support barrel (a 3' tall barrel fixed to the bottom of the pool liner. The support barrel has two inlet openings (16" diameter) located 180° apart, centered 17" above the bottom of the pool liner. The water drawn in through the inlet openings would be drawn preferentially from above. It is then assumed that the water below the centerline of these openings would not participate in the heatup process. Further, provided the flowrate is relatively slow, the water will be drawn directly from above (i.e., we could assume that water is only drawn from above in a 60° sector about the openings). This would mean that almost two-thirds of the water below the top grid plate does not participate in the heatup.

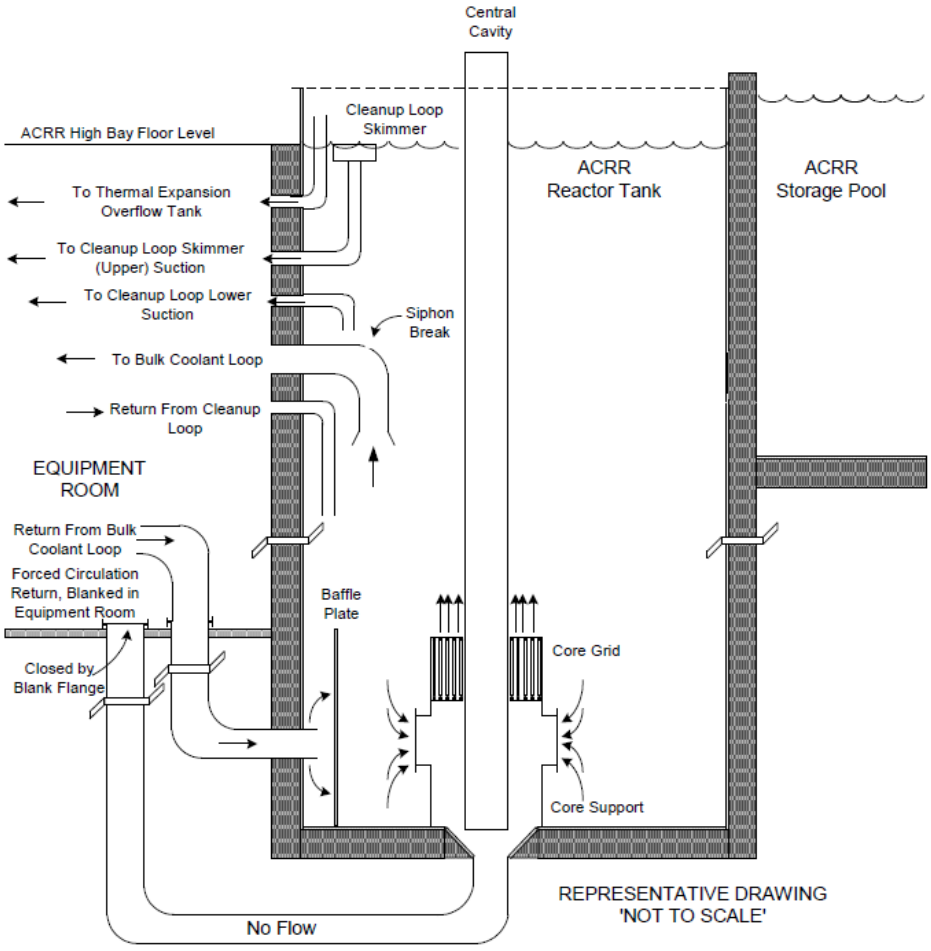

Figure D-1. Schematic of the ACRR in its reactor pool. (From ACRR Documented Safety Analysis, Change Notice 9).

For the sake of this evaluation, we will simply assume that none of the water below the top of the core grid participates in the heatup. If we utilize 14000 gal. as the nominal water volume used in the pool heatup calibration method computation, then we may conclude that the actual reactor power is ~77% (10800/14000) of the normally computed power. In other words, the conclusion of this argument is that the actual reactor power level is less than the value computed in the pool heatup calibration method, and a rough estimate indicates the actual reactor power could be about 75% of the computed value (to use a nominal fraction).

The pool heatup calibration method also assumes that the measured heatup rates are representative of the actual average heatup rate over the entire volume that participates in the heatup process. The thermocouples used for the calibration process are located vertically above the upper grid plate in grid locations 723 and 743, outside the nickel reflector elements (i.e., at the outer edge of the core). The locations are on the western and north-northeast regions, respectively, of the core. Further, the ACRR core is located off-center in the pool, toward the liner wall on the western side. Thus, it is not difficult to postulate slower heatup rates in the

water near the eastern side of the pool liner wall. In other words, the actual reactor power level may be even less than 75% of the value computed in the pool heatup calibration method.

Having made the argument that the actual reactor power is less than that computed in the pool heatup calibrations (perhaps less than 75% of the computed value), we now consider data from some coolant channel temperature measurements.

Evaluation of Coolant Channel Temperature Measurements

In his Master's thesis,[15] Farmer reports on and evaluates coolant channel temperature measurements for several steady state power operations at the ACRR in June 2002. A couple of these operations afford the data to estimate the reactor power using a simple energy balance, and to determine the power level needed by Razorback to match the temperature conditions.

Figure D-2 shows Farmer's temperature data for ACRR operation SS7572. The reactor power was raised quickly in a single step to an indicated power level of ~95% at ~13:55, while the initial pool water temperature was ~20°C. The reactor was shutdown at ~14:45 (a run of ~50 minutes). After the shutdown was initiated, the bulk cooling system was turned on in order to mix the pool water prior to the next operation. As can be seen in Fig. D-2, the temperatures equilibrated to ~40°C. Thus for a reactor energy release of ~4750 %-min., the temperature change was 20°C. Because the bulk cooling system was operated, essentially all of the 13725 gal. of pool water "participated" in the pool heatup plus the water volume in the bulk cooling system piping. The largest diameter piping of the bulk cooling system is 16", and this routes the water from the ACRR pool to the adjacent equipment room and back to the ACRR pool. At 16", the volume is ~10.4 gal/ft. A nominal 30' total run of piping from the pool and back to the pool is assumed to account for the piping volume to, from, and within the heat exchanger. This brings the total participating volume to ~14037 gal.

An energy balance of the form $\Delta E = \rho V c_p \Delta T$ may be used to compute the energy added in the operation. For a density of 0.995 g/cm^3 and a specific heat capacity of 4.185 J/g·K, the energy added is 4.425 GJ or 73759 kW·min. Using the 4750 %·min from above, one obtains a power of 1553 kW at 100%. This implies that the actual reactor power was ~65% of 2.39 MW (vs. the indicated 95%). In other words, the actual reactor power is about 68% of the pool heatup calibration method computed value.

[15] Farmer, R. A., "Critical Heat Flux Estimation for Sandia National Laboratories' Annular Core Research Reactor," Master's Thesis, University of New Mexico, Albuquerque, NM, August 2003.

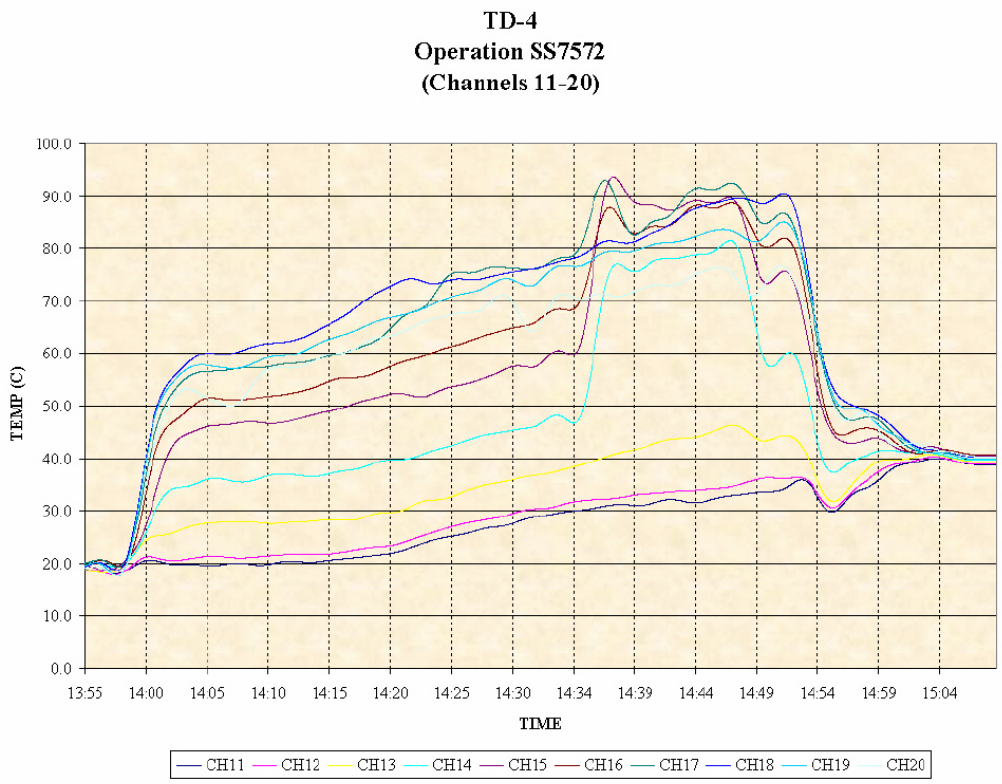

Figure D-2. Coolant channel temperature data for ACRR operation SS7572. (From Farmer, R. A., "Critical Heat Flux Estimation for Sandia National Laboratories' Annular Core Research Reactor," Master's Thesis, University of New Mexico, Albuquerque, NM, August 2003.)

Also seen in Fig. D-2 is that early in the run, the outlet temperature equilibrated to ~57°C-60°C while the inlet temperature was ~20°C. The thermocouples associated with this data were installed in either[16] the channel between core locations 202, 203, and 303 or the channel between core locations 204, 205, and 305. In either location, the average peaking factor for flow channel is ~1.32.

A steady-state Razorback run with a peaking factor of 1.32 with a 20°C inlet temperature yields an outlet temperature of 58.3°C for a power of 65% of 2.39 MW (or 1553.5 kW). Thus, the coolant channel temperature difference is consistent with the power level determined from the energy balance.

Another Razorback steady-state run at the same power level, but with a peaking factor of 1.46 to correspond to the PPS1 instrumented element position yields a measured fuel temperature result of 827°C. Figure D-3 is a plot of the ACRR log file PPS1 fuel temperature data recorded for Operation SS7572. The measured temperature is ~797°C at the time under consideration. Thus, the Razorback fuel temperature result is consistent with the power level determined from the energy balance, being just 3.8% higher.

[16] The thesis report is unclear as to which thermocouple set is installed in which precise location.

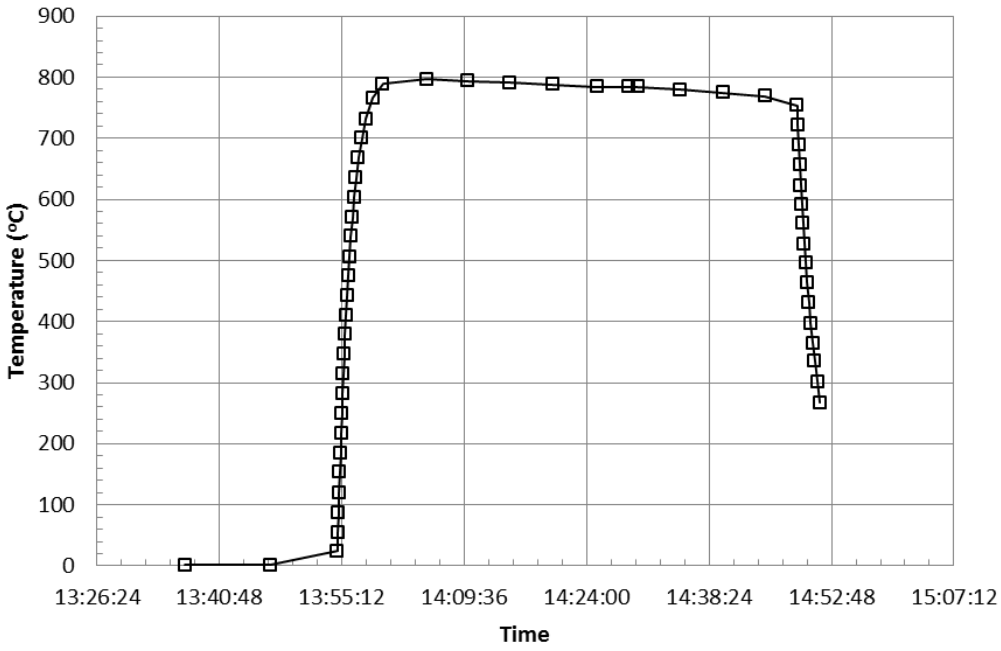

Figure D-3. Measured fuel temperature data for the PPS1 instrumented fuel element during ACRR operation SS7572.

Figure D-4 shows Farmer's temperature data for ACRR operation SS7579 for which the reactor power was raised quickly to ~95% (indicated). This operation is of interest because at 13:55, the bulk cooling system was turned on, and the result was a period of ~30 minutes where the coolant channel inlet and outlet temperatures were nearly constant. The inlet temperature was 42°C, while the outlet temperature was ~74°C-77°C. A steady-state Razorback run with a peaking factor of 1.32 with a 42°C inlet temperature yields an outlet temperature of 75.6°C for a power of 65% of 2.39 MW (or 1553.5 kW). Thus, the coolant channel temperature difference is again consistent with the power level determined from the energy balance for Operation SS7572.

Another Razorback steady-state run at the same power level, but with a peaking factor of 1.46 to correspond to the PPS1 instrumented element position yields a measured fuel temperature result of 827°C. Figure D-5 is a plot of the ACRR log file PPS1 fuel temperature data recorded for Operation SS7579. The measured temperature is ~775°C at the time under consideration. Thus, the Razorback fuel temperature result is reasonably consistent with the power level determined from the energy balance, being 6.7% higher.

The process of examining data from Operations SS7272 and SS7579 from June 2002 appears to lead to the conclusion that actual ACRR power is ~65% of the indicated power.

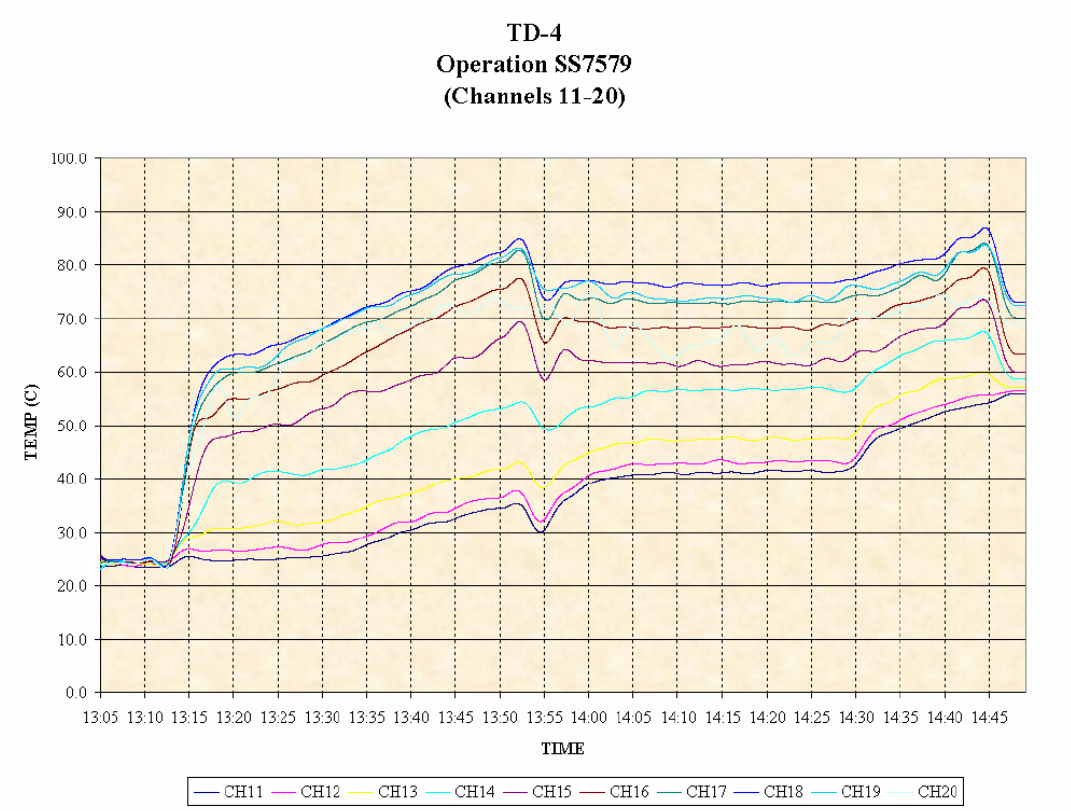

Figure D-4. Coolant channel temperature data for ACRR operation SS7579. (From Farmer, R. A., "Critical Heat Flux Estimation for Sandia National Laboratories' Annular Core Research Reactor," Master's Thesis, University of New Mexico, Albuquerque, NM, August 2003.)

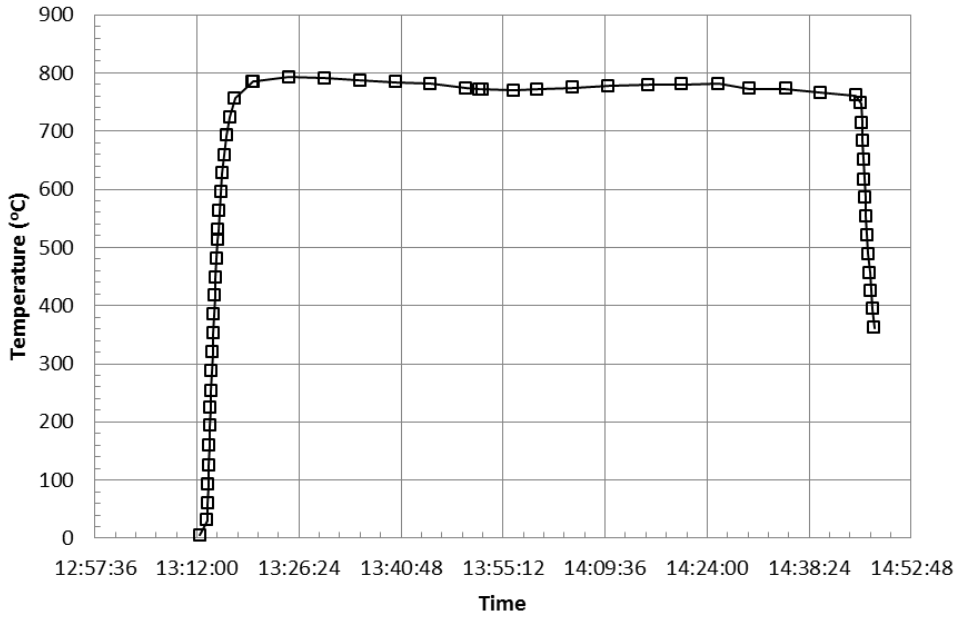

Figure D-5. Measured fuel temperature data for the PPS1 instrumented fuel element during ACRR operation SS7579.

Return to Pulse Configuration (November-December 1999)

In 1998 and 1999, the ACRR core was re-worked for a new mission of isotope production. This involved removing the dry central irradiation cavity so that a grid capable of holding fuel element shaped isotope production targets could be installed in the region where the central cavity had been. This isotope production configuration was operated (mainly in physics testing and power calibration operations) from September 1998 through September 1999.

The movement into an isotope production configuration was accomplished via a three-stage ACRR restart plan. Stage 1 included initial load-to-critical and control rod worth determinations. Stage 2 included the initial full core loading and core temperature mapping at 500°C. Stage 3 included the approach to full power, which was to be at a peak element power of 21.7 kW. The final core loading was to have 213 elements (which included 2 safety rods and 6 control rods), and the core radial peaking factor was specified to be 1.8.

For the approach to 100% power, the Stage 3 restart procedure notes that the fuel temperature was not to exceed 1330°C. This temperature corresponded to a 21.7 kW element power, and was derived from a power correlation of fuel temperature vs. element power determined in the safety analysis for isotope production operation, specifically,

$$T(°C) = 187.9[P(kW)]^{0.636}. \quad \text{(D-1)}$$

However, the Stage 3 restart procedure also says that data from Stage 2 testing suggested that this correlation was conservative (i.e., predicted higher-than-measured temperatures for a given power level), and that 1330°C would not be the temperature attained at 100% power. The fuel temperatures measured for the 50%, 75%, and 100% power calibrations (via pool heatup), along with the 500°C temperature mapping power were used to create a new power law correlation

$$T(°C) = 171.9[P(kW)]^{0.593}. \quad \text{(D-2)}$$

The records of the 100% power pool heatup calibration performed February 4, 1999 on the isotope configuration core show that the pool temperature increased from 10°C to 40°C over the time period of 16:34 to 17:21while indicated reactor power was ~100%, and the measured fuel temperature was ~1025°C. This would yield a pool heatup rate of 38.3°C/h. An electronic copy of the pool heatup calibration procedure for the February 1999 timeframe specifies the pool heatup rate factor to be 0.0159°C/kW-h. Combining this with the estimated pool heatup rate one determines 100% power to be ~2400 kW. A power of 2400 kW would result in 20.3 kW in the peak element. Equation D-1 yields a predicted temperature of 1275°C for 20.3 kW, but it also yields a power of 14.4 kW for a measured temperature of 1025°C. We note that 14.4 kW is 71% of 20.3 kW, and could conclude that the pool heatup-determined power of 2400 kW was actually 1700 kW. At the time however, it was decided that Eq. D-1 was conservative, as the confidence was in the pool heatup rather than the analytically developed correlation.

Just a few months later, the original pulse reactor core configuration was needed to meet Defense Program testing needs, and the ACRR was converted back to its pulse mission configuration. In

November 1999, physics testing of the pulse core (236 elements) with a newly-installed dry central irradiation cavity (designed to be very similar to the original cavity) was begun. The peak element power was to be 21.7 kW at 100% full power. For a 236 element core with a radial peaking factor of 1.5, this would equate to about 3420 kW at 100%. Low and high power physics testing was planned to characterize the "new" core, and by mid-November 1999 the low power physics testing was complete. High power physics testing was to begin with fuel element location power mapping. The process involved first raising reactor power to attain a measured fuel temperature of ~300°C for the PPS instrumented fuel element.

The high power physics testing began with an attempt to make use of the original power law correlation (Eq. D-1). As before, the temperatures resulting from Eq. D-1 were found to be conservative with respect to the temperatures obtained at various reactor power levels. In fact, when results were presented to the ACRR safety committee[17], the presenter noted specifically that if the power utilized in Eq. D-1 was reduced by 29% (i.e., multiplied by 0.71), then the temperature vs. power data compared much more favorably with the data measured during isotope production testing. It was then noted at the same meeting by the same presenter that Eq. D-2 had been published in the most recent safety analysis report for the ACRR, and that when the power level is reduced in Eq. D-1, the results compare well with Eq. D-2.

Conclusions and Recommendations

The application of an energy balance calculation to Operation SS7572 has shown evidence that the pool heatup power determination may be overestimating the actual reactor power, such that actual power is ~65% of the heatup-determined power. Evaluation of the coolant channel temperature measurements made in Operation SS7579 has shown that Razorback results are consistent if the assumed reactor power is 65% of the indicated power. An evaluation of the pool heatup power determination method has estimated that the actual water volume participating in the heatup may be ~75% of the volume assumed in the power determination. Examination of the data resulting from the return to pulse configuration from the isotope configuration may show that the actual reactor power was ~71% of the indicated reactor power. Taken together, there is evidence that the actual reactor power determined by the pool heatup process is 65%-75% of the indicated reactor power.

Figure D-6 presents the Razorback predicted steady-state measured fuel temperature as a function of element power. Figure D-6 also shows the temperatures measured in Operation 11278, with the associated element powers reduced to 65% and 75% of their indicated values. The result is that accuracy of the Razorback predictions is much improved if the actual reactor power is 65% of the indicated power.

[17] Minutes of the December 6, 1999 ACRR Committee meeting.

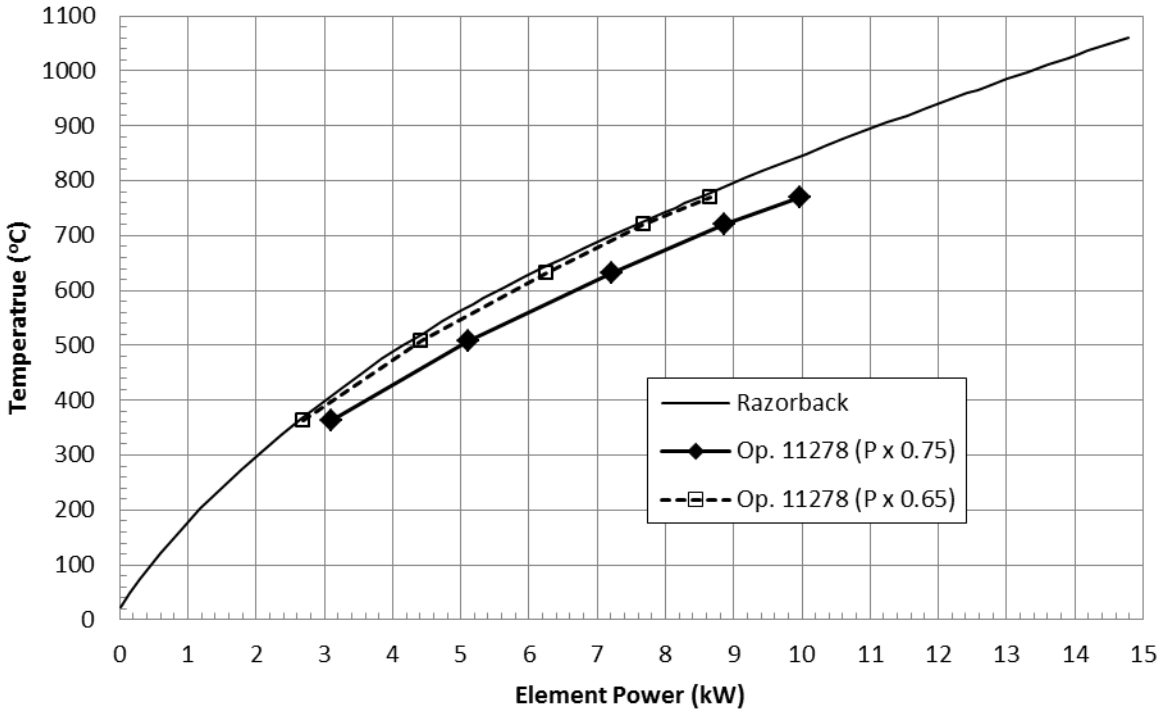

Figure D-6. Measured fuel temperature data for the PPS1 instrumented fuel element during ACRR operation SS7579.

In conclusion, we cannot state that the actual-to-indicated power for the ACRR is 65% to 75% based only on the more favorable comparison to Razorback results. However, there is adequate evidence to warrant consideration of the possibility that the actual-to-indicated power for the ACRR is less than believed. It should be noted that overestimating the actual reactor power results in conservative operation of the reactor.

The fact that the pool heatup calorimetric power determination has issues has been known, but as stated above, the results are generally conservative. With the need to better benchmark analysis codes such as Razorback, there is also a need to more closely examine the calorimetric methodology and assumptions, and consider other possible means of power calibration. Recommendations for additional work include:

1. Additional energy balance evaluations: Perform a pool heatup operation using the bulk coolant system (primary side only) for full tank mixing, so that a heat balance calculation may be performed.
2. Primary/Secondary heat balance evaluations: Perform a high power operation with the primary and secondary side coolant systems balanced so that the pool temperature is at equilibrium. Determine the power from the primary and secondary side heat transfer rates.
3. Pool water heatup uniformity evaluation: Install more temperature measurement instruments at strategic locations within the reactor pool to investigate the uniformity of the heatup rate and flow patterns.

DISTRIBUTION

1	MS1141	Jason P. Petti	01383	(electronic copy)
1	MS1141	Rachel A. Chang	01383	(electronic copy)
1	MS1141	Richard L. Coats	01383	(electronic copy)
1	MS1141	Shawn J. Henderson	01383	(electronic copy)
1	MS1141	Bennett J. Lee	01383	(electronic copy)
1	MS1141	Shivi Singh	01383	(electronic copy)
1	MS1141	Darren G. Talley	01383	(electronic copy)
1	MS1141	Michael K. Black	01385	(electronic copy)
1	MS1141	Aaron M. Miller	01385	(electronic copy)
1	MS1142	Shannon E. Kawane	01381	(electronic copy)
1	MS1142	R. David Clovis	01381	(electronic copy)
1	MS1142	Joseph Greenberg	01381	(electronic copy)
1	MS1142	Krista I. Kaiser	01381	(electronic copy)
1	MS1142	Lonnie E. Martin	01381	(electronic copy)
1	MS1146	Edward J. Parma, Jr.	01384	(electronic copy)
1	MS0899	Technical Library	9536	(electronic copy)

[This page intentionally left blank.]


Sandia National Laboratories